THE PRODUCTION OF ENDOGENOUS IL-10 BY PANETH CELLS AND ITS ROLE IN ENTEROID DEVELOPMENT

by

Huong D. Nguyen

Submitted in partial fulfilment of the requirements
for the degree of Master of Science

at

Dalhousie University
Halifax, Nova Scotia
September 2021

Dalhousie University is located in Mi'kma'ki,
the ancestral and unceded territory of the Mi'kmaq.
We are all Treaty people.

TABLE OF CONTENTS

LIST OF TABLES iv
LIST OF FIGURES v
ABSTRACT vi
LIST OF ABBREVIATION AND SYMBOLS USED vii
ACKNOWLEDGEMENTS x
CHAPTER 1: INTRODUCTION 1
1.1. Mucosal barriers 1
1.2. Intestinal epithelial cells 3
1.3. Intestinal epithelial cells as immune-modulators 8
1.4. IL-10 is an anti-inflammatory cytokine 9
1.5. IL-10 signaling pathways 11
1.6. IL-10 in the gut 13
1.7. IL-10 receptor expression in IEC 15
1.8. Effects of IL-10 on IEC 16
1.9. IL-10 expression in IEC 18
1.10. Small intestine as the research subject of interest 19
1.11. Small intestinal organoids as a model of IEC biology 20
1.12. Research Objectives 23
CHAPTER 2: MATERIALS AND METHODS 24
2.1. Animals 24
2.2. Crypt isolation and organoid culture 26
2.3. Organoid passaging 27
2.4. Cytokine treatments of organoids 28
2.5. RNA isolation 28
2.6. Reverse transcription and quantitative PCR 28
2.7. Electrophoresis 32
2.8. Immunofluorescence 32
2.9. FITC dextran permeability assay 34
2.10. Monolayer enteroid culture 35
2.11. Protein extraction 36
2.12. Western blot 37
2.13. In silico mining of publicly available RNA-sequencing datasets 38

2.14. Statistical analysis tools 38
CHAPTER 3: RESULTS 39
3.1. Establishing and standardization of enteroid cultures 39
3.2. Constitutive expression of IL-10 & IL-10R in enteroids 43
3.3. Apical expression of IL-10 in enteroids 45
3.4. Apical & basal expression of IL-10R in enteroids 47
3.5. Cellular sources of IL-10 49
3.6. Paneth cells and goblet cells express IL-10RA 52
3.7. Autocrine activity of epithelial IL-10 55
3.8. IL-10KO enteroids have deficiencies in Paneth cell markers 57
3.9. WT and IL-10KO enteroids are equally permeable 60
3.10. WT and IL-10KO enteroids express the same level of cellular lineages 63
3.11. IL-10 addition does not correct deficiencies in IL-10KO Paneth cells 66
3.12. IL-10 signaling pathway in enteroids 68
3.13. IL-10 signaling pathway in monolayers 70
3.14. Reduction of secretory markers in IFN-γ treated enteroids 73
3.15. Mining of publicly available RNA-sequencing data from mouse IECs 76
CHAPTER 4: DISCUSSION 77
4.1. Summary of expression and function of epithelial IL-10 and IL-10RA in enteroids 77
4.2. Heterogeneity in enteroid culture 80
4.2.1. Potential impact of heterogeneity of enteroid culture on characterization of constitutive expression 80
4.2.2. Potential impact of enteroid heterogeneity on characterization of enteroid permeability 80
4.3. Paneth cells express IL-10 and IL-10R and the likelihood of autocrine activity 81
4.3.1. Role of epithelial IL-10 in Paneth cell development 84
4.3.2. Role of epithelial IL-10 in Paneth cells following IFN-γ exposure 86
4.4. Inconsistent reports of the source of epithelial IL-10 89
4.5. Basal IL-10 receptors are expressed on IEC types other than Paneth cells 90
4.6. IL-10R signaling in IEC 92
CHAPTER 5: CONCLUSION 95
REFERENCES 96
APPENDICES 111
Confirmation of publication and licensing rights 111

LIST OF TABLES

Table 1. Mouse primers used in this study 30

Table 2. Antibodies used for immunofluorescence 34

LIST OF FIGURES

Figure 1. Spatial dynamics and cell lineages of the intestinal epithelium. 7

Figure 2. Enteroids resemble spatial and temporal dynamics in native intestinal epithelium. 22

Figure 3. Genotypes of WT and IL-10KO mice. 25

Figure 4. RT-qPCR primer design and melt curve 30

Figure 5. Optimization of enteroid culture through seeding density control. 41

Figure 6. Constitutive expression of IL-10 and IL-10RA in developing enteroids. 44

Figure 7. Apical expression of IL-10 in WT and GFP-IL-10 reporter mouse enteroids. 46

Figure 8. Detection and localization of IL-10RA on enteroids. 48

Figure 9. Paneth cells produce IL-10. 50

Figure 10. Cellular sources of IL-10 receptor. 53

Figure 11. Autocrine activity of epithelial IL-10 in Paneth cell. 56

Figure 12. IL-10KO has deficiencies in Paneth cell markers. 58

Figure 13. Characterization of WT and IL-10KO through permeability assay. 61

Figure 14. Cellular lineage markers in WT and IL-10KO enteroids. 64

Figure 15. IL-10 does not correct Paneth cell deficiencies in IL-10KO enteroids. 67

Figure 16. IL-10 signaling pathway through STAT3. 69

Figure 17. Western blot of pSTAT3 following apical vs basal IL-10 stimulation 71

Figure 18. Impact of IFN-γ on WT and IL-10KO enteroids. 74

Figure 19. Impacts of IL-10 on WT and IL-10KO enteroids 79

ABSTRACT

The epithelium plays key roles in maintaining immune tolerance towards the microbiota while facilitating luminal inspection and defense. The epithelium is arguably an important player of gut immune defense, given that it can secrete a wide range of anti-microbial products, cytokines, and chemokines.

In this study, we investigate the production and the role of IL-10, a potent anti-inflammatory cytokine, in intestinal epithelial cells. IL-10 has been established to be a key player of the intestinal innate immune system, and plays critical roles in gut homeostasis. Interest in intestinal IL-10 has mainly focused on how leukocyte-derived IL-10 influences the activity of other leukocytes, which consequently affect the state of the epithelium. Yet emerging evidence has claimed that the IL-10 receptors, as well as IL-10, are both detectable in the epithelium. Nevertheless, there are still knowledge gaps regarding the specific cell source and the role of IL-10 in the epithelium.

Using multiple means of detection, Paneth cells within murine enteroids are shown to produce IL-10 and possess the IL-10 receptor. Additionally, other cells also possess the IL-10 receptor. The evidence from this study speaks to the likelihood of autocrine activity of IL-10 in Paneth cells and its impacts on the development of Paneth cell. Moreover, characterization of STAT3 activation through the IL-10 receptor revealed differential epithelial responses when stimulated from the apical versus basal membranes. Evidently, epithelial IL-10 might play a role in the regulation of STAT3 signaling through apical IL-10 receptor in intestinal epithelial cells.

This study draws attention to intestinal epithelial cell as an unconventional contributor to the pool of mucosal IL-10. Importantly, the study further highlights the pleiotropism of IL-10, the effect of which greatly depends on the source, the target, and, for polarized cells such as intestinal epithelial cell, the polarity of exposure.

LIST OF ABBREVIATIONS AND SYMBOLS USED

ANOVA	Analysis of variance
BSA	Bovine serum albumin
cDNA	Complementary deoxyribonucleic acid
DAPI	4′,6-diamidino-2-phenylindole
DEFA	Defensin (human) or cryptdin (mouse)
DLL	Delta Like Canonical Notch Ligand
DMEM/F12	Dulbecco's Modified Eagle Medium/Nutrient Mixture F-12
DNA	Deoxyribonucleic acid
DSS	Dextran sulfate sodium
ECL	Enhanced chemiluminescence
EDTA	Ethylenediaminetetraacetic acid
EGF	Epidermal growth factor
FBS	Fetal bovine serum
FITC	Fluorescein isothiocyanate
G-CSF	Granulocyte colony stimulating factor
GFP	Green fluorescent protein
GM-CSF	Granulocyte-macrophage colony-stimulating factor
HRP	Horseradish peroxidase
IBD	Inflammatory bowel disease
IEC	Intestinal epithelial cell
IEL	Intraepithelial lymphocyte

IFN	Interferon
IgG	Immunoglobulin G
IL	Interleukin
ILC	Innate lymphoid cell
IP-10	Interferon gamma-induced protein 10 (also known as CXCL10)
JAK	Janus kinase
KO	Knockout
LPS	Lipopolysaccharide
LYZ	Lysozyme
MCP	Monocyte chemoattractant protein
MIP-2	Macrophage inflammatory protein-2 (also known as CXCL2)
mRNA	Messenger ribonucleic acid
MUC	Mucin
PAGE	polyacrylamide gel electrophoresis
PBS	Phosphate-buffered saline
PFA	Paraformaldehyde
PIPES	Piperazine-N,N′-bis(2-ethanesulfonic acid)
RANTES	Regulated on Activation, Normal T Cell Expressed and Secreted (also known as CCL5)
RIPA	Radioimmunoprecipitation assay
RT-qPCR	Reverse transcription - quantitative polymerase chain reaction
SDS	sodium dodecyl sulfate
STAT	Signal Transducer and Activator of Transcription

TAE	Tris-acetate-EDTA
TBS	Tris-buffered saline
TLR	Toll-like receptor
TNF	Tumor necrosis factor
TYK	Tyrosine kinase
WT	Wild-type

ACKNOWLEDGEMENTS

I am grateful for the support and mentorship from Dr. Andrew Stadnyk. Thank you for all the precious hours that you spend on answering my questions and editing my writing with such patience and understanding. Your enthusiasm in every project motivates me to stay curious and critical with my research.

Thank you, Dr. Francesca DiCara, for always coming to my rescue when I need reagents, and Dr. Jun Wang, for providing me with IL-10-GFP reporter mouse. Thank you both for your helpful inputs toward improving my research and your encouragement in every committee meeting.

Thank you Rean, for all the help around the lab and for always keeping an eye on the orders and supplies for my project. My last few months would not have been a smooth sail without your assistance.

CHAPTER 1: INTRODUCTION

1.1. Mucosal barriers

The well-being of the gut depends on the fine interplay between 3 major aspects of mucosal homeostasis: the intestinal epithelium, the mucosal adaptive immune elements and the resident microbiota (Soderholm & Pedicord, 2019). The goal is to keep the balance between two seemingly opposing functions: maintaining immune tolerance towards intestinal commensals while staying acutely responsive against pathogens. In order to carry out this task, the gut is equipped with multiple levels of protection and regulation: the physical barrier, the chemical barrier and the “functional” immunological barrier (Moens & Veldhoen, 2012).

The physical barrier in direct contact with the gut microbes is the thick mucus layer secreted by goblet cells, which covers all of the apical (lumen) side of the intestinal mucosa. The small intestine has one thick mucus layer, while the large intestine, which has a more abundant microbial population, has more goblet cells and consequently has 2 layers of mucus: a firm inner layer and a loose outer layer (Pelaseyed et al., 2014).

The other important physical barrier for the mucosa is the intestinal epithelial monolayer itself. The epithelium segregates the external microbes from the host effector leukocytes, presumably to avoid unwanted interaction between the two while still modulating selective permeability. This layer is composed of multiple cell types, each of them having distinguishing roles in homeostasis, and

cells are tightly sealed together by cell junctions to sustain barrier integrity (Allaire et al., 2018).

The chemical barrier is composed of antimicrobial peptides and proteins, such as lysozyme, defensins, C-type lectins and phospholipase A2, secreted by Paneth cells (Elphick & Mahida, 2005). Another component of the chemical barrier is secretory IgA (SIgA), dimeric antibody produced by plasma cells from the lamina propria, which following directed transport across the epithelium, has a residual fragment of the polymeric Ig receptor attached. SIgA inhibits microbial access to epithelial receptors, entraps microbes in the mucus and facilitates microbial removal (Mantis et al., 2011).

The immunological barrier is exceptionally important in the case of microbes overcoming the chemical barrier and penetrating the physical barrier to enter the mucosa. The first immune cells to encounter and react to antigen are intraepithelial lymphocytes, a subset of T-cells that reside in between epithelial cells. Beneath the epithelium are populations of immune cells in the lamina propria, which includes several cell types, all contributing to the maintenance of gut homeostasis and responsiveness to potential pathogens (Sheridan & Lefrançois, 2010). During the homeostatic state, epithelial cells and leukocytes maintain a tolerogenic environment, which allows the existence of commensal microbes without eliciting pathogenic inflammatory responses (Soderholm & Pedicord, 2019).

1.2. Intestinal epithelial cells

The epithelium is the outermost cellular layer of the intestinal mucosa, with the apical membrane facing the exterior/luminal environment and the basal side in contact with a basement membrane, resting on the lamina propria. The luminal environment constantly exposes the epithelium to ingested materials and resident microbiota. Changes to the luminal environment can directly influence the epithelium and the underlying mucosal immune system (Goto, 2019). The epithelium, as a physical barrier between the external environment versus the host, becomes the crucial bridge that connects and balances these 2 sides of the intestinal environment (Soderholm & Pedicord, 2019).

In conducting the principal function of nutrient digestion and absorption, the intestinal epithelium is thrown into folds, organized into crypts and villi in the small intestine, and crypts in the large intestine (Krndija et al., 2019). Cells along the crypt-villus axis are organized into specialized niches. At base of crypts in both intestines is the intestinal stem cell niche, consisting of intestinal stem cells (ISC) and in the small intestine, Paneth cells. The pocket-shaped crypt is supported by stromal cells, smooth muscle cells, and neural cells from the basal side (Meran et al., 2017). The ISC are multipotent adult stem cells that continuously divide and give rise to undifferentiated cells, named transit-amplifying cells, which eventually differentiate into specialized cells such as Paneth cells, goblet cells, enteroendocrine cells, tuft cells and enterocytes. ISC proliferation and differentiation not only generate epithelial cell populations to maintain the barrier function and integrity but also push the cells progressively

out of the crypt up the villi, like an escalator. At the top of the escalator, the villus tip, the oldest cells are shed (Strzyz, 2019).

Paneth cells are highly specialized secretory cells residing at the crypt base that can be observed under the microscope by dense cytoplasmic granules, which are packed with antimicrobial peptides and immunomodulating mediators (Bevins & Salzman, 2011). These granule contents are released upon detection of microbial signals (Ayabe et al., 2000). Paneth cells also play a crucial role in regulating the stem cell niche for epithelial renewal via secretion of proliferative factors such as EGF, WNt3 and the Notch ligand DII4 (Clevers & Bevins, 2013; Sato, Van Es, et al., 2011). Unlike in the small intestine, the large intestine does not seem to have Paneth cells except during certain mucosal inflammatory conditions (Fahlgren et al., 2003). Interestingly, although lacking Paneth cells, the large intestine crypt niche is still supported and protected, thanks to unique subsets of goblet cells. Although the labeling of these goblet cell types is inconsistent between studies, the cells are unanimously characterized as being at the colonic crypt base and interspersed between stem cells. Specifically, deep-crypt-secretory cells and/or cKit+ goblet cells reside at the colonic crypt base and support the stem cell with proliferative factors such as DLL1, DLL4, and EGF, similar to Paneth cells in small intestine (Rothenberg et al., 2012; Sasaki et al., 2016).

Goblet cells are specialized secretory cells that are scattered across the epithelium though still interspersed between enterocytes. These cells produce gel-forming mucins such as MUC2, MUC5AC, MUC6 and MUC5B, that make up

the large polymers of mucous layers. Together, Paneth cells and goblet cells form an antibacterial gradient in the mucus that hinders the penetration of microbes (Pelaseyed et al., 2014). The mucus is not only important to protect against antigen invasion but also self-digestion by intestinal proteases (Pelaseyed et al., 2014). Surprisingly, in addition to the secretory role, small intestinal goblet cells can also uptake and deliver luminal antigens to the lamina propria dendritic cells (LP-DC) through goblet cell-associated antigen passages, which are now believed to be the dominant mechanism to facilitate the process of luminal sampling by LP-DC (McDole et al., 2012; Miller et al., 2014). As mentioned, colonic goblet cells not only maintain the mucus layers but also support the colonic stem cell niche. Depending on the position in the gut (small or large intestine) and the position within the epithelium (crypt base, crypt opening or villi surface), different goblet cell subsets can differentially respond to various secretagogue and secrete different endogenous factors (Birchenough et al., 2016; Nyström et al., 2021; Prandi et al., 2013).

Enterocytes are specialized digestive and absorptive cells that are responsible for the digestion of food products and absorption of ions, water, nutrients, and resorption of bile acids. The most abundant cell type of the epithelium, the role of enterocytes expands beyond digestion/absorption. Enterocytes contribute to mucosal immune activities by capturing, processing and presenting antigens to immune cells (Snoeck et al., 2005). Enterocytes can also produce transmembrane mucins such as MUC3, MUC12 and MUC17 that make up the matrix of glycocalyx, a layer resting just above the apical microvilli of

enterocytes. The glycocalyx is believed to be the sensing tool of enterocytes to examine the luminal environments (Pelaseyed et al., 2014).

Two other cell types, enteroendocrine and tuft cells, make up a very small fraction of the IEC population yet play important roles that support gut function and homeostasis. Enteroendocrine cells are specialized secretory cells responsible for the release of hormone-like molecules which can either act locally on enteric neurons or enter the circulation and affect extrinsic neurons. In this role, enteroendocrine cells are essential elements of the gut-brain axis, the connection responsible for a variety of activities such as secretion, motility and metabolism (R. Latorre et al., 2016). Notably, within the enteroendocrine cell population, there are various subtypes scattered along the GI tract which express heterogeneous markers and functions (Beumer et al., 2020; S. Wang et al., 2004). Tuft cells share similarities with enteroendocrine cells in the sense that the cells release neurotransmitters. However, tuft cells can also play distinguishing roles in type 2 immunity by producing an array of effector cytokines (Schneider et al., 2019). Similar to enterocytes, both enteroendocrine and tuft cells act as chemosensory sentinels that examine the luminal content and communicate with leukocytes and neuronal cells through diverse means (Gribble & Reimann, 2016; Schneider et al., 2019)

Figure 1. Spatial dynamics and cell lineages of the intestinal epithelium. Stem cells residing at the crypt base give rise to all other cell lineages. Stem cell-derived progenitors undergo multiple steps of cell fate determination and differentiation before reaching maturation to become specialized IECs (Gerbe et al., 2011) (Created with BioRender.com).

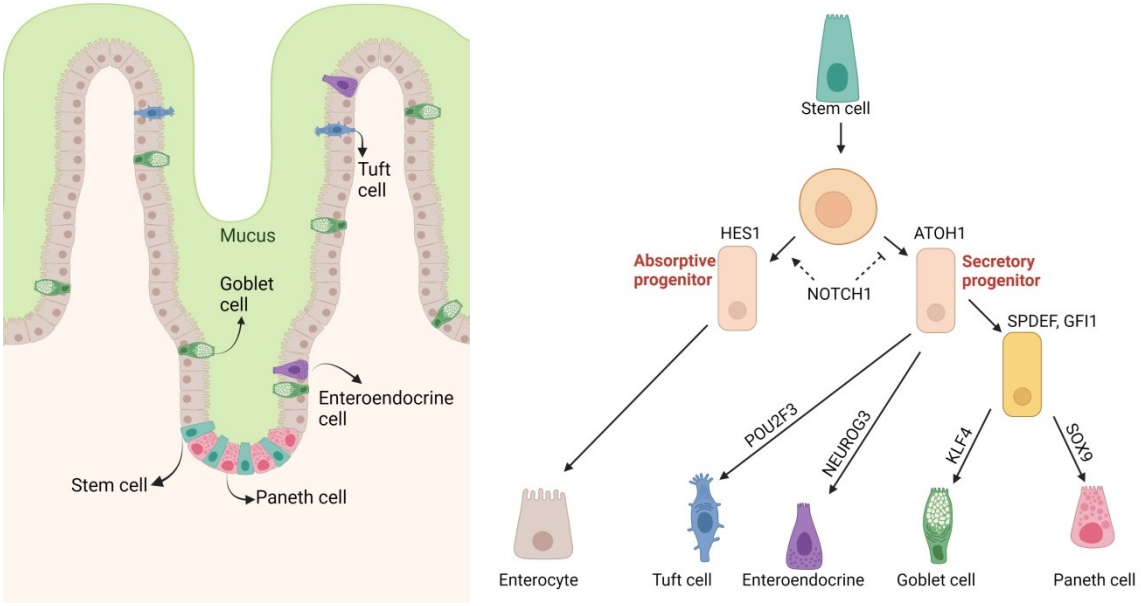

1.3. Intestinal epithelial cells as immune-modulators

When it comes to mucosal immune regulation, leukocytes have been presumed to be the major effectors, while IECs were considered a physical barrier and bystander during inflammatory and immune processes. Yet a growing volume of studies has revealed that IECs also directly participate in the immune activities in the local response, indicating that IECs are noteworthy players of the mucosal immune system. IECs can produce a myriad of cytokines and chemokines, as well as carry the corresponding receptors, making it quite an interactive component of the mucosal immune system (Stadnyk, 2002).

Through the secretion of mediators IECs contribute to mucosal tolerance, and homeostasis (Iliev et al., 2007). For example, epithelial IL-6 was shown to induce IEC proliferation, while epithelial TGF-β was shown to promote differentiation (Jeffery et al., 2017; R. D. Smith, 1995). Pooling the results from multiple IEC research models, the list of detected epithelial-derived constitutively expressed cytokines includes IL-1α, IL-1β, IL-2, IL-4, IL-5, IL-6, IL-8, IL-10, IL-15, IL-18, TNF, TGF-β and even IFN-γ (Eckmann et al., 1993; Panja et al., 1995).

In addition to constitutive expression, the expression of immunoregulatory proteins in IECs are especially heightened in response to infections (Jung et al., 1995; Li et al., 1998; Michalsky et al., 1997; Steiner et al., 2000). Regarding the mechanisms, epithelial-derived cytokines and chemokines can be stimulated and enhanced by a wide range of stimuli, including microbial antigens, other chemokines or cytokines, and interaction with various leukocytes (Cella et al., 2009; Hyun et al., 2015; Stadnyk, 2002). Consequently, depending on the stage

of the infection, the outcomes can include leukocyte recruitment and activation, antimicrobial release by IECs, and epithelial repair (Beck et al., 2003; Farin et al., 2014; Goto, 2019). Overall, either during inflammatory conditions or in the homeostatic state, IECs are capable of producing cytokines and chemokines, constitutively and upon stimulation.

1.4. IL-10 is an anti-inflammatory cytokine

Of all cytokines, IL-10 arguably has the most potent anti-inflammatory effects upon both innate and adaptive immunity (Sabat et al., 2010). The mechanisms behind these effects are diverse. Conforming to its early name as "human cytokine synthesis inhibitory factor", IL-10 suppresses the secretion of multiple pro-inflammatory cytokines and chemokines from a wide variety of leukocytes, including IFN-γ, TNF, IL-1α/β, IL-2, IL-4, IL-5, IL-6, IL-12, IL-18, G-CSF, GM-CSF, MCP1, MCP5, RANTES, IL-8, IP-10, and MIP-2 (Couper et al., 2008; Iyer & Cheng, 2012). Simultaneously, IL-10 induces the release of multiple anti-inflammatory molecules such as the IL-1 receptor antagonist and soluble TNF receptor (Cassatella et al., 1994; Dickensheets et al., 1997) Other effects of IL-10 include limiting the activation and proliferation of CD4+ T cells and macrophages, suppressing CD8+ T cell cytotoxicity, as well as inhibiting maturation of Th1-type dendritic cells (De Smedt et al., 1997; O'Farrell et al., 1998; L. K. Smith et al., 2018; Ye et al., 2007). Interestingly, depending on the the stimulus, the cell source, the location and the phase of inflammation, IL-10 can act on certain subsets of leukocytes without interfering with others (Brooks et al., 2010), highlighting the versatile immunoregulatory role of IL-10. While most

immune effector cell activities are dampened in response to IL-10, in the case of B cells, IL-10 can lead to cell activation, proliferation, differentiation and survival (Itoh & Hirohata, 1995). Taken together, that IL-10 has paradoxical activities, inhibiting of cell-mediated immunity and inflammation yet stimulating humoral immunity becomes evident.

Since the discovery of IL-10, multiple cell sources of IL-10 have been discovered. The major sources of IL-10 are T cells, particularly Th2 and subsets of regulatory T cells such as Treg and Tr1 (Mosser & Zhang, 2008). Proinflammatory effector T cells such as cytotoxic CD8+ T cells, Th1 and activated monocytes also produce IL-10 under certain conditions. In this case, IL-10 acts as a self-control mechanism to hamper immunopathological damage caused by cytokine-dependent and cell-mediated immunity (Abrams et al., 1991; Noble et al., 2006; Trandem et al., 2011; Trinchieri, 2007). Professional antigen-presenting cells such as dendritic cells, monocytes and stimulated macrophages are also important producers of IL-10 under certain immune conditions such as allergy, and parasitic and bacterial infection, to limit tissue damage by inflammatory activities (Sanin et al., 2015; Schülke, 2018). Additionally, at the site of infection during sepsis, neutrophils emerge as the early and dominant producers of IL-10 (Kasten et al., 2010). In the setting of autoimmune disease, IL-10-producing B cells can play a significant regulatory role. Researchers proposed that IL-10-producing naive B cells prevent the onset of inflammation, while memory B cells, through secretion of IL-10, ameliorate the inflammatory burden in autoimmune disease (Rieger & Bar-Or, 2008).

Like a double-edged sword, IL-10 can also be wielded in favor of the pathogens. Specifically, granulocytes such as mast cells and eosinophil were found to produce IL-10 in response to fungal and parasitic infections, which contribute to an ineffective immune response and persistent survival of the pathogens. In a different scenario, the emergence of IL-10-producing macrophages and T-cells during viral infection hindered viral clearance and lead to chronicity of the viral infection (Richter et al., 2013). Additional evidence has shown that IL-10-producing Th17 can promote an immunosuppressive state that increases susceptibility to infection and tumor escape (Musuraca et al., 2015). Therefore, the temporal and spatial dynamics of IL-10 release is precisely executed in order to allow efficient pathogen clearance while still attenuating immunopathological damages (Ernst et al., 2019).

1.5. IL-10 signaling pathways

The IL-10R is a membrane-spanning tetramer that consists of two α (IL-10R1) and two β (IL-10R2) chains. IL-10R1 binds exclusively to IL-10 with high affinity (Shouval et al., 2014). IL-10R2 is shared with other cytokines of the IL-10 family, such as IL-19, IL-20, IL-22, IL-24, IL-26, IL-28, IL-29, and IFN-λ (Commins et al., 2008). Binding of IL-10 to the IL-10 receptor results in the phosphorylation of IL-10Rα-associated JAK1 and IL-10Rβ-associated TYK2 (Kotenko et al., 1997). Following JAK1 phosphorylation, tyrosine residues of the IL-10Rα intracellular domain are phosphorylated and serve as the docking site for STAT molecules. At this site, phosphorylated JAK1 phosphorylates STAT molecules which then form heterodimers, which are translocated into the nucleus to exert

gene regulation effects (Verma et al., 2016). On the other hand, events following IL-10β-associated TYK2 phosphorylation remain less clear, some evidence suggesting that IL-10β-associated TYK2 phosphorylation supports early and optimal STAT1 and STAT3 phosphorylation (Shaw et al., 2006; Wilbers et al., 2017).

IL-10 activation through the IL-10 receptor commonly results in STAT3-phosphorylation. Two important residues of STAT3 for phosphorylation critical to operation as a transcription factor are Y705 and S727. While phospho-TYR705 stabilizes the STAT3 dimer and is necessary for translocation of the dimer to the nucleus, phospho-SER727 reportedly regulates the longevity of STAT3 activation through tyrosine-dephosphorylation (Wakahara et al., 2012; Yang et al., 2019). In addition to STAT3, STAT1 and STAT5 can also be phosphorylated upon IL-10 stimulation (Wehinger et al., 1996). However, the biological effects following IL-10-stimulated STAT1 or STAT5 phosphorylation have not been determined. Generally, STAT1 is reported to have multiple opposite effects to STAT3. Specifically, STAT3 activation is associated with proliferation, immune tolerance and cell survival, while STAT1 activity was thought to restrain cell growth and induce inflammation and apoptotic responses (Avalle et al., 2012). STAT3 and STA5 exert some similar biological effects upon activation, but they can also have some opposing effects on key genes such as BCL6 (Tanabe et al., 2005; S. R. Walker et al., 2013).

Although better studied in hematopoietic cells such as macrophages, IL-10R/STAT3 signaling was also reported in non-hematopoietic cells. STAT3 plays

a role in IEC as knockout of IEC-specific STAT3 has been shown to aggravate DSS-induced colitis in mice (Jung et al., 2019; Willson et al., 2013). STAT3 was shown to play an indispensable role in quiescent stem cell maintenance, crypt renewal following epithelial damage, and antimicrobial peptide regulation upon intestinal infection (Matthews et al., 2011; Oshima et al., 2019; Wittkopf et al., 2015). Notably, in addition to IL-10, there is a wide range of cytokines that signal through STAT3 in IEC including IL-6, IL-15, IL-22 and IFN-γ, some of which can be either endogenous or from exogenous sources (Jeffery et al., 2017; Mizoguchi, 2012; Pickert et al., 2009; Reinecker et al., 1996; Serrano et al., 2019; Stadnyk, 2002; Yue et al., 2021). As it was reported that STAT3-knockout enteroids have severe maturation deficiencies, it can be concluded that endogenous STAT3 activation plays a significant role in epithelial homeostasis (Jung et al., 2019).

1.6. IL-10 in the gut

The gut, as the largest and most dynamic immunological environment in the body, depends on the immune regulation by IL-10 to maintain healthy homeostasis (Pabst et al., 2008). The crucial role of IL-10 in gut homeostasis was indisputably demonstrated by the discovery that the absence of IL-10 spontaneously resulted in enterocolitis in mice (Kühn et al., 1993). Several subsequent studies reported IL-10 and IL-10R mutation phenotypes in humans and revealed similar outcomes, which reinforced the fact that the IL-10 signaling pathway is absolutely required for gut maintenance (Kotlarz et al., 2012; Moran et al., 2013; Zhu et al., 2017).

Depending on the location and stimulation, IL-10 can be secreted by almost all types of leukocytes. In the gut, intraepithelial lymphocytes (IEL) are the main producer of IL-10 (Kamanaka et al., 2006). Among leukocytes producing IL-10, a small subset of type 2 innate lymphoid cells (ILC2) were found secreting IL-10 in the lamina propria, during steady-state and following stimulation with certain cytokines and neuropeptides (Bando et al., 2020). However, during inflammation, macrophages become the most significant producer of IL-10 and facilitate the wound healing process of the epithelium (Morhardt et al., 2019).

The gut is in constant contact with products from the gut microbiota, thus it is no surprise that this relationship also influences mucosal immunity in general, and mucosal IL-10 expression in particular. Compared to conventionally raised mice, germ-free mice or antibiotic-treated mice have similar or lower mucosal IL-10 levels (Kennedy et al., 2018). At the cellular level, IL-10 production by Tregs was found lower in germ-free mice than in colonized mice (Strauch et al., 2005). In a refinement of these observations, researchers have identified several intestinal microbial species and metabolites that modulate IL-10 levels. For example, polysaccharide A produced by *Bacteroides fragilis* was found to induce IL-10 production in $CD4^+$ T cells, which protected mice from colitis (Mazmanian et al., 2008). The gut microbiota was found to promote expansion of IL-10-producing B cells in the colonic lamina propria, as well as IL-10 production in Treg cells and macrophages (Jeon et al., 2012; Mishima et al., 2019; Ueda et al., 2010). Additionally, *Clostridium* species were shown to induce IL-10 production in a variety of mucosal immune cells including Tregs, macrophages and dendritic

cells, all of which contribute to the prevention and attenuation of colitis (Alameddine et al., 2019; Atarashi et al., 2011; Rossi et al., 2016). In addition to IL-10, expression of IL-10R on IEC was also induced by microbial metabolites, specifically, indole-3-propionic acid and butyrate, which exerted protection from model colitis in mice (Alexeev et al., 2018; Zheng et al., 2017). These observations indicate that the gut microbiota can affect IL-10/IL-10R pathways in diverse targets, including leukocytes and IEC.

1.7. IL-10 receptor expression in IEC

There is evidence across different IEC models confirming the expression of IL-10R on IEC. Indeed, researchers detected mRNA for both IL-10R subunits from freshly isolated cells from the murine intestine. Concurrently, they also detected surface protein expression in murine IEC cell lines, including mode-K and MCA-38 (Denning et al., 2000). IL-10R1 mRNA was reported in human IEC, specifically from isolated colonic IEC and SW1116 cell lines, but surprisingly not in HT-29 nor T84 (Bourreille et al., 1999). On the other hand, T84 can express apical IL-10R1 after being stimulated with IFN-γ (Kominsky et al., 2014). In this study, the essential role of IEC-specific IL-10R was highlighted, as knockdown of IEC-specific IL-10R1 increased permeability in T84 monolayers and after DSS treatment in mice. Reports of apical IL-10R on IEC in colonic IBD biopsies but not non-IBD biopsies further supports the idea that apical IL-10R on IEC are induced. Apical expression of IL-10R was observed in the distal colon of mice with DSS-induced colitis, although these authors did not localize the receptor to any particular epithelial cell type (Kominsky et al., 2014). From the evidence

available, it remains unclear whether all IEC express the IL-10R or whether it is unique to a specific cell type; the most comprehensive study to date indicates the IL-10R is expressed on the goblet cells (of the mouse distal colon) and on goblet cell-differentiated LS174T colon carcinoma cells (Hasnain et al., 2013).

The expression of the IL-10R2 subunit is expected to be more abundant on the epithelium because it makes up the receptor for several cytokines in addition to IL-10. Yet, immunofluorescent-staining in human stem cell-derived intestinal organoids demonstrated that the localization of IL-10R2 was restricted to cells also possessing an enteroendocrine cell marker (Forbester et al., 2018). It is noteworthy that organoids lack interactions with cells of the lamina propria and microbiota, which might be required to stimulate IL-10R2 expression. Despite conflicting published characterization of IL-10R localization (IL-10R1 colocalizes with goblet cells while IL-10R2 colocalizes with enteroendocrine cells), researchers have investigated the effect of IL-10 on the intestinal epithelium, which infers the presence of functional receptors on IEC.

1.8. Effects of IL-10 on IEC

IL-10 can have indirect effects on IEC by acting on immune effector cells, to ameliorate epithelial injury caused by these cells. In general terms, the response of IEC to IL-10 also seems to promote epithelial barrier integrity and homeostasis. IL-10 can also directly influence IEC activity.

The impacts of IL-10 upon epithelial integrity is evident even during steady-state since the absence of IL-10 or IL-10R on IEC results in increased permeability and altered expression of intercellular junctions (Kominsky et al.,

2014; Shi et al., 2014). Following DSS-induced colitis, disruption of IL-10 signaling through knockout of IEC-specific IL-10R exacerbates the damage to the epithelial barrier, which can be restored by adding IL-10 (Kominsky et al., 2014; Madsen et al., 1997; Shi et al., 2014; Sun et al., 2007). Additionally, IL-10 was found to play a significant role *in vivo* in epithelial wound healing (Morhardt et al., 2019; Quiros et al., 2017).

The mechanisms behind how IL-10 exerts effects on IEC varies from anti-apoptosis, maintaining subcellular proteostasis, influencing IEC secretions, to possibly even influencing IEC differentiation. Specifically, a lack of IL-10 was shown to associate with reduced specialized cell types such as Paneth and goblet cells, as well as secretory products such as antimicrobial peptides and mucin. The difference was observable from proteomic profiles (Werner et al., 2007). Furthermore, IL-10 was shown to exert direct anti-apoptotic effects on IEC by decreasing expression of Fas protein and caspase 3/8 activity (Bharhani et al., 2006). IL-10 can also contribute to the cross talk between IEC with other immune cells and the microbiota. With regard to the microbiota, IL-10 affects fucosylation of glycans by IEC, an important component of the mucus composition, which act as receptors and nutrient source for certain mucus-resident microbial populations (Goto et al., 2014). By inhibiting the expression of chemokines such as MCP-1 (CCL2), IL-10 regulates the interaction of IEC with immune cells (Kucharzik et al., 1998). Overall, IL-10 can directly target IEC to exert intrinsic effects, as well as mediate the relationship between IEC with both

mucosal immunity and microbes, all of which contribute to balancing of mucosal homeostasis and tolerance.

1.9. IL-10 expression in IEC

The evidence is unequivocal that IL-10 modulates IEC activities, more often positively, affecting the balancing act of homeostasis. Yet, do IEC contribute to the pool of IL-10? Interestingly, studies have shown evidence of IL-10 produced by IEC, yet the identification of the specific cell type responsible for IL-10 production remains unclear. IL-10 protein and mRNA have been reported in IEC from multiple species, including human, mouse and rhesus macaques (Panja et al.,1995; Autschbach et al., 1998; Pan et al., 2014). The evidence that IEC expression of IL-10 is regulated is derived mainly from cell culture experiments. Human COLO 205 cells can be stimulated with cytokines produced by NK cells to secrete IL-10 (Cella et al., 2009). IEC isolated from the colon of colon cancer patients, and SW480-APC colon carcinomas, increased IL-10 production when stimulated through TLR4 using LPS, or through macrophage-epithelial cell interaction (Hyun et al., 2015). Another study showed that in Caco-2 cells and mice, IL-10 production could be induced via TLR4 or TLR2 stimulation (Latorre et al., 2018). Such evidence suggests that the expression of IL-10 in IEC can be influenced by the microbiota and the interaction with mucosal immune cells.

The functional role of epithelial-sourced IL-10, especially regarding autocrine roles, is still a relatively unexplored territory in mucosal immunology. One study reported transgenic mice producing IL-10 in mature enterocytes along

the villi and showed that several leukocyte activities were altered; however, any direct effect on the epithelium was not interrogated (De Winter et al., 2002). The role of epithelial-sourced IL-10 during infection has been explored. During infection with *E. faecalis*, isolated IL-10KO IEC overexpressed grp-78 and cleaved caspase-3, but under-expressed E-cadherin compared to the infected WT, suggesting a high ER stress response and likely a compromised barrier in the epithelium (Shkoda et al., 2007). IEC from IL-10KO organoids possessed a higher level of double-stranded DNA breaks. This phenomenon was partially reversible by adding IL-10 to the IL-10KO organoids after 24 hours (Frick et al., 2018). The observation that IL-10KO organoids differ from WT and that the difference is corrected by added IL-10 suggests that endogenous IL-10 is not only present but also has a functional role in epithelial biology. Observations of IL-10 are not limited to small intestinal organoids. Compared to the WT, aberrant patterns of E-cadherin and a reduced level of desmoglein-2 was detected in IL-10KO colon organoids (Khare et al., 2019). The use of an organoid model for the investigation of IL-10 in IEC has advantages, the model not only preserves the *in vivo* cellular dynamics but also exclude the leukocyte sources of IL-10, which allow the researcher to confidently attribute the observed effect to autocrine IL-10.

1.10. Small intestine as the research subject of interest

The small and large intestines, while populated with similar epithelial cells, have some significant differences in terms of anatomy and function, as well as cellular and microbiota composition (Bowcutt et al., 2014). For example, Paneth

cells play significant roles in maintaining the stem cell niche and defend against microbes in the small intestine while the detection of Paneth cells in the large intestine is limited to pathological states (Simmonds et al., 2014; Tanaka et al., 2001). TEER measures are typically higher in colonoid monolayers compared to enteroid monolayers, suggesting there are differences in tight junctions (Altay et al., 2019; Kozuka et al., 2017). Interestingly, compared to the small intestine, IELs in the large intestine express significantly more IL-2, IL-4, IL-5, and IL-10 mRNA (Beagley et al., 1995), which can establish distinctive immunological microenvironments in the two compartments. Similarly, the microbiota composition is also different between small and large intestine (Crespo-Piazuelo et al., 2018; Vuik et al., 2019). Thus it is inappropriate to simply extrapolate findings from the small intestinal epithelium to the large intestine and vice versa.

Although IBD, specifically Crohn's disease, can affect both the small and large intestine, the majority of studies intended to provide insights into IBD use colonic cell models. The popular gut carcinoma cell lines (T84, Caco-2, HT-29, LS 174T, MCA-38, COLO205, SW1116, SW480-APC) used in studies of IL-10 are derived from the large intestine. Yet in 30% of Crohn's disease cases inflammation is confined to the small intestine (Cheifetz, 2013). Clearly, the small intestine is not spared from IBD, and in fact becomes inflamed in a number of other conditions. Thus, IEC biology in the small intestine is important to study.

1.11. Small intestinal organoids as a model of IEC biology

Before the breakthrough of organoid technology, most health or disease studies of IEC biology utilized common research models such as whole animals

and transformed cell lines. The limitations of these models include the lack of capacity to differentiate the cells into the major phenotypes and therefore the inability to study the interplay between specialized cell types (Noben et al., 2017). Organoid technologies have opened a door to explore the biology of intestinal epithelia.

Organoids are 3-dimensional constructs that develop from stem cells of the original tissue and contain all mature cell types of the derived-tissue. In the case of the gut epithelium, the spatial organization of cells in organoids closely resembles that of the native epithelium, preserving the native crypt-villi axis and cell polarity (Almeqdadi et al., 2019). Importantly, IEC within organoids conduct functions found in the native epithelium, such as secretion, absorption, endocrine activity, and motility (George et al., 2019). Handily, possessing stem cells, organoids are self-renewing and can be readily cryopreserved, allowing researchers to manipulate the genetic and environmental factors in the organoid culture easily (Sato et al., 2011). Additionally, because ISC are the only proliferative units in organoid culture, the passages of organoid culture is presumably free of other non-epithelial cell types, which allow the researchers to confidently attribute observed function to IEC. Therefore, when it comes to IEC biology, *ex vivo* organoid model provides the combination of advantages from both *in vitro* and *in vivo* models.

Figure 2. Enteroids resemble spatial and temporal dynamics in native intestinal epithelium.

Enteroids contain all specialized cell types found in native epithelium. Red arrows describe the direction of cell migration starting from the crypt base to the villus (Gerbe et al., 2011; Sato et al., 2009)(Created with BioRender.com).

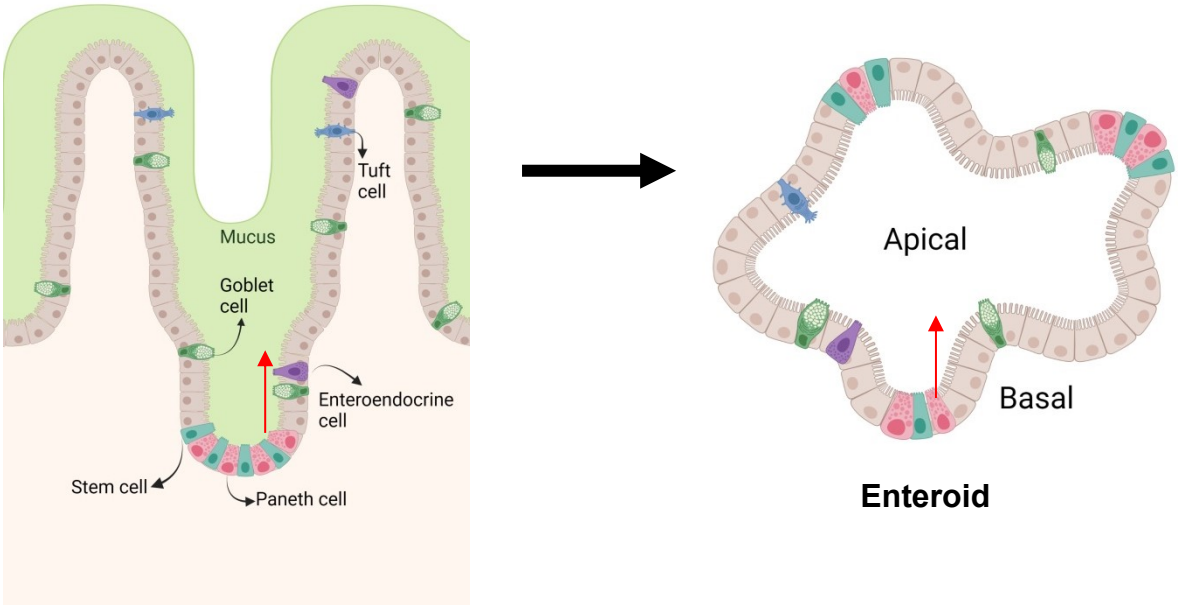

1.12. Research Objectives

Although there is evidence for IL-10 production by IEC, the specific cell type of the epithelium that produces IL-10 is not confidently confirmed, nor has the target of epithelial-sourced IL-10 been identified. Using freshly isolated IEC, studies can provide point-in-time evidence that the epithelium is a source of IL-10 but until highly specific cell sorting is conducted, there is a risk that non-epithelial cells contaminating the preparations confound the results. Consequently, the detection of IL-10 and IL-10 activities on IEC has been conducted mainly using transformed carcinoma cells, which likely do not correctly represent non-transformed cells. Therefore, in this study, enteroids were used to address 3 major questions:

1) What is the cellular source of IL-10 and which cell type(s) possess the IL-10 receptor in the intestinal epithelium?

2) What is the function of epithelial-derived IL-10 in the intestinal epithelium including during challenge with IFN-γ?

3) What is the polarity of epithelial IL-10 secretion and IL-10 receptors on the intestinal epithelium?

CHAPTER 2: MATERIALS AND METHODS

2.1. Animals

C57BL/6 (Wildtype, WT) and B6.129P2-Il10^{tm1Cgn}/J (IL-10 knockout, IL-10KO) mice were initially purchased from The Jackson Laboratory (Bar Harbor, ME), then bred in the IWK Health Centre facility. IL-10-GFP expressing congenic mice were available in a collaboration with Dr. Jun Wang (Dalhousie University) who had obtained the animals from Dr. Richard Flavell (Yale University). Mice that were sacrificed for crypt isolation were male, 6 to 14-weeks old. Animal use was approved by the University Committee on Laboratory Animals (most recently, 20-012). The WT and IL-10KO genotypes were confirmed using the polymerase chain reaction (PCR), the products of which were demonstrated on agarose gel electrophoresis (Figure 3).

Figure 3. Genotypes of WT and IL-10KO mice.

Mouse DNA was extracted from mouse ear pierce and amplified using the KAPA Mouse Genotyping Kit. Genotyping primers are described in The Jackson Laboratory protocol: common forward 5'CTTGCACTACCAAAGCCACA3'; WT reverse 5'GTTATTGTCTTCCCGGCTGT3'; KO reverse 5' CCACACGCGTCACCTTAATA3'. The amplicon from WT mice is 137 base pairs and the amplicon from KO mice is 312 base pairs. PCR products were separated by electrophoresis on a 2% agarose gel with 0.5 µg/mL ethidium bromide.

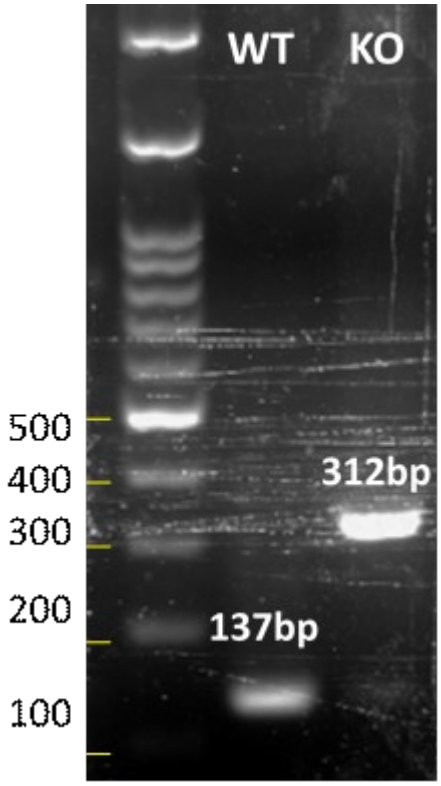

2.2. Crypt isolation and organoid culture

Enteroids were grown from crypts isolated from small intestine, respectively. WT mice were euthanized and small intestine including duodenum, jejunum and ileum was harvested and flushed with cold phosphate buffered saline (PBS). Small intestine was cut open longitudinally and cut into fragments of 3-4 cm. The apical side of each fragment was scraped to remove adherent solids, mucous and villi. The fragments were subsequently further dissected into pieces of 2-3 mm and washed with ice-cold PBS before being incubated in 30 ml of cold 1 mM EDTA in PBS for 30 minutes on ice, with shaking at 200 rpm. The pieces were transferred to 30 ml of pre-chilled 5 mM EDTA in PBS for 30 minutes on ice. The pieces were transferred to 25 ml DMEM/F12 (Gibco, Waltham, MA) and manually shaken vigorously to dissociate the crypts from the mucosa. The resulting suspension was strained through a 100 µm Falcon® cell strainer (Corning, Corning, NY, US) to separated large tissue fragments from dissociated crypts. The suspension was centrifuged at 130×g at 4°C for 4 minutes to separate crypts from cell debris. The supernatant was aspirated and the pellet was resuspended in 1 ml of complete DMEM/F12, then the centrifugation repeated. The final supernatant was aspirated to remove any cell debris left.

To seed 8 wells with approximately 100-200 crypts each, pellets were suspended with 300 µl ice-cold Cultrex® (Trevigen, Gaithersburg, MD) and 100 µl of ice-cold Intesticult™ (STEMCELL Technologies, Vancouver, BC). A droplet of 50 µl of the suspension was placed on each well of pre-warmed 24-well culture plate (Sarstedt, Newton, NC) to form matrix domes that embed the organoids.

Once the dome solidified, 500 µl of Intesticult™ – growth medium was added to each well to provide nutrition for the organoids. The medium was changed on days 3 and 5. All organoids were grown at 37°C in a humidified atmosphere with 5% carbon dioxide.

2.3. Organoid passaging

On day 7 of enteroid cultures, the cells were passaged at 1:5 ratio. Medium was aspirated out of the wells. To dissolve the Cultrex® matrix that embeds the organoids, 1 ml of ice-cold DMEM/F12 + 5% FBS (Gibco) was added to each well. The contents of each well, including the dome matrix, was repeatedly pipetted (20 times) using a P1000 pipette tip ice-cold DMEM/F12 to dissolve the matrix and dissociate the organoids. The content of each well was then pipetted 20 times using a P200 pipette tip to further break down the organoids into crypts. The contents of all the wells was combined into a 15 ml tube pre-coated with fetal bovine essence (VWR, Radnor, PA), and centrifuged at 300×g for 5 minutes at 4°C. The supernatant, containing cell debris, was discarded. The pellets were resuspended in 1 ml of ice-cold DMEM/F12 + 5% FBS before centrifugation, also at 300×g for 5 minutes at 4°C. After the supernatant was removed, the pellets were resuspended in ice-cold Intesitcult™ and Cultrex® at 2:1 ratio, and the suspension was placed in droplet of 50 µl into each well of pre-warmed 24-well culture plate. Intesticult™ was added to each well after the matrix had solidified.

2.4. Cytokine treatments of organoids

Unless indicated otherwise, for qPCR experiments enteroids had 5-days of treatment with 10 ng/ml murine recombinant IL-10 (Peprotech, Rocky Hill, NJ). Medium was renewed every two days. For overnight treatment (less than 24 hours) of organoids, IL-10 was used at 20 ng/ml, and recombinant murine IFN-γ (Peprotech) was applied at 10 ng/ml. For Western blot experiments, enteroids were treated for 20 minutes with 100 ng/ml of IL-10.

2.5. RNA isolation

Organoids were washed with ice-cold sterile PBS and pooled from all 2-3 wells of each biological replicate for each treatment and processed immediately for RNA following instructions from the ReliaPrep™ RNA Tissue Miniprep System (Promega, Madison, WI) RNA samples were stored at -80℃.

2.6. Reverse transcription and quantitative PCR

RNA quality and quantity was determined using NanoDrop™ One Microvolume UV-Vis Spectrophotometer (Thermo Scientific, Waltham, MA). Depending on the RNA yield, 0.1-1µg of RNA was used for cDNA synthesis following the manufacturer's instructions for the High-Capacity cDNA Reverse Transcription Kit (Applied Biosystems, Waltham, MA). For RT-qPCR, the cDNA was amplified for target genes using the PowerUp SYBR Green Master Mix (Applied Biosystems) following the manufacturer's instructions. The reactions (20 µl final volume) were run on a CFX96 Dx Real-Time PCR Detection System (Bio-Rad, Hercules, CA). The reaction temperature started with Uracil-DNA glycosylases (UDG) activation set for 1 time at 50°C for 2 minutes, followed by

Dual-Lock Taq DNA polymerase activation at 95°C for 2 minutes. Subsequently, for 40 cycles, the cDNA was denatured at 95°C for 15 second, followed by an annealing step at 58°C for 30 seconds. Additional reverse-transcription controls were run for the first replicate and non-template controls were run for all replicates. Primers were designed by Primer Blast to span an exon-exon junction, with Tm ranging from 59^{o}C to 62^{o}C, and contain 40-60% GC content. The signal for genes of interest were normalized using TATA-box-protein (TBP) gene, suggested to be the most stable reference gene for murine intestinal epithelial cells (Wang et al., 2010).

To amplify IL-10, the primer pairs were designed such that the forward primer was within exon 1 and the reverse primer spanned the exon 1-exon 2 junction. As codon 5 – 55 on exon 1 are replaced by a 500bp linker in the IL-10KO (Figure 4A), the primer pair ensures specific amplification of the IL-10 transcript in WT but not KO (Figure 5B). Representative RT-qPCR melt peaks showed a single peak for each gene of interest, indicating the presence of only a single amplicon and therefore high specificity (Figure 4B).

Figure 4. RT-qPCR primer design and melt curve

A) The IL-10 transcript in WT is encoded in 5 exons. Compared to WT IL-10 transcript, in IL-10KO, codons 5-55 of exon 1 of IL-10 transcript was replaced with a 500 bp linker containing a stop codon followed by a neomycin-resistance cassette. Additionally, another stop codon was inserted into exon 3. Red arrows mark the position and direction of primer sequences, as well as the corresponding amplicon. **B)** Representative RT-qPCR melt peaks of the IL-10 amplicon from WT and IL-10KO enteroids, and the IL-10RA amplicon from WT enteroids.

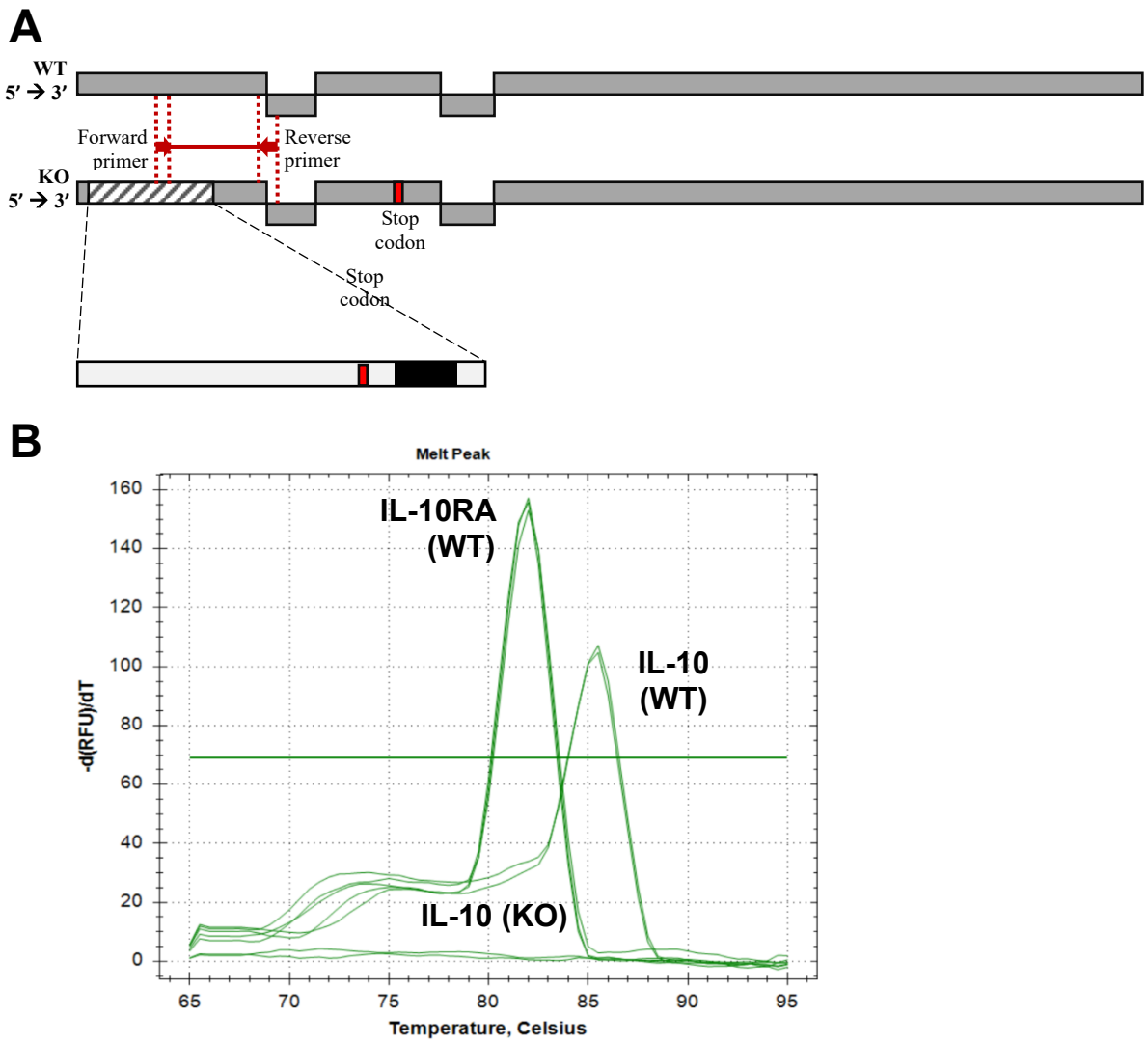

Table 1. Mouse primers used in this study

TARGET GENES	DIRECTION	PRIMER SEQUENCE (5′ → 3′)	PRODUCT SIZE
LYZ1	Forward	GGTCTACAATCGTTGTGAGTTGGC	95bp
LYZ1	Reserve	TGAGCTAAACACACCCAGTCAGC	
MUC2	Forward	TCTGGAGGACGCCGGATCTA	102bp
MUC2	Reserve	TCTCAAAGCTGCGGTTCCCA	
TBP	Forward	AGCTCTGGAATTGTACCGCAGC	134bp
TBP	Reserve	ATGATGACTGCAGCAAATCGCTTG	
IL-10	Forward	TGGCATGAGGATCAGCAGGG	144bp
IL-10	Reserve	TCCAGCTGGTCCTTTGTTTGAAAG	
IL-10RA	Forward	GTGGCCCTCAAACAGTACGGA	134bp
IL-10RA	Reserve	ACTCTGGCCCGGTAGCCATA	
DEFA 5	Forward	AGGCCAAGAAGGGTCTGCTC	107bp
DEFA 5	Reserve	TTCTGCAGGTCCCAAAAACGC	
NOTCH1	Forward	CTGCGCAAGCACCCAATCAA	127bp
NOTCH1	Reserve	GGTAGACAATGGAGCCACGGA	
HES1	Forward	CAAACCAAAGACGGCCTCTGA	143bp
HES1	Reserve	TGGAATGCCGGGAGCTATCTTT	
ATOH1	Forward	CAGCTGCGCAACGTTATCCC	104bp
ATOH1	Reserve	AGCAACTCCGACAGAGCGTT	

2.7. Electrophoresis

The amplicons from PCR were resolved by electrophoresis through 1.5% agarose/Tris-acetate-EDTA (TAE) gels containing 0.5 µg/ml ethidium bromide for visualization. Loaded content included 4 parts PCR reaction and 1 part Novel juice DNA stain (Sigma). DNA ladder (FroggaBio, Concord, ON) was 1:2 diluted with dH2O. Samples and the DNA ladder were electrophoresed for 40 minutes at 130 V. Following electrophoresis, the products were imaged using a ChemiDoc™ Touch Imaging System (Bio-Rad).

2.8. Immunofluorescence

Between 20-30 µl of Cultrex® containing enteroids was added into each well of a Millicell EZ SLIDE 8-well glass chamber (Millipore Sigma, Burlington, MA). The Cultrex® droplet was incubated for 20 minutes then 300 µl of Intesticult™ was added to each well. Enteroids in the chamber were grown untill day 4. When ready for immunofluorescence, the medium was replaced with ice cold PBS, followed by 300 µl 4% paraformaldehyde in 1X PME buffer (10x PME buffer: 500 mM PIPES, 25 mM $MgCl_2$, 50 mM EDTA). Enteroids were incubated in this fixing solution 20 minutes on a shaking platform. The fixing solution was removed and 300 µl of ice-cold permeabilization solution (PBS containing 0.5% Triton X-100) was added and the enteroids incubated on ice on a shaking platform for 20 minutes. The chamber was washed once with PBS containing 0.2% Triton X-100 & 0.05 % Tween. To quench autofluorescence, the enteroids were incubated in 100 mM glycine in PBS or Image-iT™ FX Signal Enhancer (Thermo Fisher, Waltham, MA) for 30 minutes at room temperature.

Subsequently, enteroids were treated with 300 µl of blocking buffer (wash buffer containing 1% BSA), for 30 minutes, at room temperature, shaking. Primary antibodies were diluted in 150 µl of antibody signal enhancer (Recipe:10 mM glycine, 0.05 % Tween20, 0.1 % Triton X-100 and 0.1 % hydrogen peroxide in PBS (Rosas-Arellano et al., 2016)). The dilution ratio was 1:50 for anti-IL-10 (Thermo Fisher), 1:200 for anti-lysozyme (Bioss, Woburn, MA) and anti-mucin-2 (Thermo Fisher). The enteroids were incubated with the primary antibody overnight at 4^{o}C, then the chamber was washed 3 times with wash buffer before adding secondary antibodies. Secondary antibodies were diluted in blocking buffer at ratio 1:400. A list of antibodies used is presented in Table 2. The organoids were incubated with secondary antibodies for 2 hours at room temperature. All organoids were counterstained with DAPI in blocking buffer (1 µg/ml) for 5 minutes. The organoids were washed 3 times with wash buffer before the chamber was detached from the slide. A coverslip was applied using Antifade Gold mounting medium (Thermo Fisher). All slides were imaged using either EVOS FL Imaging System (Thermo Fisher) or a confocal microscope (LSM 710, Carl Zeiss).

Table 2. Antibodies used for immunofluorescence

Antibody order	Target	host/target species	Conjugation	Clonality/ Isotype	Catalogue#	Source
Primary	Lysozyme (Paneth cell)	rabbit anti-mouse	AF555	Polyclonal IgG	BS-0816R-A555	Bioss USA
Primary	IL-10RA	rabbit anti-mouse	AF488	Polyclonal IgG	BS-2459R-A488	Bioss USA
Primary	IL-10	rat anti-mouse	N/A	Monoclonal IgG2b, kappa	14-7101-85	Invitrogen
Primary	DCAMKL1 (tuft cell)	rabbit anti-mouse	AF647	Polyclonal IgG	ab202755	Abcam
Primary	Mucin-2 (goblet cell)	rabbit anti-mouse	N/A	Polyclonal IgG	PA5-79702	Invitrogen
Secondary	Rabbit antibody	goat anti-rabbit	AF488	IgG	A11008	Invitrogen
Secondary	Rat antibody	goat anti-rat	AF555	IgG	A21434	Invitrogen
Secondary	Rat antibody	chicken anti-rat	AF647	IgG	A21472	Invitrogen
Secondary	Rabbit antibody	goat anti-rabbit	AF647	Fab2'	4414S	Cell Signaling
Secondary	Isotype control	rabbit	AF488	IgG	NBP2-24982	Novus Biologicals

2.9. FITC dextran permeability assay

The organoid culture medium was removed, and the wells were washed 3 times with room temperature PBS, each time for 5 minutes. A solution of 1 μM FITC-dextran (3 kDa, Thermo Fisher) in PBS was added to the wells and incubated on a gently shaking platform for 30 minutes at room temperature. After this incubation, the FITC-dextran was removed and the organoids were washed 5 times with PBS on a gently shaking platform, each time for 5 minutes, to remove free FITC. The organoid image was captured by an EVOS FL Imaging System (Thermo Fisher). Images were taken from multiple representative organoids from different wells. Fluorescence levels within the organoid lumen and its background fluorescence was measured by ImageJ 1.53e (National

Institutes of Health, Bethesda, MD, USA). The corrected total fluorescence (CTF) was calculated as follows:

CTF = Integrated Density – (Area of selected cell X Mean autofluorescence readings)

2.10. Monolayer enteroid culture

Transwell® inserts (6 mm, 0.4 µm pore size, Corning, Darmstadt, Germany) were used to establish 2D organoid monolayers. The insert was coated with 40 µl of diluted (1 part 7.48 mg/ml collagen type I (Millipore): 1 part 0.2% acetic acid: 1 parts 70% ethanol) and air-dried overnight at room temperature in a biological safety cabinet.

Day-7 enteroids were treated with TrypLE Express (Gibco) for 5 minutes at 37°C to achieve a suspension of fine crypt fragments, which was seeded in Cultrex® following the procedure for typical organoid passage but excluding the 1:5 dilution step, in order to achieve a dense- and stem cell-enriched spheroid culture. To make a single 2D monolayer, 3 wells of dense spheroids were used. At day 3, spheroids were incubated in TrypLE Express at 37°C for 5 minutes and passed through an 18-gauge syringe needle to be further dissociated into a cell suspension. The suspension was centrifuged at 130xg for 5 minutes. The supernatant was removed, and the cell pellets were resuspended in 100 µl of Intesticult™, which was added to the collagen-coated insert. Simultaneously, 500 µl of Intesticult™ was added to the bottom well. After overnight incubation, medium from the insert was replaced with 200 µl fresh Intesticult™ to clean up unattached cells. Medium was changed every 2 days.

2.11. Protein extraction

For phosphorylated targets, organoids were pre-treated with 30 μM phenylarsine oxide, a cell-permeant phosphatase inhibitor, for 15 minutes before treatment with cytokines of interest. To harvest organoids, the Cultrex® matrix was dissociated by vigorous pipetting in ice-cold Cell Recovery Solution (VWR) and left shaking in this solution for 20 minutes at 4°C. The released enteroids were then centrifuged at 200xg for 4 minutes into a pellet and the pellet washed with ice-cold PBS, then centrifuged at the same settings. The pellet of enteroids was lysed in 150 μl RIPA buffer (50 mM Tris HCl - pH 7.4, 150 mM NaCl, 1% Triton X-100, 0.5% sodium deoxycholate, 0.1% SDS, 1 mM EDTA, 10 mM sodium fluoride, 1X freshly added Halt™ protease inhibitor cocktail (Thermo Fisher), and freshly added phosphatase inhibitor cocktail (5 mM sodium orthovanadate, 10 mM sodium pyrophosphate decahydrate and 10 mM β-glycerophosphate)) for 30 minutes, shaking at 4°C. The preparation was centrifuged for 10 minutes at 13000xg. The supernatant containing proteins was recovered and diluted with 4X SDS-PAGE loading buffer (25% glycerol, 12% SDS, 20 % β-mercaptoethanol, 0.04% bromophenol blue in 150 mM Tris), which was subsequently boiled at 90°C for 5 minutes.

To extract protein from organoid monolayers, Transwell® insert membranes containing a monolayer of cells were detached from the inserts using a scalpel. The insert membranes were then directly incubated in 150 μl RIPA buffer for 30 minutes, shaking at 4°C. Subsequent steps of protein extraction are described above. The protein concentration of the lysates was determined using

the Qubit Protein Assay following the manufacturer's instructions (Thermo Scientific). Protein lysates were stored at -80^{o}C.

2.12. Western blot

Proteins were separated by 8% SDS-PAGE electrophoresis for 2 hours at 100V with Tris-Glycine running buffer (10X buffer contains 14% glycine, 3% Tris base and 1% SDS in dH_2O). In some experiments, proteins were separated on gradient TGX Stain-Free™ Mini-PROTEAN precast gels (Bio-Rad Laboratories) for 1 hour at 120V. Following electrophoresis, the proteins were transferred to a low fluorescence PVDF membrane using the Bio-Rad Turbo Transfer system (Bio-Rad Laboratories) for immunoblotting. In some experiments, to enhance the protein signal, the membrane was pretreated with SuperSignal™ Western Blot Enhancer (Thermo Fisher). Subsequent to this incubation, the membrane was blocked for 1 hour at room temperature in blocking buffer (TBS-T (20 mM Tris, 150 mM NaCl and 0.1% Tween® 20 detergent) + 3% BSA) before incubation with antibodies. All antibodies were diluted in blocking buffer. The membrane was incubated in the primary antibody solution overnight at 4^{o}C. Primary antibodies utilized for these analyses consisted of anti-pSTAT3 (TYR705 and SER727) (1:2000, Cell Signaling Technologies), and anti-STAT3 (1:2000, Cell Signaling Technologies). Following the incubation with primary antibodies, the membrane was washed 3 times, each time for 5 minutes, in TBS-T washing buffer (as are all subsequent washes). The membrane was then incubated with secondary HRP-linked goat anti-rabbit antibody for 1 hour at room temperature (1:10000, Cell Signaling Technologies). Subsequently, the membrane was washed 4 times,

each time for 10 minutes. The membrane was incubated with Clarity™ Western ECL Substrate (Bio-Rad Laboratories) or with SuperSignal™ West Atto Ultimate Sensitivity Chemiluminescent Substrate (Thermo Fisher) for low-abundance protein, before being imaged using Bio-Rad ChemiDoc™ Touch Imaging System.

2.13. *In silico* mining of publicly available RNA-sequencing datasets

Transcriptome data was obtained from NCBI's Gene Expression Omnibus. RNA-sequencing data from enteroids were obtained from GEO accession numbers GSE115955, GSE100274 and GSE92332. RNA-sequencing data from native murine epithelial cells were obtained from GEO accession numbers GSE92332 and GSE113536. Single-cell RNA-sequencing data exclusively from Paneth cells were obtained from GEO accession number GSE117216 and GSE76408. For each GEO dataset, raw counts matrix (under "Supplementary file" section) was downloaded and assessed for the number of reads and sequences aligning to each gene.

2.14. Statistical analysis tools

Unpaired two-tailed Student's t-test was used when comparing 2 groups. To compare more than 2 groups that involve 1 independent variable, one-way analysis of variance (ANOVA) was used, followed by Tukey's post hoc test. If 2 independent variables were involved, two-way ANOVA was used, followed by Sidak's post hoc test. Differences between groups were considered to be significant when P-value was less than 0.05. Statistical analyses and graphs were generated with GraphPad Prism 8 (GraphPad Software, San Diego, CA).

CHAPTER 3: RESULTS

3.1. Establishing and standardization of enteroid cultures

To obtain enteroid cultures, crypts were isolated from murine small intestine and embedded in extracellular matrix (Cultrex®), to facilitate the formation of 3D structures (Figure 5A). At this stage of culture, in addition to the isolated crypts, mucosal leukocytes, especially IELs can also be present in the newly-established culture. The purification of enteroids is necessary to ensure that the detected IL-10 signal is strictly limited to an IEC source. Notably, CD3 and CD45 transcripts were investigated in an effort to confirm the absence of leukocytes yet both were detected through RT-qPCR. It was later learned from the single-cell RNA-sequencing (scRNA-seq) data that these markers can be found in moderate to abundant amounts on IECs (Haber et al., 2017), making these markers unsuitable for confirming the absence of leukocytes in the enteroid culture. As alternate evidence for a lack of leukocytes, it has been reported that in the absence of IL-2, IL-7, and IL-15 supplements, IELs co-cultured with enteroids do not last until day 7 (Nozaki et al., 2016). Therefore, to ensure the purification of enteroids, experiments were only conducted from second-passage enteroids and onward.

It has been reported that sex hormones can affect the proliferation of IEC, which can be a potential confounder in IEC experiments (Lee et al., 2019). Additionally, age is another factor that affects the population and the distribution of different IEC types (Moorefield et al., 2017). Therefore, to minimize these

confounding effects, enteroids were grown from crypts isolated from 6- to 14-week-old male mice.

The seeding density is the number of viable crypts per matrix “dome” (Figure 5A). During the period that enteroids mature, it was noted that the seeding density can greatly affect the morphology, which can reflect the cell composition of the enteroids. For example, rounder enteroids contain more KI67-positive proliferative cells (Figure 5B). Specifically, in over-diluted cultures (< 50 enteroids/50 µl Cultrex®), organoid growth was delayed. On the contrary, dense cultures (> 200 enteroids/50 µl Cultrex®) resulted in restriction of organoid size and an increase in apoptosis, seen as black cells accumulating in the enteroid lumen (Figure 5C). Therefore, to optimize enteroid growth and ensure consistency between experiments, the density of enteroid culture was standardized to range from 100 to 150 organoids per 50 µl Cultrex® dome.

Figure 5. Optimization of enteroid culture through seeding density control. **A)** Freshly isolated crypts from murine small intestines were seeded and embedded in 50 µl of basement membrane extracellular matrix (Cultrex®) (Created with BioRender.com). **B)** Day 4 enteroids were stained for KI67 and images were captured with EVOS FL Imaging System. Measurements of the KI67-positive area (left) and whole enteroid area (right) were quantified with ImageJ. **C)** Enteroids were grown to full maturation and passaged after 7 days of culture. Enteroids from the same passage were dissociated into suspension and re-seeded in basement membrane extracellular matrix at different seeding densities. Seeding densities were determined as the number of crypts per 50 µl dome: Low density (< 50 crypts/dome), medium density (100-150 crypts/dome), and high density (>200 crypts/dome). The scale bars are 1000 µm, 400 µm and 200 µm for day 3, 5 and 7 images, respectively.

A

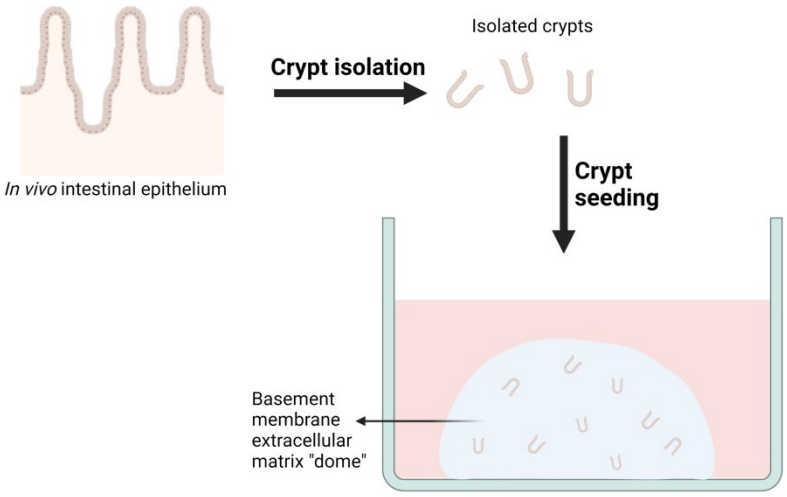
Isolated crypts
Crypt isolation
Crypt seeding
In vivo intestinal epithelium
Basement membrane extracellular matrix "dome"

B

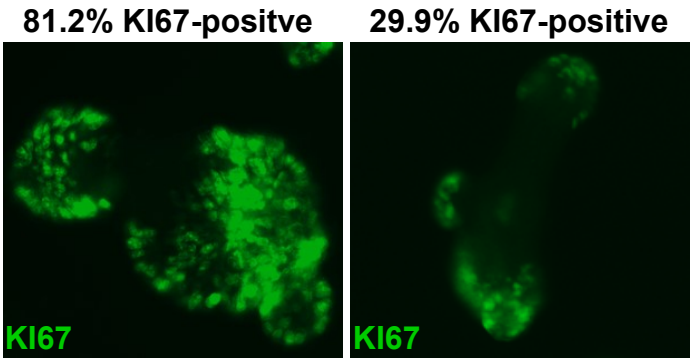
81.2% KI67-positve
29.9% KI67-positive
KI67
KI67

C

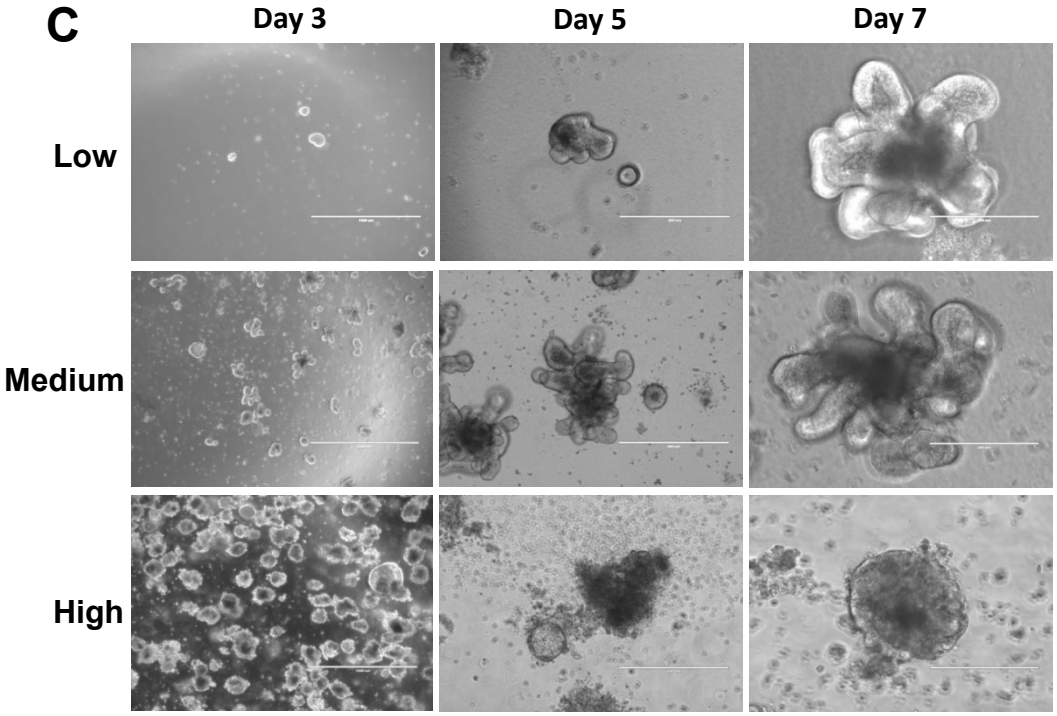
Day 3
Day 5
Day 7
Low
Medium
High

3.2. Constitutive expression of IL-10 & IL-10R in enteroids

In order to determine whether IL-10 production in enteroids is constitutive (intrinsic), IL-10 mRNA throughout developmental stages of organoids was investigated. Also, since autocrine activity of IL-10 is commonly observed, IL-10-producing cells usually also express IL-10 receptor. Therefore, the temporal dynamics of IL-10RA, the ligand-specific subunit of the IL-10 receptor, was also investigated.

Regarding constitutive expression, enteroids on days 2, 4 and 6 were harvested for mRNA. RT-qPCR experiment results demonstrated that constitutive expression of IL-10 and IL-10RA was detected throughout all the stages of enteroids. In the case of IL-10, day 4 enteroids possess the most IL-10 mRNA relative to the total mRNA recovered from the culture (Figure 6). As this experiment was conducted on whole enteroids, it remains unclear whether a change in IL-10 or IL-10RA mRNA was due to increased copies in a few cells or an increase in the numbers of IL-10 or IL-10RA producing cells.

Figure 6. Constitutive expression of IL-10 and IL-10RA in developing enteroids.

Enteroids were harvested on the indicated day and mRNA assessed for IL-10 and IL10RA. For each experiment, on each day, 2 wells of WT enteroids were pooled to collect total RNA. Levels of IL-10 and IL-10RA transcripts were determined by RT-qPCR and the result normalized to the TBP level for the same culture. Results are the mean ± standard deviation of 3 independent experiments (* $p < 0.05$, ** $p < 0.01$, one way ANOVA followed by Tukey's post hoc test)

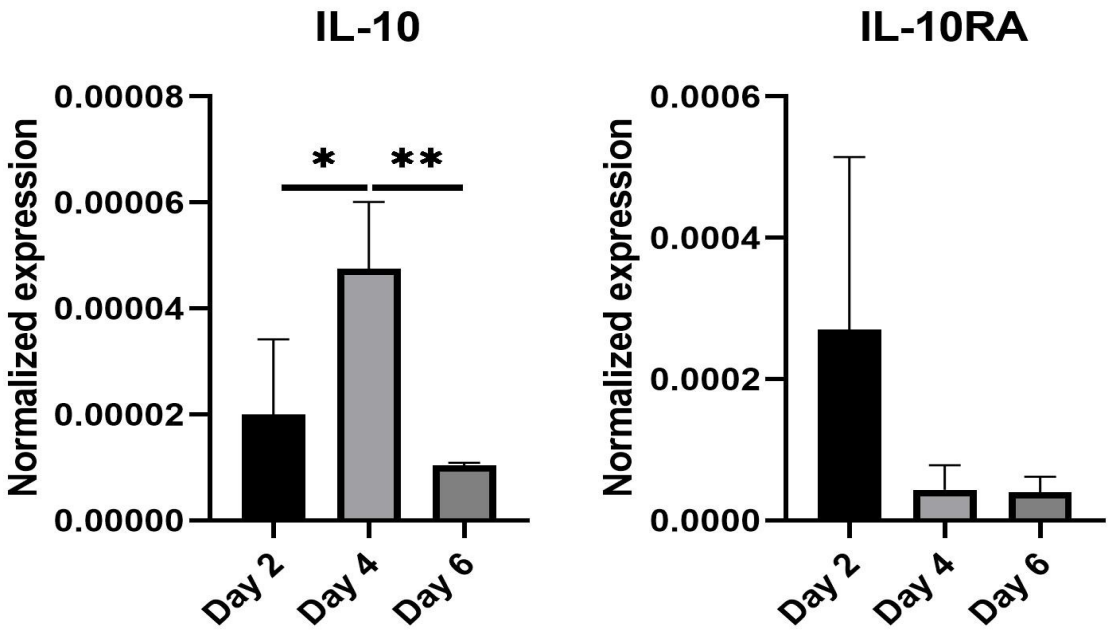

3.3. Apical expression of IL-10 in enteroids

Despite evidence from whole epithelial preparations that cells make IL-10, the specific cell type within the epithelium that produces IL-10 is still unclear. To address this knowledge gap, immunofluorescent detection of IL-10 was conducted on enteroids. Considering the previous RT-qPCR data showed the highest relative expression of IL-10 mRNA occurred on day 4 of the enteroid culture, all immunofluorescence staining was conducted 4 days after passage. Notably, enteroids within a single dome on any single day are morphologically heterogenous, indicating heterogeneity of enteroid developmental stages. For this experiment, two different mouse phenotypes were used: C57BL/6 (WT) and homozygous GFP-IL-10 reporter mice on the C57BL genetic background. Preliminary confocal microscopic observations of GFP-IL-10 enteroids did not show a GFP signal in enteroids; therefore, these enteroids were examined using anti-GFP-antibody as primary antibody.

In enteroids of both mouse genotypes, a product was observed in the crypts. From the pattern of staining within the cell, it can be believed that epithelial IL-10 is most likely secreted apically (Figure 7A). Two negative controls were used to confirm the specificity of the staining. One was to apply the anti-IL-10 to IL-10KO enteroids. The second negative control was staining of WT enteroids with conjugated secondary antibodies only. No signal was detected in these negative controls (Figure 7B).

Figure 7. Apical expression of IL-10 in WT and GFP-IL-10 reporter mouse enteroids.

A) Day 4 WT enteroids were stained with monoclonal rat anti-mouse IL-10 antibodies, which were subsequently detected using polyclonal chicken anti-rat conjugated to AlexaFluor647. For GFP detection, GFP-IL-10 reporter enteroids were treated with polyclonal rabbit anti-GFP antibody which were subsequently detected using polyclonal goat anti-rabbit antibodies conjugated to AlexaFluor488. **B)** Left panel: first negative control; IL-10KO enteroids were stained for IL-10 following similar steps as in A. Right panel: second negative control; WT enteroids were stained with secondary antibodies conjugated with AlexaFluor647. All enteroids were counterstained with DAPI to highlight the nuclei. All images were taken by confocal microscope (LSM 710, ZEISS)(Scale bar = 10 µm).

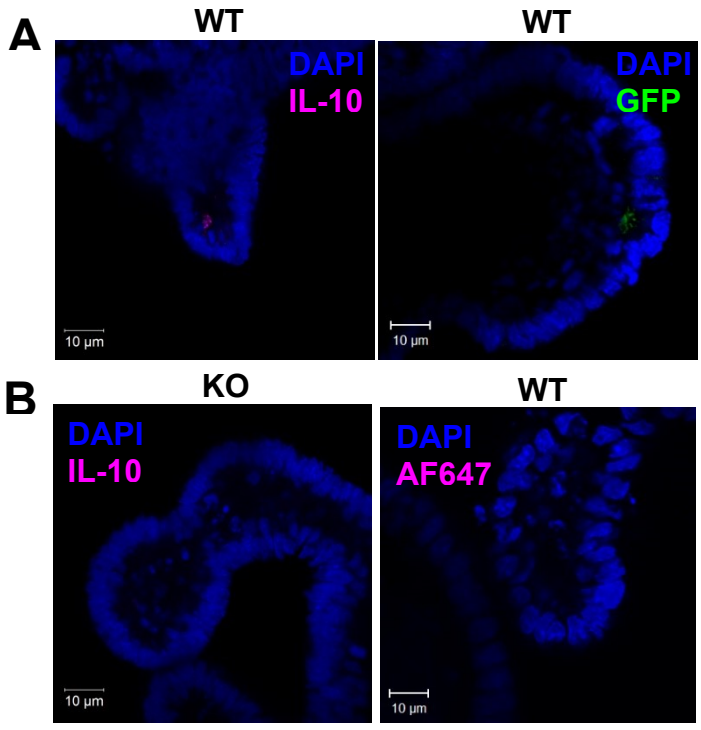

3.4. Apical & basal expression of IL-10R in enteroids

Given that apical expression of IL-10 was detected through immunofluorescence, it is reasonable to suspect that this cell source of IL-10 requires the simultaneous expression of IL-10R apically to exert an autocrine effect; however, the only published evidence of apical IL-10R expression was in T84 carcinoma cells following IFN-γ stimulation and in colonic biopsies of IBD patients (Kominsky et al., 2014). Epithelial IL-10 was detected in unstimulated enteroids; therefore, immunofluorescence staining for IL-10 receptor was also conducted in unstimulated enteroids. Anti-IL-10RA antibody was used to detect the IL-10 receptor. Interestingly, IL-10RA was observed on both apical and basal sides of the enteroid epithelium (Figure 8A). The IL-10RA signal is abundant on the basal side of the crypt base. IL-10RA was also observed on the apical side of cells in the crypt (Figure 8A). Since the IL-10RA signal was detected using directly labeled primary antibodies, an isotype-matched antibody (AlexaFluor488-conjugated rabbit IgG anti-mouse) was used as negative control. No signal was detected in the negative control, indicating that the staining for IL-10RA was specific (Figure 8B).

Figure 8. Detection and localization of IL-10RA on enteroids.

A) WT and IL-10KO enteroids were stained with polyclonal rabbit anti-mouse IL-10RA antibody conjugated with AlexaFluor488. **B)** Enteroids were stained with isotype control rabbit polyclonal IgG1, Alexafluor488 conjugated. All enteroids were counterstained with DAPI for nuclei. All images were taken by confocal microscope (LSM 710, ZEISS)(Scale bar = 10 μm).

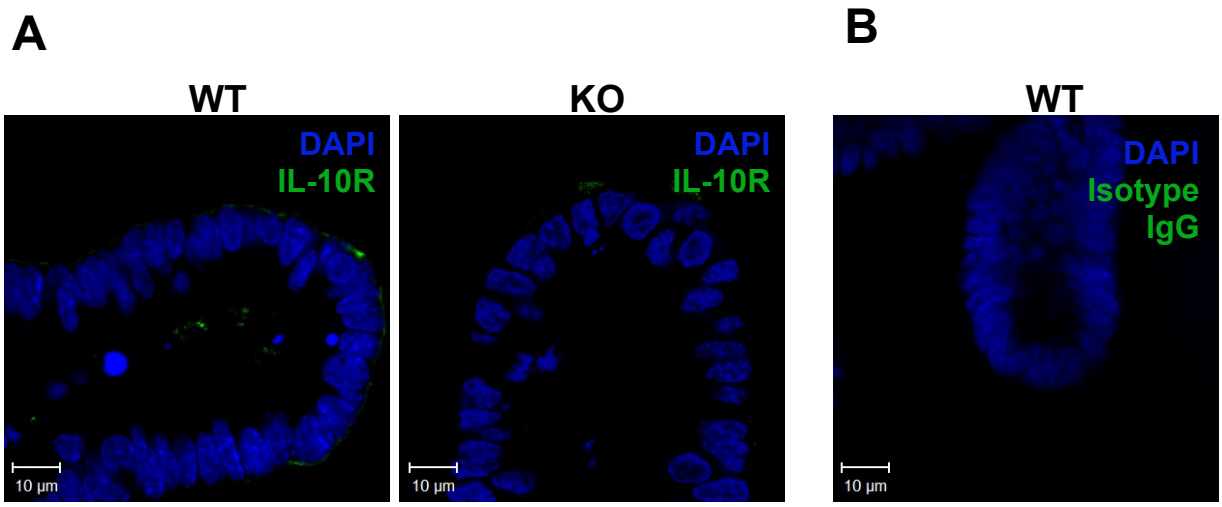

3.5. Cellular sources of IL-10

Since the preliminary immunofluorescent staining localized IL-10-positive cells to the crypt, the cell type that produces IL-10 can be narrowed down to 2 candidates: stem cells and Paneth cells. The cell marker for stem cells is Leucine-rich repeat-containing G-protein coupled receptor 5 (LGR5), a member of Wnt pathway (Kumar et al., 2014). One marker for Paneth cells is lysozyme (LYZ1), an antibacterial protein (Elphick & Mahida, 2005). Attempts to stain for LGR5 in WT enteroids were unsuccessful. However, in WT enteroids, it was observed that IL-10 and LYZ1 co-localized in the same cell (Figure 5). Similarly, co-staining for LYZ1 and GFP on IL-10-GFP reporter enteroids showed co-localization of these two markers (Figure 9A).

Hasnain et al. showed IL-10RA expression on goblet cells, and since IL-10 tends to act in an autocrine fashion, co-staining for IL-10 and mucin-2 was conducted (Hasnain et al., 2013). Additionally, a single cell transcriptome survey detected IL-10 within the population of tuft cells (Haber et al., 2017); therefore, tuft cells were also investigated for IL-10 production. As shown in Figure 9B and Figure 9C, IL-10 did not co-localize with either goblet cell or tuft cell marker (double cortin-like kinase 1, or DCLK1), indicating that either goblet nor tuft cells produce IL-10 under these conditions.

Figure 9. Paneth cells produce IL-10.

A) WT enteroids were co-stained for IL-10 and LYZ1. For IL-10 detection, WT enteroids were stained with monoclonal rat anti-mouse IL-10 antibody, which was subsequently detected using AlexaFluor 647 conjugated polyclonal chicken anti-rat anti-sera. For LYZ1 detection, enteroids were stained with AlexaFluor555-conjugated polyclonal rabbit anti-mouse LYZ1 antibodies. IL-10-GFP organoids were stained for GFP and LYZ1. For GFP detection, IL-10-GFP reporter enteroids were stained with polyclonal rabbit anti-GFP antibodies, which were subsequently detected with polyclonal goat anti-rabbit antibodies conjugated to – AlexaFluor647. **B)** WT enteroids were co-stained for IL-10 and MUC2. For IL-10 detection, WT enteroids were stained with monoclonal rat anti-mouse IL-10 antibody, which was subsequently detected with AlexaFluor 555 conjugated polyclonal goat anti-rat antibodies. For MUC-2 detection, WT enteroids were stained with polyclonal rabbit anti-mouse IL-10 antibodies, followed by AlexaFluor647 conjugated polyclonal goat anti-rabbit antibodies. **C)** WT enteroids were co-stained for IL-10 and DCLK1. For IL-10 detection, WT enteroids were stained as in A. For DCLK1 detection, WT enteroids were stained as in B). All enteroids were counterstained with DAPI for observing the nucleus. All images were taken by confocal microscope (LSM 710, ZEISS)(Scale bar = 10 μm).

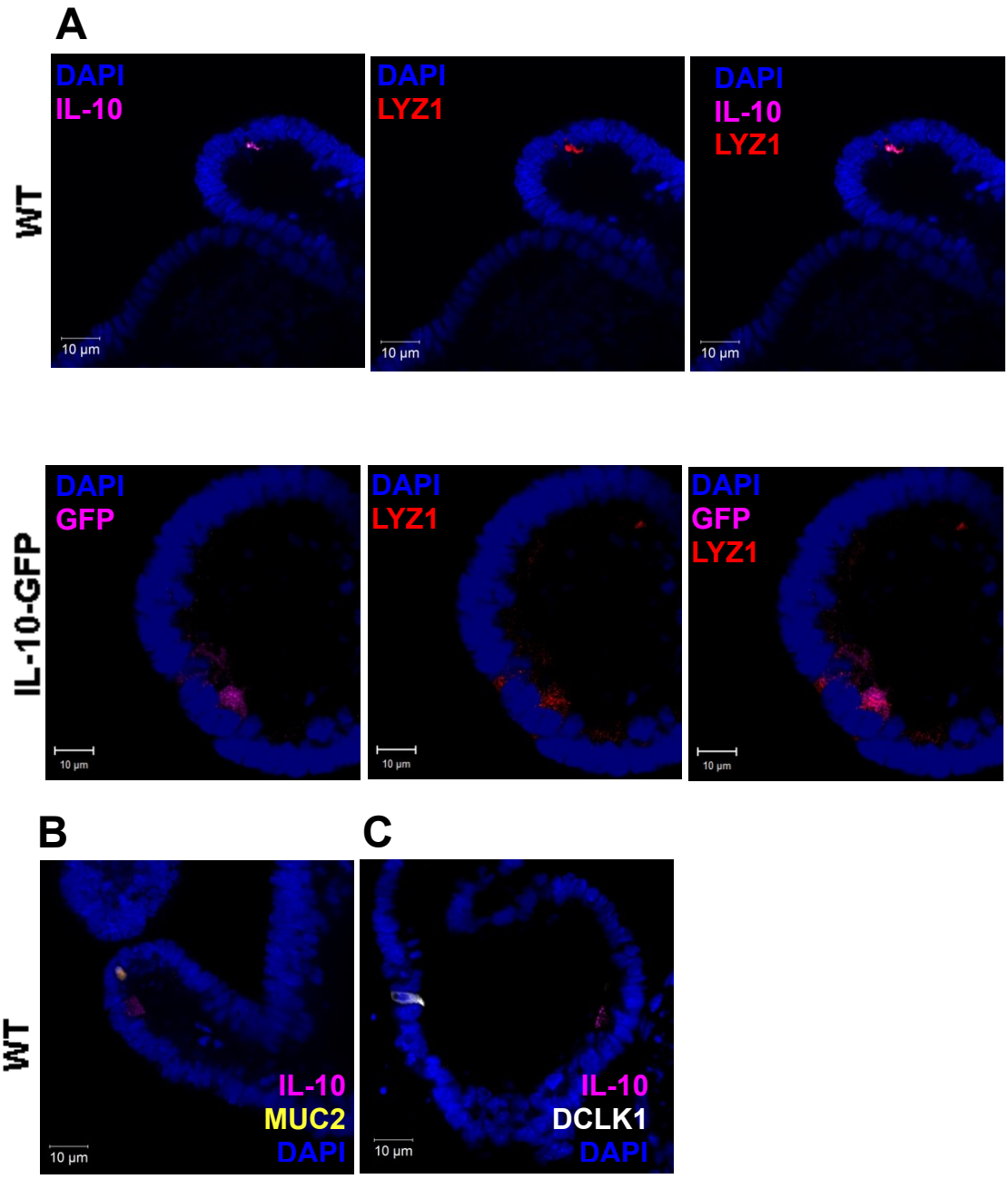
A
WT
DAPI
IL-10
DAPI
LYZ1
DAPI
IL-10
LYZ1
IL-10-GFP
DAPI
GFP
DAPI
LYZ1
DAPI
GFP
LYZ1
B
C
WT
IL-10
MUC2
DAPI
IL-10
DCLK1
DAPI
10 µm

3.6. Paneth cells and goblet cells express IL-10RA

Presently, there is no report of cell-type specific localization of IL-10RA in the small intestinal epithelium. The only study that localized IL-10 receptor was conducted on colon tissue (Hasnain et al., 2013). Here, the authors showed positive IL-10RA staining on goblet cells. Nevertheless, several studies have demonstrated an effect of IL-10 administration to IEC, including both goblet cells and Paneth cells, which implies that these cells must have functional IL-10 receptors (Deng et al., 2020; Hasnain et al., 2013). Therefore, immunofluorescence staining was conducted to investigate the potential expression of IL-10RA on these cell types. The results reveal that apical IL-10RA is exclusively expressed on LYZ1-positive Paneth cells (Figure 10A). Meanwhile, basal IL-10RA staining is found on both LYZ1-positive Paneth cell and MUC-2-positive goblet cell (Figure 10A,B). Additionally, IL-10RA staining does not co-stain with the tuft cell marker – DCLK1 (Figure 10C). Notably, the staining signal of basal IL-10RA can also be located at the crypt base area is cells that are not LYZ1 positive, suggesting stem cells also express basal IL-10 receptor. This speculation could not be confirmed due to the lack of confident stem cell staining.

Figure 10. Cellular sources of IL-10 receptor.

A) WT enteroids were co-stained for IL-10RA and LYZ1. For IL-10RA detection, WT enteroids were stained with conjugated polyclonal rabbit anti-mouse IL-10RA antibodies conjugated to AlexaFluor488. For LYZ1 detection, enteroids were stained with AlexaFluor555 conjugated polyclonal rabbit anti-mouse antibody. **B)** WT enteroids were co-stained for IL-10RA and MUC2. IL-10RA was stained as described from panel A. For MUC2 detection, WT enteroids were stained with polyclonal rabbit anti-mouse MUC2 antibodies, which were subsequently detected using AlexaFluor647-conjugated polyclonal goat anti-rabbit antibody. **C)** WT enteroids were co-stained for IL-10RA and DCLK1. IL-10RA was stained as described in panel A. For DCLK1 detection, WT enteroids were stained with AlexaFluor647-conjugated polyclonal rabbit anti-mouse DCLK1 antibody. All enteroids were counterstained with DAPI for visualizing the nuclei. All images were taken by confocal microscope (LSM 710, ZEISS)(Scale bar = 10 μm).

A

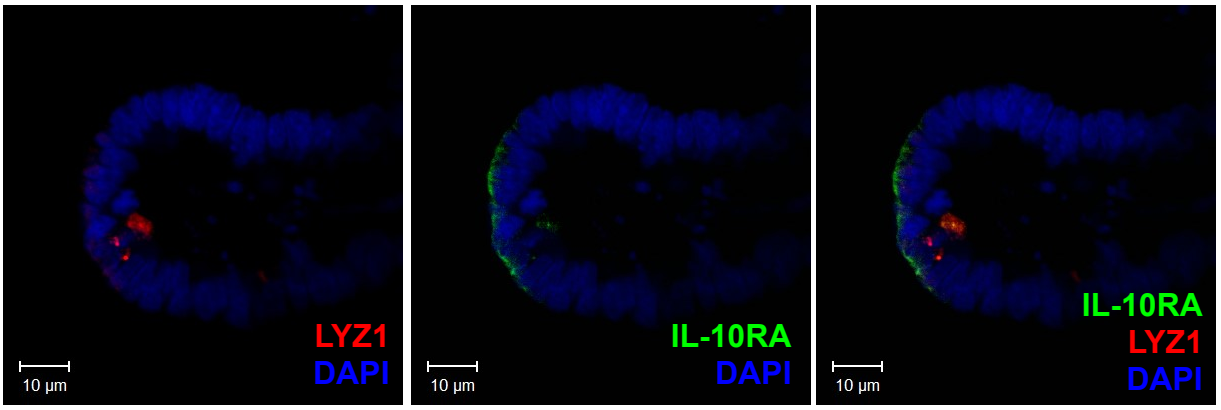
LYZ1
DAPI
10 µm
IL-10RA
DAPI
10 µm
IL-10RA
LYZ1
DAPI
10 µm

B

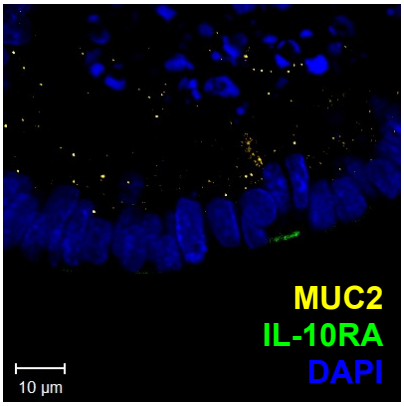
MUC2
IL-10RA
DAPI
10 µm

C

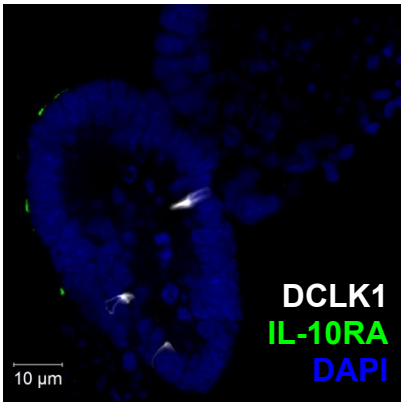
DCLK1
IL-10RA
DAPI
10 µm

3.7. Autocrine activity of epithelial IL-10

Most leukocytes are able to produce IL-10 depending on the context. Yet, IL-10 has short half-life and limited range of activity, which might explain the need for this cytokine to commonly act in autocrine and paracrine fashions (Saxena et al., 2015). It was shown in separate immunofluorescent staining experiments that IL-10 and IL-10RA are expressed on Paneth cells, implying potential autocrine activity of IL-10 on Paneth cells. In order to confirm this observation, WT enteroids were stained for IL-10 and IL-10RA simultaneously. Despite some cells being positive for the IL-10RA alone, the immunofluorescent data revealed that IL-10 and IL-10 receptor indeed co-localized in the same cell (Figure 11A). Furthermore, in addition to the detection of individual staining of IL-10 (magneta) and IL-10RA (green), there is also overlapping signal (gray) that speaks to the likelihood of IL-10 autocrine activity in IEC (Figure 11B).

Figure 11. Autocrine activity of epithelial IL-10 in Paneth cell.

WT enteroids were co-stained for IL-10 and IL-10RA. For IL-10RA detection, WT enteroids were stained with AlexaFluor488-conjugated polyclonal rabbit anti-mouse IL-10RA antibody. For IL-10 detection, WT enteroids were stained with monoclonal rat anti-mouse IL-10 antibody, which were subsequently detected using AlexaFluor647-conjugated polyclonal chicken anti-rat antibody. Enteroids were counterstained with DAPI. Images were taken by confocal microscope (LSM 710, ZEISS)(Scale bar = 10 μm). **B)** The area of simultaneous detection of IL-10 and IL-10RA is enlarged for better visualization of staining colors.

A

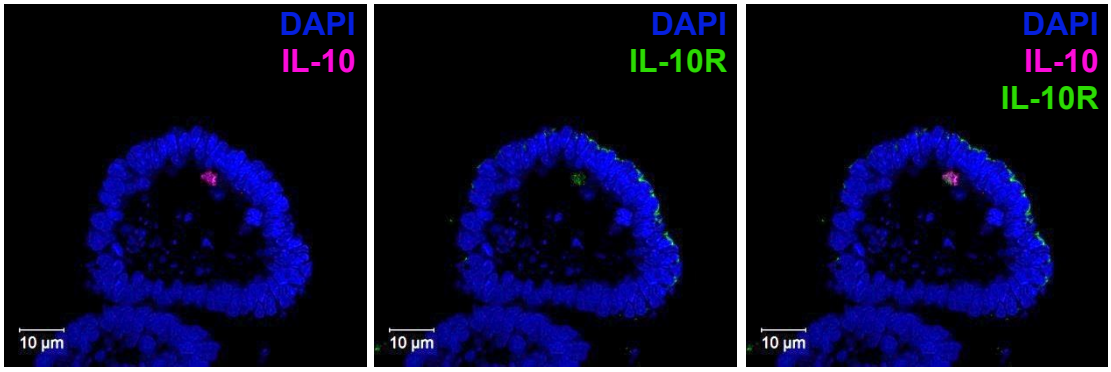

B

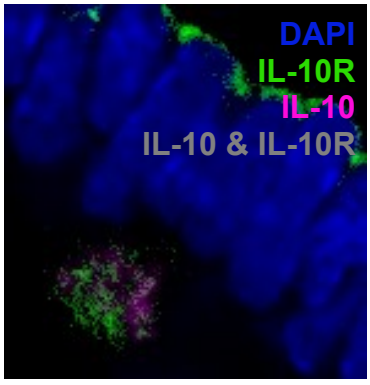

3.8. IL-10KO enteroids have deficiencies in Paneth cell markers

As it was determined that enteroids, at steady-state, produce IL-10, it was hypothesized that there is a functional role of IL-10, in this case epithelial cell-derived, in homeostasis of the epithelium. To address this hypothesis, IL-10KO genotypes were used. Importantly, enteroids from KO mice developed and could be passaged, similar to WT. Additionally IL-10KO enteroids undergo similar morphological changes corresponding to developmental stages similar to WT enteroids (Figure 12A). Characterization of the 2 genotypes at the level of gross morphological observation suggests that epithelial IL-10 has no discernable impact on the development of intestinal epithelium.

Considering the lack of differences in terms of enteroid morphology or permeability, I next examined cell phenotypes in the two genotypes. It was reported in several studies that IL-10KO mice have aberrant Paneth cells and goblet cells (Berkowitz et al., 2019); if this is directly due to the lack of IL-10, then it should be observable in IL-10 KO enteroids. Thus, levels of transcripts of cell-specific markers were assayed. The targets included LYZ1, DEFA5 and MUC2. RT-qPCR data demonstrated that transcripts of LYZ1 and DEFA5 were significantly lower in IL-10KO enteroids on day 5. However, these two targets in IL-10KO caught up with levels in WT enteroids on day 7 (Figure 12B). With regards to MUC2, no significant difference was detected in transcript levels (Figure 12B). These data suggested that epithelial-derived IL-10 might play a role early in Paneth cell development.

Figure 12. IL-10KO has deficiencies in Paneth cell markers.

A) Small intestinal crypts of WT and IL-10KO mice were isolated from tissues and seeded in basement membrane matrix. Enteroids were grown to full maturation and passaged after 7 days. Pictures of enteroids were taken on day 7 after passage. **B)** Days 5 and 7 enteroids were collected for total RNA. Following cDNA synthesis, levels of tata-binding protein (TBP, the reference gene), LYZ1, DEFA5 and MUC2 were measured by qPCR. Results are displayed as mean ± standard deviation (n = 6-9) (* $p < 0.05$, ns – not significant, one way ANOVA followed by Tukey's post hoc test).

A

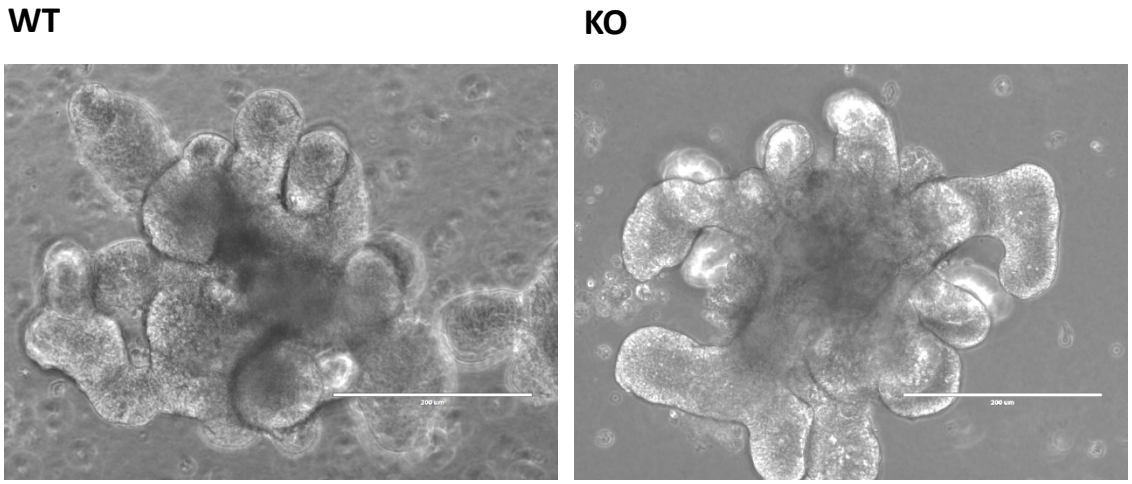
WT
KO

B

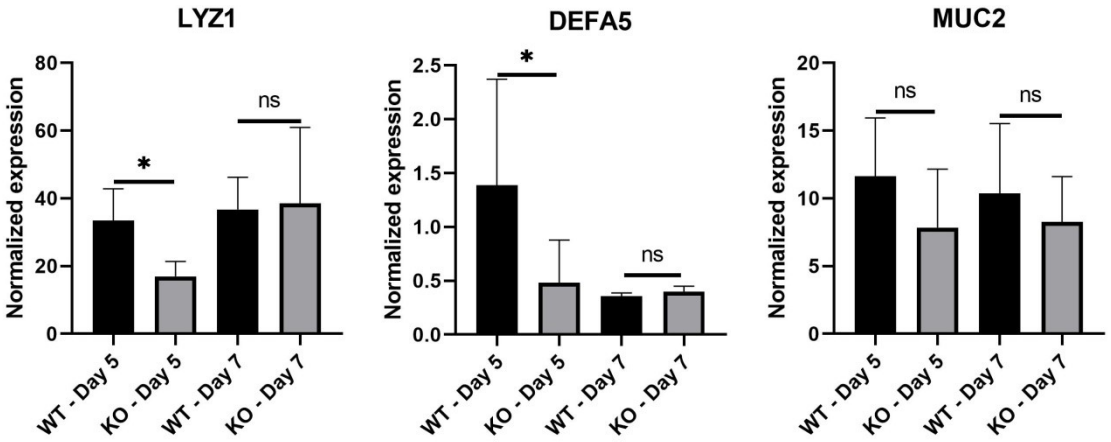
LYZ1
DEFA5
MUC2
Normalized expression
80
60
40
20
0
2.5
2.0
1.5
1.0
0.5
0.0
15
10
5
*
ns
WT - Day 5
KO - Day 5
WT - Day 7
KO - Day 7

3.9. WT and IL-10KO enteroids are equally permeable

Some studies reported that the IL-10KO mouse gut epithelium has increased permeability compared to the WT (Shi et al., 2014); however, it is unclear whether this phenotypic difference is the direct result of intrinsic factors within the IEC or the indirect result of heightened immune responses in the absence of IL-10. Using enteroids should overcome the indirect effects that are difficult to control in whole animal experiments. For this experiment, enteroids of WT and KO genotypes were grown at the same density and pulse-treated with 1μM FITC-dextran 4kDa for 30 minutes, on day 4 after passage (Figure 13A). Images of treated enteroids were taken and processed by ImageJ to quantify the fluorescent intensity. The corrected total fluorescence represents the total FITC-dextran accumulated in the enteroid lumen (Figure 13B).

The data demonstrated insignificant difference in FITC-dextran flux across the epithelium of WT and IL-10KO enteroids, which suggests no phenotypic difference in terms of barrier permeability between these two genotypes. However, it is noteworthy that there are a few confounders in the experimental design. Due to heterogeneity, even enteroids within the same Cultrex® dome showed great variation in lumen fluorescent intensity. For example, enteroids with spherical morphology, also called spheroids, were less permeable than budded enteroids (Figure 13C). Apoptotic cells within the lumen being autofluorescent can also be a confounder of the fluorescent intensity from FITC-dextran.

Figure 13. Characterization of WT and IL-10KO through permeability assay. **A)** Day 4 enteroids of both WT and IL-10KO genotypes were treated with 1 μM FITC-Dextran 4 kDa for 30 minutes and subsequently washed 3 times with PBS before observing the fluorescence. Images were taken with EVOS FL Imaging system. **B)** The fluorescent signal of the background and the lumen were quantified with ImageJ and used to calculate the corrected total cell fluorescence which is displayed as mean ± standard deviation from 4 independent experiments (n = 4, unpaired Student's t test). Each independent experiment includes the mean signal of 4 enteroids. **C)** IL-10KO enteroids from the same basement membrane extracellular "dome" were similarly treated with FITC-Dextran as described in panel A. Representative enteroids of the same culture have different morphologies, which manifest as drastic differences in FITC-dextran permeability (Scale bars = 200 μm).

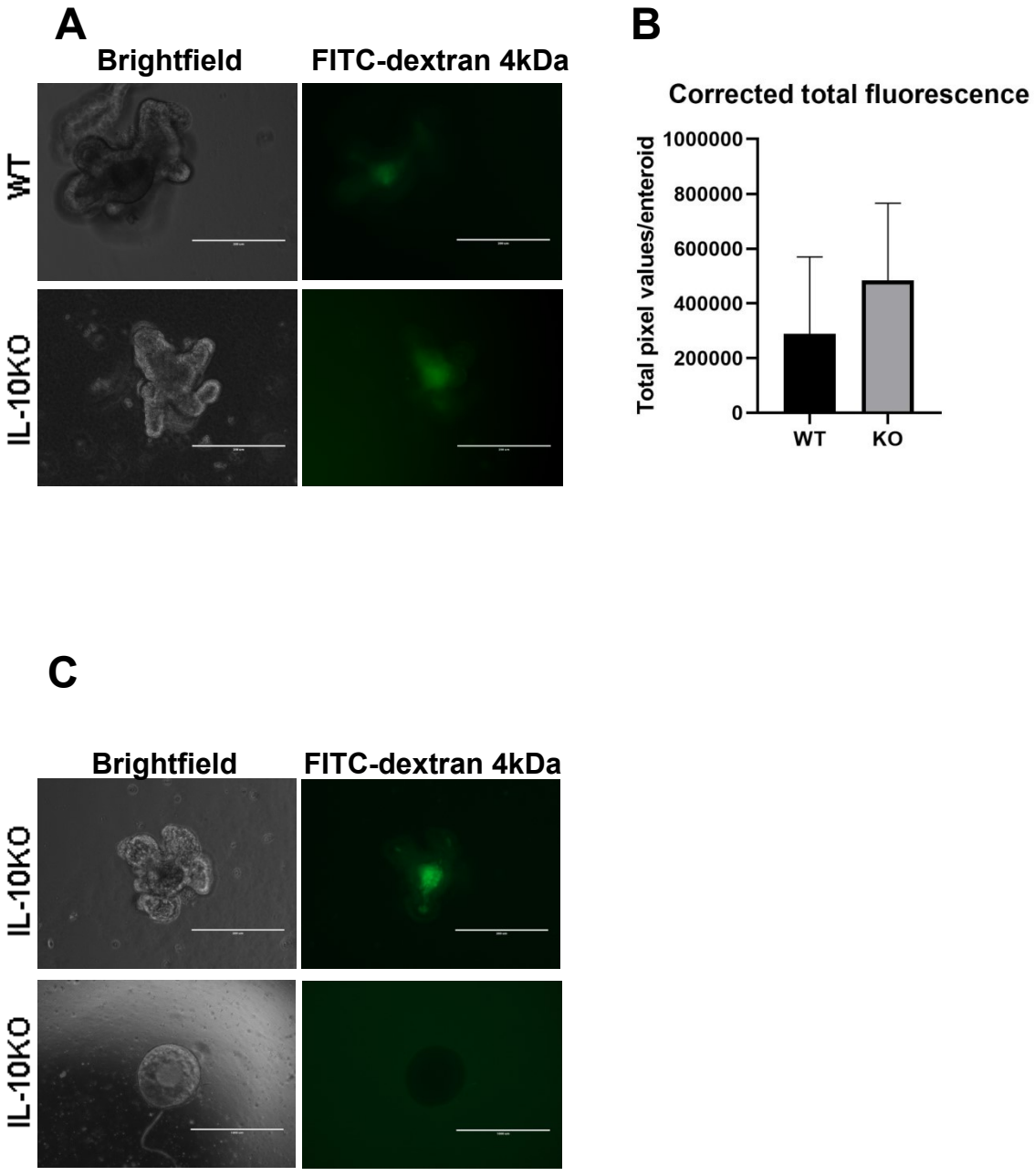
A
Brightfield
FITC-dextran 4kDa
WT
IL-10KO
B
Corrected total fluorescence
Total pixel values/enteroid
1000000
800000
600000
400000
200000
0
WT
KO
C
Brightfield
FITC-dextran 4kDa
IL-10KO
IL-10KO

3.10. WT and IL-10KO enteroids express the same level of cellular lineages

Considering that the Paneth cells of IL-10KO enteroids lag behind WT developmentally, one possibility is that IL-10 act at the early lineage-determination stage. To address this possibility, cell lineage markers including NOTCH1, HES1, and ATOH1 were investigated using RT-qPCR, as mRNA levels of mentioned genes were shown to represent protein levels (Tamagawa et al., 2012). NOTCH1 and HES1 are markers for the absorptive lineage (i.e., enterocytes); and ATOH1 is a marker for the secretory lineage (Paneth cells, goblet cells, enteroendocrine cells and tuft cells). The enteroids of WT and IL-10KO mice were collected for mRNA as early as day 3 after passage. The RT-qPCR data indicated that there was no significant difference in mRNA levels of these lineage markers between the two genotypes (Figure 14A). Interpreting this outcome suggests the deficiency in LYZ1 and DEFA5 is the result of IL-10 affecting an event downstream of lineage determination (Figure 14B).

Figure 14. Cellular lineage markers in WT and IL-10KO enteroids.

A) The key regulators that determine cell fate and differentiation of mature cell types in the epithelium (Created by BioRender.com). **B)** Day 3 enteroids were collected for total RNA. mRNA levels for TATA-binding protein (TBP, reference gene), ATOH1, HES, NOTCH1 by RT-qPCR (n = 3). Results show the mean ± standard deviation (ns – not significant, unpaired two-tailed Student's t-test).

A

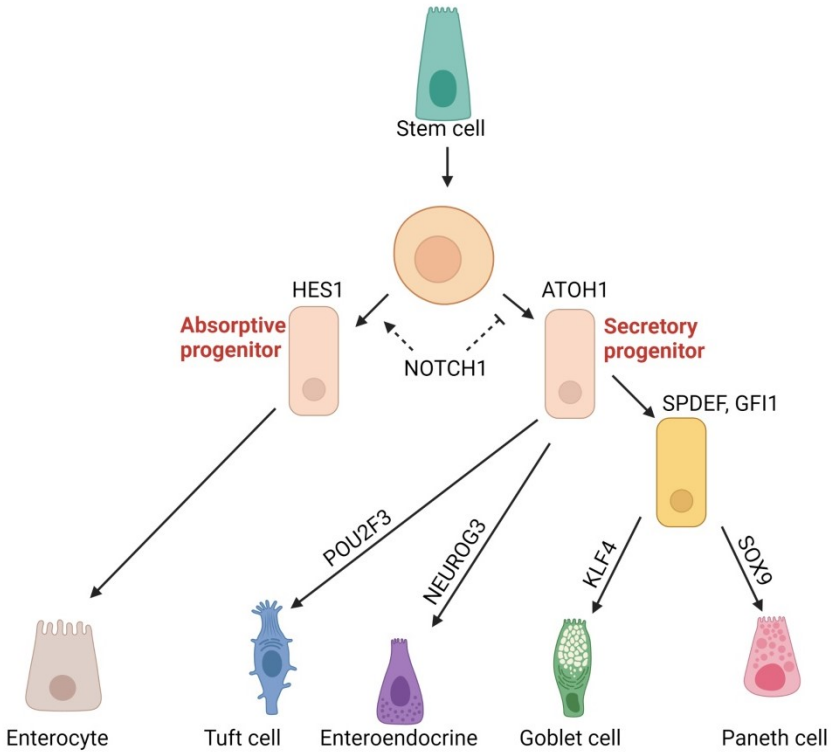
Stem cell
HES1
Absorptive progenitor
NOTCH1
ATOH1
Secretory progenitor
SPDEF, GFI1
POU2F3
NEUROG3
KLF4
SOX9
Enterocyte
Tuft cell
Enteroendocrine
Goblet cell
Paneth cell

B

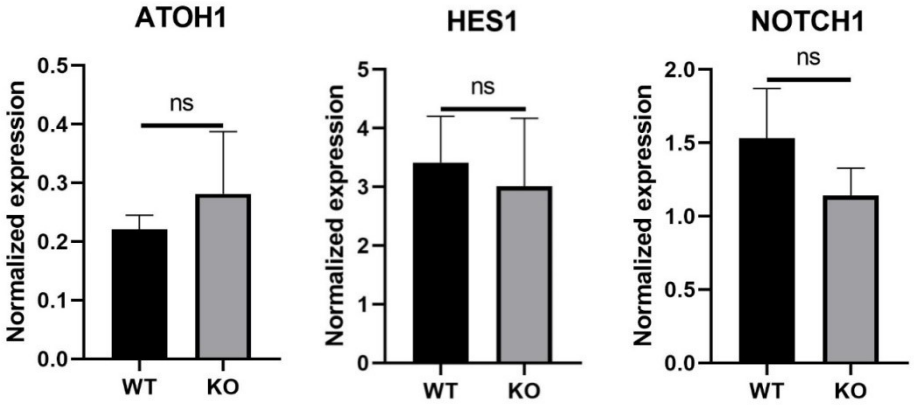
ATOH1
Normalized expression
0.5
0.4
0.3
0.2
0.1
0.0
ns
WT
KO
HES1
Normalized expression
5
4
3
2
1
0
ns
WT
KO
NOTCH1
Normalized expression
2.0
1.5
1.0
0.5
0.0
ns
WT
KO

3.11. IL-10 addition does not correct deficiencies in IL-10KO Paneth cells

Deficiencies of Paneth cell LYZ1 and DEFA5 secretory products were observed in developing IL-10KO enteroids. This observation encouraged the next experiment, to introduce IL-10 into the IL-10KO enteroid culture with the goal to correct the Paneth cell deficiencies. IL-10 was added to growth medium, which bathes the basal side of enteroids embedded in the Cultrex® dome, presumably engaging basal IL-10 receptors (Figure 15). IL-10 was added on day 1 after passage and replenished every other day along with growth medium until the enteroids were harvested for mRNA on day 5. The results from the RT-qPCR experiment showed IL-10KO enteroids treated with IL-10 still possessed lower mRNA levels of the Paneth cell markers compared to WT enteroids (Figure 14). This result indicated that IL-10, at least through basal exposure, did not correct the Paneth cell deficiency in IL-10KO organoids.

Figure 15. IL-10 does not correct Paneth cell deficiencies in IL-10KO enteroids.

IL-10 KO enteroids were treated with 20 ng/ml IL-10 for 5 days, from day 1 until day 5 of culture. Day 5 enteroids of untreated WT, untreated IL-10KO, and IL-10 treated IL-10KO were collected for total RNA. mRNA levels for TATA-binding protein TBP (reference gene), LYZ, DEFA5 and MUC2 were measured by RT-qPCR. Results were displayed as mean ± standard deviation, n = 6-9 (* $p < 0.05$, ** $p < 0.01$, *** $p < 0.001$, ns – not significant, one way ANOVA followed by Tukey's post hoc test).

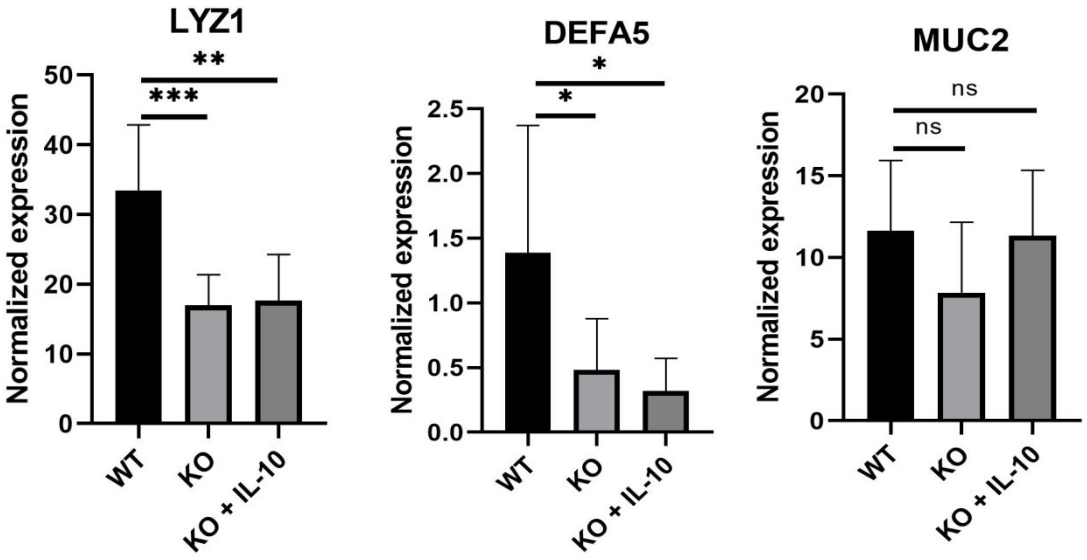

3.12. IL-10 signaling pathway in enteroids

The IL-10 receptor signals through several pathways, depending on the cell type and environmental context (Verma et al., 2016). The most common pathway triggered by IL-10 interaction with IL-10 receptor is through JAK1-STAT3 phosphorylation. Since basally administered IL-10 did not correct the Paneth cell marker deficiencies in IL-10KO enteroids, it was questioned whether IL-10 signals through the basal IL-10 receptor by the STAT3 pathway. Day 4 enteroids were treated with a phosphatase inhibitor cocktail upon IL-10 addition to ensure intact harvest of phosphorylated STAT3 (pSTAT3). Both WT and IL-10KO enteroids were treated with IL-10 for 20 minutes before being lysed for protein extraction. STAT3 and pSTAT3 were observed by Western blotting.

The Western blot data demonstrated there is a low level of constitutive pSTAT3 (at both TYR705 and SER727 positions) in untreated enteroids of both genotypes, implying the signal was not due to IL-10 (Figure 16A). Interestingly, quantification of pSTAT3 (TYR705) revealed that there was no significant difference between the two genotypes regarding level of STAT3 activation upon IL-10 addition to the medium (Figure 16B). This result suggested that enteroid responded poorly to IL-10 through STAT3 phosphorylation.

Figure 16. IL-10 signaling pathway through STAT3.

A) All enteroids were pre-treated with a phosphatase inhibitor cocktail for 20 minutes. WT and IL-10KO (or KO) enteroids were treated with 100 ng/ml of IL-10 for 20 minutes before being harvested for protein. Protein levels of STAT3 and phosphorylated STAT3 at TYR705 (SER727 and TYR705) were measured by Western blot. The level of phosphorylated STAT3 (pSTAT3) is compared to the total amount of unphosphorylated STAT3 (STAT3). **B)** Fold change of pSTAT3 (TYR705) in IL-10 treated relative to untreated enteroids was quantified using Image Lab. (n = 3) (one way ANOVA followed by Tukey's post hoc test).

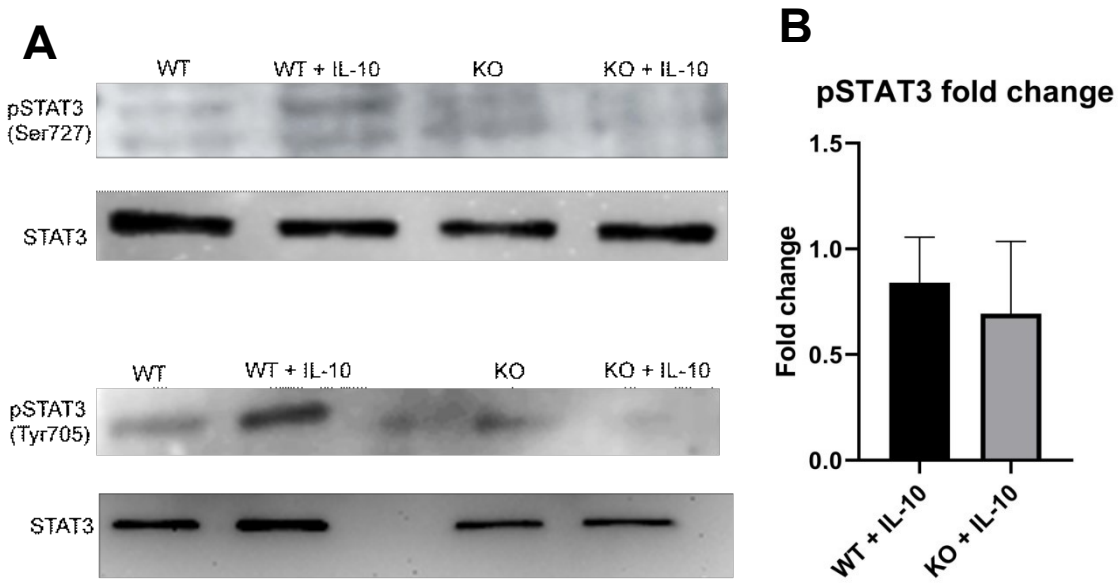

3.13. IL-10 signaling pathway in monolayers

Previous immunofluorescent findings indicated that the IL-10 receptor is present apically on cells in the enteroids; there is reason to believe that apical receptors may signal differently than basal receptors. Enteroids growing 3-dimensional in extracellular matrix have restricted access to the apical side of the epithelium. To administer IL-10 apically, enteroids were dissociated into a cell suspension and seeded onto Transwell™ insert, where the cells established a monolayer (Figure 16A). Enteroid monolayers contain proliferative cells, as well as differentiated specialized cell types (Thorne et al., 2018). Judging by the number of KI67-positive cells, it can be seen that the longer the confluent monolayer is maintained on Transwell™, the less proliferative cells there are (Figure 16B). To match day 4 enteroids regarding the relative abundance of proliferative cells (as seen previously in Figure 4B), monolayers were collected for protein lysates as soon as the culture reached confluency to maintain a highly proliferative cell population (Altay et al., 2019). To evaluate the role of epithelial polarity in STAT3 activation by IL-10, IL-10 was administered to either the apical or the basal side of the monolayer. Western blot results showed noticeable STAT3 phosphorylation (Tyr705) by IL-10 in WT monolayer, with the apically-treated monolayer being more distinct than the basally-treated one. Yet in KO monolayer, STAT3 phosphorylation (Tyr705) by IL-10 was only observed in basally-treated monolayer. This observation suggests that there is a distinct role for apical IL-10 receptor in WT epithelium. In contrast, KO epithelium is less responsive to apically-administrated IL-10, at least through STAT3 activation.

Figure 17. Western blot of pSTAT3 following apical vs basal IL-10 stimulation

A) To establish 2D monolayer from 3D enteroids, enteroids were dissociated into a suspension of single cells and fine crypt fragments, which were subsequently seeded onto Transwell™ insert. The epithelial cells expand until reaching confluency within the insert and polarize, with apical access being on the insert (top well) and basal access being on the bottom well (Created with Biorender.com). **B)** 2D monolayers were maintained on Transwell™ for different amount of time. Day 4 and day 20 monolayers were stained from KI67 and occluding, and counterstained for nuclei with DAPI. Images were taken by confocal microscope (LSM 710)(Scale bar = 20 μm). **C)** For Western blot analysis of 2D monolayers, all monolayers were pre-treated with a phosphatase inhibitor cocktail for 20 minutes. WT and IL-10KO (or KO) monolayers were treated with 100 ng/ml IL-10 for 20 minutes, either through the apical side (top well) or basal side (bottom well) before being harvested for protein. Protein levels of STAT3 and phosphorylated STAT3 at TYR705 (SER727 and TYR705) were measured and compared to the total amount of unphosphorylated STAT3. **D)** Fold change of pSTAT3 (TYR705) in IL-10 treated monolayers relative to untreated monolayers was quantified using Image Lab (n = 3) (** $p < 0.01$, two-way ANOVA followed by Sidak's post hoc test).

A

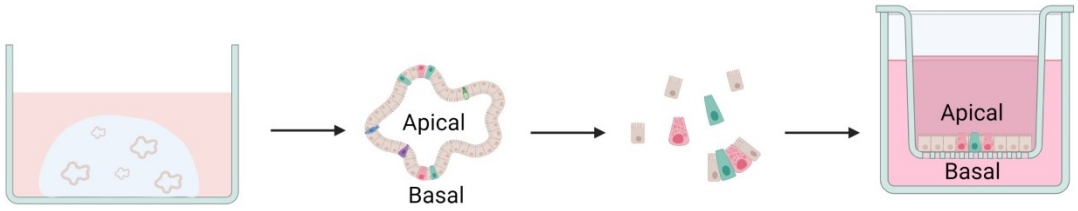
Apical
Basal
Apical
Basal

B

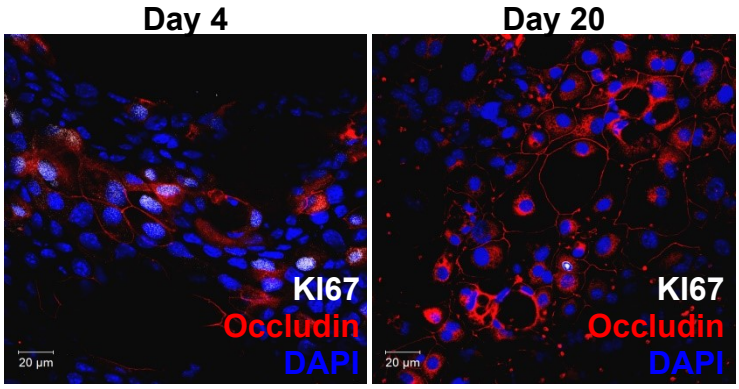
Day 4
Day 20
KI67
Occludin
DAPI
20 µm
KI67
Occludin
DAPI
20 µm

C

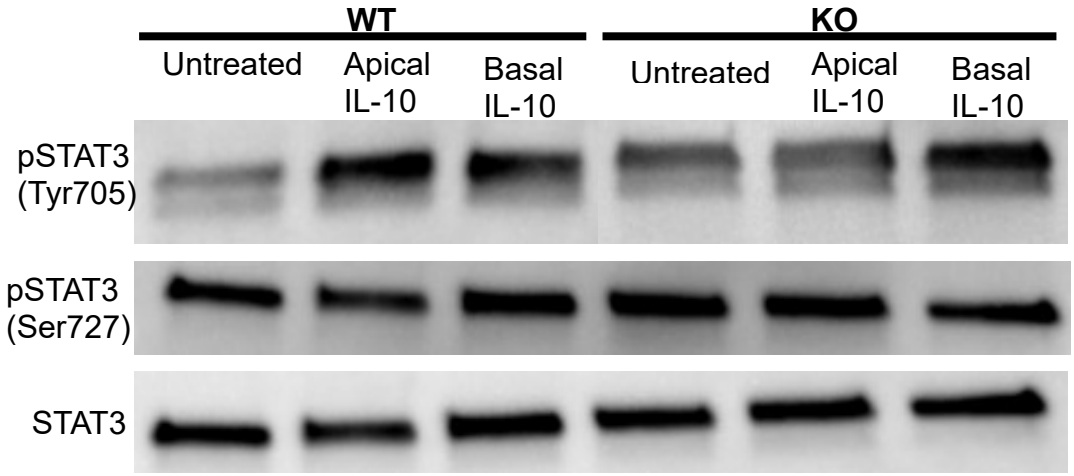
WT
KO
Untreated
Apical IL-10
Basal IL-10
Untreated
Apical IL-10
Basal IL-10
pSTAT3 (Tyr705)
pSTAT3 (Ser727)
STAT3

D

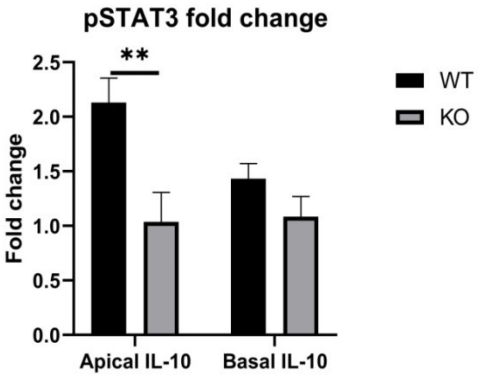
pSTAT3 fold change
**
2.5
2.0
1.5
1.0
0.5
0.0
Fold change
Apical IL-10
Basal IL-10
WT
KO

3.14. Reduction of secretory markers in IFN-γ treated enteroids

Up to this point, the experimental design has focused the potential role of epithelial IL-10 in the homeostatic epithelium. We were also interested in seeing the impact of IL-10 when the cells are challenged by pro-inflammatory signals. Among the proinflammatory cytokines reported in the intestines, IFN-γ is a common signature of small bowel inflammation (Fuss et al., 1997; Strober et al., 2013). Additionally, published *in vitro* experiments consistently demonstrate an adverse effect of IFN-γ on epithelial barrier integrity (Smyth et al., 2011). Also, IFN-γ was shown to increase the expression of apical IL-10 receptors on (Kominsky et al., 2014). Therefore, IFN-γ became the “antagonist” of interest to challenge IEC, as we investigated epithelial IL-10 function during model inflammation. Here, enteroids were treated with IFN-γ 24 hours prior to RNA extraction. It was morphologically shown that IFN-γ induced considerable apoptosis, observed as a dark lumen due to an accumulation of dead cells, and blurry luminal edges due to disruption of the barrier integrity (Figure 18A). Cell markers for Paneth cells and goblet cells were examined for transcript levels in WT and IL-10KO enteroids on day 7 (levels observed to be similar in Figure 12). In WT enteroids, IFN-γ treatment led to reduced secretory cell markers. Interestingly, although IL-10KO enteroids also had reduced levels of LYZ1 and MUC2, the level of DEFA5 remained unchanged in WT, and IFN-γ treated IL-10KO enteroids had significantly higher level of DEFA5 than IFN-γ treated WT enteroids (Figure 18B). These data suggest that upon barrier disruption with IFN-γ, epithelial IL-10 might play a role in regulating DEFA5 expression.

Figure 18. Impact of IFN-γ on WT and IL-10KO enteroids.

A) IL-10 KO enteroids were treated with 10 ng/ml of IFN-γ on day 5 of culture, for 24 hours. Representative images were taken before and after treatment with IFN-γ using the EVOS FL Imaging System (Scale bar = 200 μm). **B)** IL-10 KO enteroids were treated with 10 ng/ml of IFN-γ on day 5 in culture, for 24 hours. On day 6 of culture, untreated enteroids, and IFN-γ treated enteroids were collected for total RNA. mRNA levels for TBP (reference gene), LYZ, DEFA5 and MUC2 were measured by qPCR (n = 6). Results were displayed as mean ± standard deviation (** $p < 0.01$, ns – not significant, one-way ANOVA followed by Tukey's post hoc test).

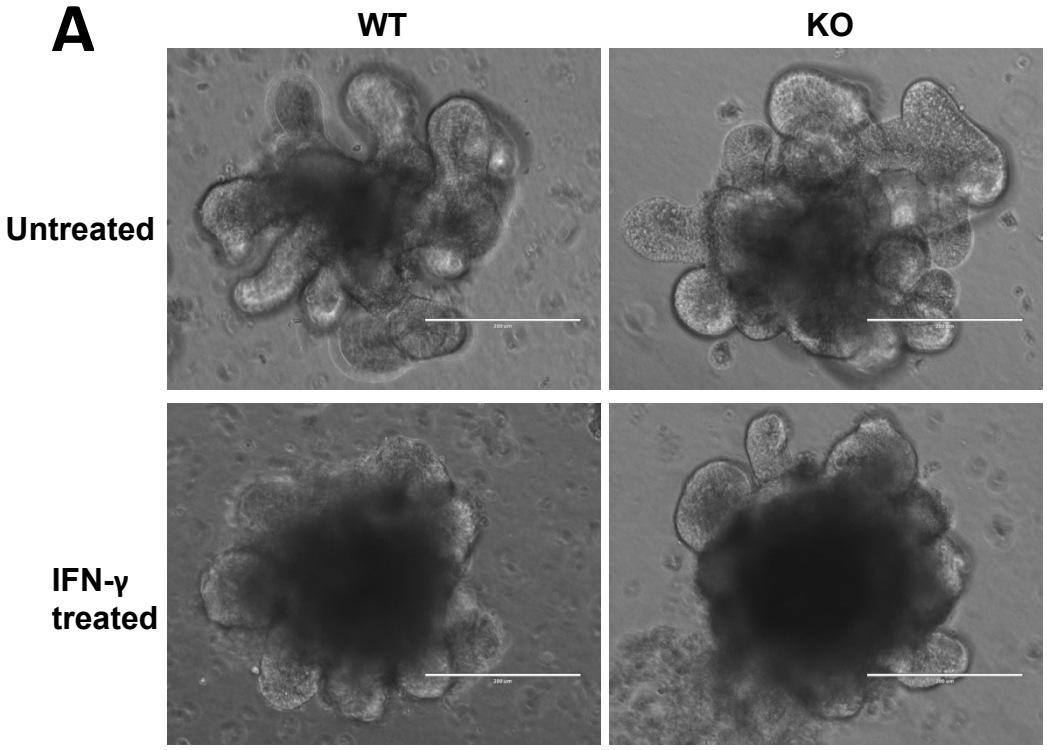
A
WT
KO
Untreated
IFN-γ
treated

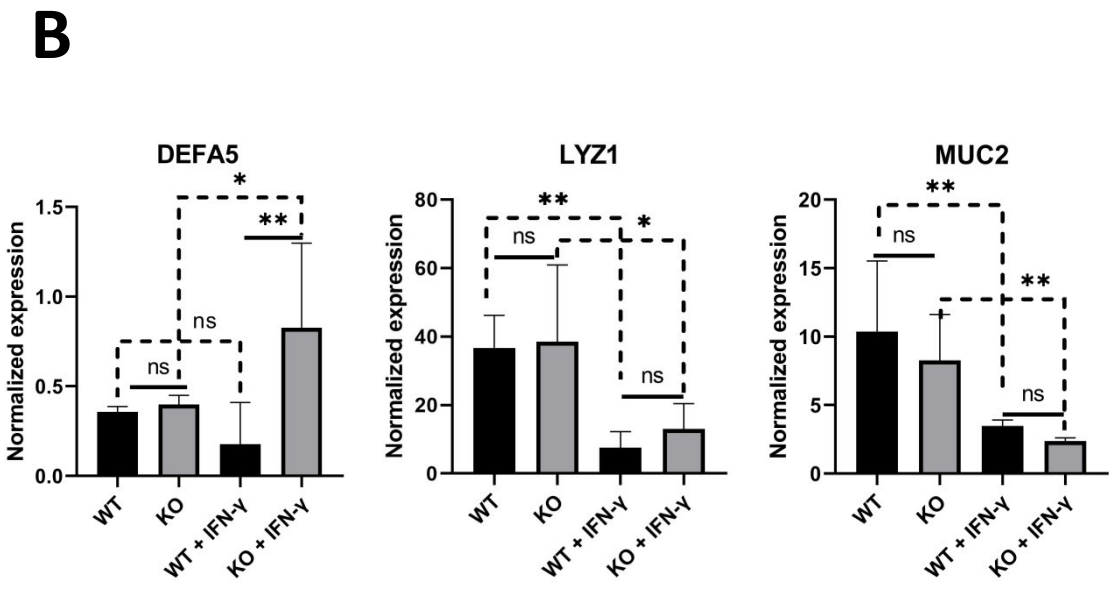
B
DEFA5
LYZ1
MUC2
Normalized expression
ns
*
**
WT
KO
WT + IFN-γ
KO + IFN-γ

3.15. Mining of publicly available RNA-sequencing data from mouse IECs

Publicly available sequence data set can provide some clues into cell-specific products. Mining single-cell RNA sequencing (scRNA-seq) data of freshly isolated murine small intestinal epithelial cells revealed the IL-10 signal was associated with some tuft cells and transit-amplifying cells (GSE92332). The IL-10 signal also associated with goblet stem cells upon *Salmonella* infection. One study of bulk and sc-RNA-seq data derived from mouse enteroids failed to detect IL-10 transcripts (GSE115955, GSE100274). Another scRNA-seq report using enteroids showed rare counts of IL-10 transcripts associated with early enterocyte progenitors, enteroendocrine and M cell (GSE92332). Regarding IL-10RA, the signal was found to be strongest in Paneth cells in one study (GSE113536), yet in another, the signal is attributed to transit-amplifying cells (GSE92332).

Paneth cells are easily under-presented in single-cell studies of the epithelium (Haber et al., 2017) and considering my principal finding that Paneth cells are a source of IL-10, I specifically probed Paneth cell scRNA-seq data. RNA sequencing of freshly isolated Paneth cells from murine small intestine (GSE117216) showed low-abundant but detectable counts of IL-10 transcripts. Additionally, scRNA-seq data of Paneth cell maturation traced from early progenitor LGR5+ cells (GSE76408) also revealed rare but detectable levels of IL-10 transcripts.

CHAPTER 4: DISCUSSION

4.1. Summary of expression and function of epithelial IL-10 and IL-10RA in enteroids

Enteroid cultures offer a unique opportunity to study intestinal epithelial cells in the absence of factors from non-epithelial cell types. Presumably any signal detected among the cells within enteroids is “hard-wired”, the cells express the molecule without exogenous stimuli. In this study, IL-10 was shown to be expressed near the apical membrane of Paneth cells, which speaks to the likelihood of IL-10 being secreted apically. The presence of IL-10RA on the apical side of Paneth cells, along with the co-staining of IL-10 and IL-10RA, provide evidence that IL-10 can act in an autocrine manner on Paneth cells.

Paneth cells in IL-10KO enteroids demonstrate deficiencies in secreted products, implying that epithelial IL-10 has a functional role in WT enteroid Paneth cell development. Upon exposure to IFN-γ, DEFA5, another Paneth cell marker, was significantly higher in IL-10KO compared to WT enteroids, further suggesting a role for epithelial IL-10 possibly including during inflammation.

In addition to the apical expression and not surprising, IL-10RA was also detected on the basal side of crypt base and goblet cells, which indicates that cells within the intestinal epithelium are equipped with receptors to respond to IL-10 from cellular sources in the lamina propria. Lastly, IL-10 receptor signaling through STAT3 was impaired in IL-10KO compared to WT cells within enteroids, suggesting an aberrant pattern of receptor regulation in IL-10KO cells. Thus, epithelial IL-10 influences the STAT3 signaling pathway with the epithelium.

Interestingly, STAT3 signaling was more potent through stimulation of the apical receptors, which suggests the cell response of IEC toward IL-10 depends on the side to which the ligand is delivered. The sum of these findings suggests there is a unique role for epithelial IL-10 in epithelial homeostasis, acting primarily if not exclusively apically, compared to other possible IL-10 sources which act upon the epithelium basally.

Figure 19. Impacts of IL-10 on WT and IL-10KO enteroids

This study demonstrated the likelihood of IL-10 autocrine activity in Paneth cells and how it impacts Paneth cell development. Additionally, this study speaks to the unique role of apical epithelial-derived IL-10, which is non-redundant to exogenous IL-10 (created with Biorender.com).

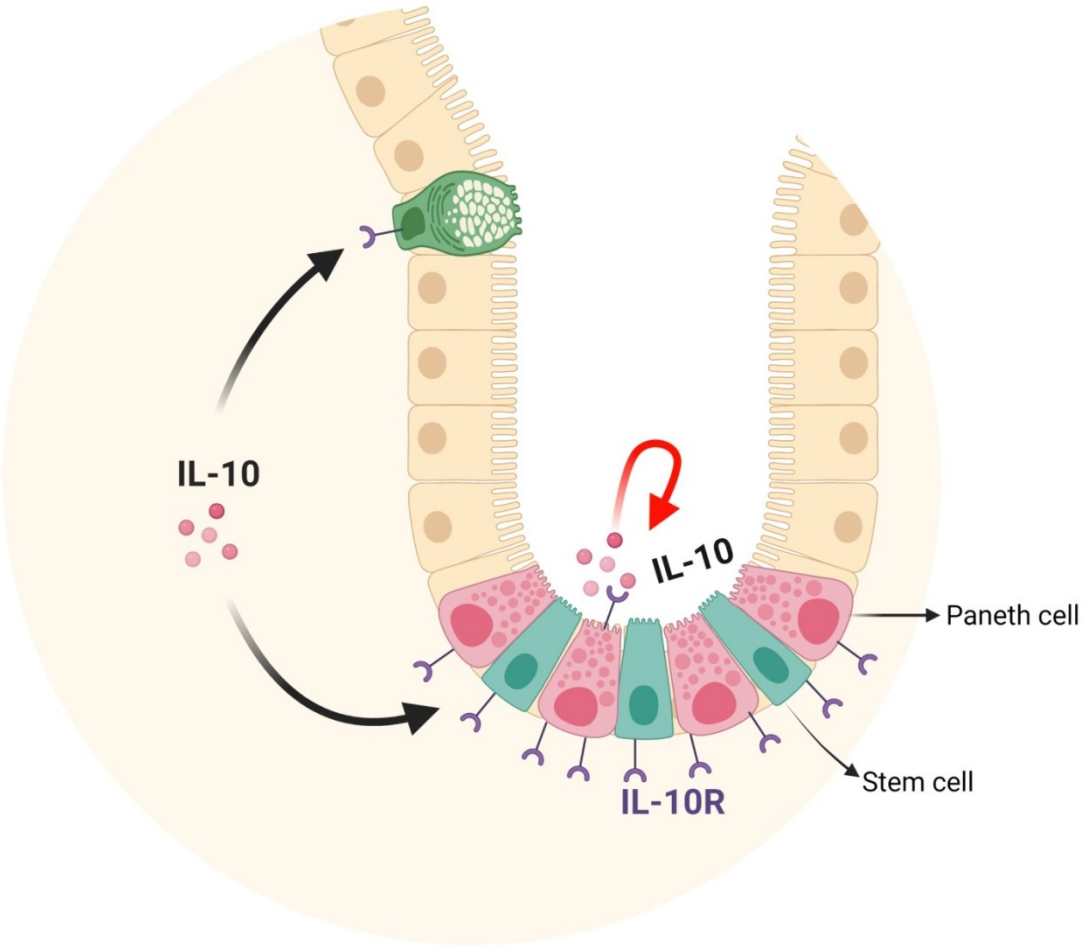

4.2. Heterogeneity in enteroid culture

4.2.1. Potential impact of heterogeneity of enteroid culture on characterization of constitutive expression

Over the 7-days of enteroid cultures, IL-10 and IL-10RA mRNA was always detectable by RT-qPCR, suggesting constitutive expression of these two targets in the epithelium. It remains a possibility that this consecutive expression is limited to a particular stage of enteroid development. At every day there is heterogeneity in terms of development among enteroids within the same matrix dome due to the spatiotemporal gradient and instability of certain growth factors (Shin et al., 2020). As a result, since enteroids from multiple domes were pooled together for RNA isolation, the RNA pool represents a mixture of IL-10-positive enteroids and possibly IL-10-negative enteroids. This study was limited to examining mainly “mature” budded enteroids for the cellular sources of IL-10 and the receptor. In order to confirm the true constitutive nature of IL-10 and IL-10RA cellular production, future experiments may choose to longitudinally trace IL-10 and the IL-10 receptor on IEC at single-cell level through enteroid development.

4.2.2. Potential impact of enteroid heterogeneity on characterization of enteroid permeability

It has been reported that the epithelium of IL-10KO mice is more permeable than the epithelium of WT mice (Shi et al., 2014). Despite this precedent, no significant difference in permeability was observed in the present experiments comparing IL-10KO versus WT enteroids. However, the permeability assay has several limitations which can confound the observed outcome.

Specifically, the FITC-dextran marker was added to PBS, replacing the medium bathing the enteroid matrix “dome”, creating a gradient of diffusion across and into the enteroids. The alternative is to administer the FITC-dextran into the lumen of the enteroids, which is very challenging. Consequently, at the single-enteroid level, it was observed that despite coming from the same Cultrex® dome, enteroids with different morphologies varied in the amount of FITC-dextran that diffused into the lumen. Future experiments could use enteroid monolayers in the FITC-diffusion assay or TEER measurements, as this model might offer a more homogenous representative of the epithelium and facilitate more accurate measurement and quantification. The results of the FITC-dextran experiment were inconclusive.

4.3. Paneth cells express IL-10 and IL-10R and the likelihood of autocrine activity

In this study, Paneth cells were observed to be the IL-10-positive cell though not all Paneth cells in a single crypt were positive. Thus, constitutive expression of IL-10 corresponds with the continuous presence of Paneth cells during the course of enteroid culture, beginning with fresh crypts. Paneth cells are also long-lived one (>30 days *in vivo)* and go through extensive development stages before reaching maturation and termination (Lueschow & McElroy, 2020). Whether IL-10 production was constitutive throughout the entire course of Paneth cell development or limited to a specific development stage cannot be concluded with the data available.

RT-qPCR showed that levels of IL-10RA remained statistically unchanged throughout the course of enteroid culture. Yet, with such significant standard deviation on day 2 measurements (Figure 6), the presence of IL-10RA in early-stage enteroids is questionable. In a future experiment, *in situ* hybridization could be used as an alternative method to simultaneously confirm IL-10 or IL-10RA transcript expression and co-localization of cell markers. Levels of enteroid IL-10 transcripts peaked on day 4 of culture, when the majority of enteroids go through the “budding” event, signifying the transition from proliferative stage to differentiative stage. Reasonably, it can be speculated that epithelial IL-10 might be involved in the downstream pathway of cellular differentiation. Nevertheless, the differences in IL-10 expression throughout the course of enteroid culture can be explained in various ways. IL-10-positive Paneth cells may multiply with day 4 budding events and the emergence of new crypts. Following Paneth cell emergence, other cell types rapidly arise which dilutes the relative abundance of IL-10 transcripts, resulting in an apparent decrease on day 6. Alternatively, there exists a temporary phase of Paneth cell development linked to day 4 during which Paneth cells produce substantially more IL-10. It is also possible that a combination of these events occur. Future studies will require the development of a fluorescent reporter system to study the dynamic of IL-10 in Paneth cells in real time. Paneth cells have been reported to be deeply impacted by epithelial extrinsic factors, especially the commensal microbes, which has been shown to significantly induce Paneth cell numbers and immune-competent functions (Schoenborn et al., 2019; Walker et al., 2013).

Although the production of antimicrobial proteins are typical signatures of Paneth cells, studies have shown that there are subtypes within the Paneth cell population, and that not all Paneth cells express the same level and the same composition of secreted products (Haber et al., 2017; Heida et al., 2016). Such heterogeneity within the Paneth cell population supports the finding that not all Paneth cells are positive for IL-10. It is noteworthy that the enteroid cultures were established from crypts isolated from jejunum and ileum. Significant regional variation in Paneth cell subset distribution has been demonstrated in murine small intestinal epithelium (Haber et al., 2017). Therefore, we have reasons to suspect that IL-10-positive Paneth cells in our enteroid cultures represent a subpopulation, possibly from a particular region of the intestine. Moreover, studies have shown that Paneth cells and goblet cells do not fully diverge in WT organoids (Biton et al., 2018). In WT murine adult epithelium, intermediate cells that express the markers for both goblet and Paneth cells are rare, at a ratio of 1 cell for every 10 crypts (Berkowitz et al., 2019). Such scarcity implies that the intermediate cell is a temporary and very brief phase. It is not clear how well cells in enteroid cultures recapitulate this development and maturation; for example, a brief stage *in vivo* may be prolonged *ex vivo* due to a lack of exogenous signals. The true source of IL-10 in enteroids might not be a fully mature Paneth cell but rather the common progenitor of Paneth cells and goblet cells. If that is the case, a question arises over whether Paneth cells continue to make IL-10 beyond the developmental window observed in enteroids, or possibly whether other cell type(s) emerge to become IL-10-producing cells. The only *in vivo* study to assign

IL-10 production to an epithelial cell type is a single-cell sequencing survey of freshly isolated murine epithelium. Our analyses of these authors' data revealed very rare IL-10 signals associated with tuft cells (Haber et al., 2017). However, because the objective of this RNA-seq study did not prioritize low abundant transcripts, the expression threshold possibly resulted in several other IL-10-positive IEC appearing negative (Haber et al., 2017). In our enteroid immunofluorescent staining, DCLK-positive tuft cells did not co-localize with IL-10. Perhaps extrinsic factors are required to induce IL-10 production in tuft cells. We conclude from our enteroid-derived data that IL-10 production is an intrinsic feature of cells clearly on the Paneth cell lineage.

4.3.1. Role of epithelial IL-10 in Paneth cell development

In addition to producing IL-10, Paneth cells were shown to express the IL-10 receptor, implying that IL-10 can affect the cell. This hypothesis was confirmed by comparing WT and IL-10KO enteroid Paneth cell secretory markers and observing deficiencies in day 5 IL-10KO enteroids. Interestingly, this difference was not evident in day 7 enteroids. The latter finding suggests that such deficiencies would not be evident *in vivo*. Interestingly, this does not seem to be the case, for example, although lysozyme mRNA levels were similar between WT and IL-10KO small intestinal epithelium, cells in the IL-1KO reportedly had aberrant lysozyme packing in granules, and significantly lower cryptdin mRNAs and protein levels, findings were observed prior to onset of symptomatic inflammation (Berkowitz et al., 2019; Inaba et al., 2010). Still, the IL-10KO mouse experiences alterations in basal cytokine levels prior to developing

inflammation; therefore, it is difficult to rule-out indirect effects of cells in the lamina propria impacting the epithelium *in vivo*.

Finally, there is a possibility that the outcomes observed in day 7 enteroids are an artifact due to the peculiar conditions that enteroids are exposed to. For example, enteroids have an enclosed lumen and endure an irreversible increase of intraluminal pressure due to the accumulation of apoptotic bodies. Such mechanical tension has been shown to directly affect the cellular dynamics and can confound the results (Gayer & Basson, 2009).

The Paneth cell marker deficiencies were detected on day 5 in IL-10KO enteroids, how is this transient deficiency explained? Epithelial IL-10 may affect the transition from intermediate cells to fully mature secretory cells. In line with this argument, researchers have shown that intermediate cells co-expressing both Paneth and goblet cell markers are 3 times more abundant in IL-10KO mice than in WT mice, suggesting that IL-10 is required for the complete maturation of specialized secretory cells (Berkowitz et al., 2019). Yet, it can also be an indication of proliferation-versus-differentiation imbalance. IL-10KO IECs are hyperproliferative and produce unregulated amount of new undifferentiated cells before the old ones can reach complete differentiation. Interesting, this scenario is supported by both *in vivo* and *ex vivo* studies. IL-10KO mice are reported to have more proliferative cells per crypts and addition of IL-10 to enteroids reduced proliferation while increasing differentiation simultaneously (Deng et al., 2020; Xue et al., 2016). Another, and not necessarily independent hypothesis proposes that epithelial IL-10 affects the production of antimicrobial products. If the

numbers of Paneth cells are the same between IL-1KO and WT crypts, the amounts of antimicrobial products may be different. In this case, IL-10 will affect the immune-competent function of Paneth cells and not the number of cells. Although Paneth cell numbers are reported to be equal or slightly less in IL-10KO compared to WT crypts, expression of cryptdins is consistently shown to be significantly lower in IL-10KO (Berkowitz et al., 2019; Inaba et al., 2010; Xue et al., 2016). Therefore, we have reason to believe that IL-10 can have an influence on antimicrobial peptide output. Whether this influence can be attributed to all exogenous sources of IL-10 or exclusive to epithelial IL-10, can be elucidated in future studies by comparing the ratio of antimicrobial peptide level over Paneth cell number.

4.3.2. Role of epithelial IL-10 in Paneth cells following IFN-γ exposure

The absence of IL-10 might weaken the barrier integrity of the intestinal epithelium but in the absence of microbes it is not enough to tip the scale of homeostasis and trigger inflammation. Conventionally-raised IL-10KO mice develop colitis but germ-free IL-10KO mice do not (Sellon et al., 1998). Once inflammation is triggered, the compromised IL-10KO epithelium and intestine experiences severe symptoms and more difficulty recovering (Zhou et al., 2004). This speaks to IL-10 critically and favorably influencing epithelial integrity in the presence of gut microbes, whether directly or indirectly.

An important mediator that emerges in the absence of IL-10 is IFN-γ and this is the most commonly implicated and impactful cytokine during gut

inflammation (Fuss et al., 1997; Ito et al., 2006). With the objective of exploring the role of epithelial IL-10 in an inflammatory setting, enteroids were exposed to IFN-γ. Notably, IFN-γ is not limited to inflammation as it can also play a regulatory role during homeostasis. Specifically, steady-state microbiota-driven IFN-γ mediates Paneth cell autophagy, an essential cellular process required for homeostasis (Burger et al., 2018).

In this study, it was observed that secretory marker mRNAs examined such as LYZ1 and MUC2 were decreased following overnight stimulation with IFN-γ. The reduction in Paneth cell marker transcripts (LYZ) is in agreement with the findings by Eriguchi et al. who also treated enteroids with IFN-γ (Eriguchi et al., 2018). These authors showed that IFN-γ promoted Paneth cell degranulation, extrusion and apoptosis, which might explain the decrease in Paneth cell markers. Since the observations were made in enteroids, the outcomes are direct responses of IEC to IFN-γ (Farin et al., 2014). Mucus extrusion in goblet cells was also induced by IFN-γ, although the downregulating effect of IFN-γ on MUC2 transcript is more modest (Eriguchi et al., 2018; Farin et al., 2014).

While we registered an effect of IFN-γ on WT enteroids, there also was a difference between WT and IL-10KO enteroids following IFN-γ stimulation in DEFA5 transcript abundance. Opposite to what was observed in steady-state enteroids on day 5, IFN-γ treated IL-10KO enteroids expressed higher mRNA levels of DEFA5 than IFN-γ treated WT enteroids. There are at least two scenarios that may apply to explain these findings. First, if protein levels correspond with mRNA levels, the data imply that IL-10KO enteroids produce

more cryptdin-5 than WT enteroids following treatment with IFN-γ. Interestingly, opposite to the outcomes observed in IFN-γ overnight treatment (Eriguchi et al., 2018; Farin et al., 2014), a 3-hour IFN-γ treatment was shown to induce expression of DEFA5 in enteroids (Yue et al., 2021). Thus, in WT enteroids, it is speculated that although short-exposure to IFN-γ temporarily increases DEFA5 expression, a long exposure results in decreased DEFA5 expression due to Paneth cell autophagy and extrusion. Yet, in IL-10KO enteroids, DEFA5 expression remained elevated after a long-exposure to IFN-γ, inferring that perhaps “normal” Paneth cell responses to IFN-γ such as autophagy and/or extrusion are dysregulated in IL-10KO enteroids. In a second scenario, mRNA levels of DEFA5 do not parallel the quantity of DEFA5 protein, given that murine cryptdin-5 (or human α-defensin-5) requires post-translational modifications prior to achieving an active form (Ghosh et al., 2002; Wilson et al., 1999). An example of where this may apply is in necrotizing enterocolitis (NEC). In NEC, DEFA5 mRNA levels are 2-3 times greater compared to non-NEC infants, yet the protein levels were similar. The authors inferred that Paneth cell homeostasis was disrupted which resulted in hypersecretion of immature α-defensin-5 resulting in low level of α-defensin-5 remaining intracellular. Interestingly, this dissociation between mRNA and protein levels of DEFA5 was only observed in NEC, as DEFA5 mRNA levels corresponded with protein levels in the healthy gut (Salzman et al., 1998). Future studies can confirm DEFA5 changes along with other Paneth cell secretory products proteins in WT versus IL-10KO enteroids due to IFN-γ; for example, metalloproteinase-7, the enzyme responsible for

processing cryptdin maturation ought to be examined (Vandenbroucke et al., 2014).

Cryptdin-5/α-defensin-5 has been shown to play beneficial roles in shaping the microbiota landscape and enteric mucosal immunity *(Salzman et al., 2003)*; however, this potent cytotoxic peptide can be a double-edged sword in certain settings. At high concentrations, α-defensin-5 can induce apoptosis, actin disruption and upregulation of CXCL8 - a neutrophil chemokine (shown in Caco-2 cells) (de Leeuw et al., 2007; Lu & de Leeuw, 2013). Additionally, a short exposure to a high concentration of α-defensin-5 induced CD4+ T cell production of IL-2, CXCL8 and IFN-γ, while prolonged exposure to low dose α-defensin-5 induced apoptosis in CD4+ T cells (Lu & de Leeuw, 2013). It is important that future experiments not only measure the level of DEFA5, but also demonstrate the consequences on the integrity of the epithelium. Additionally, as IL-10 has been consistently shown to directly act on epithelial wound healing (Lorén et al., 2015; Quiros et al., 2017), it would be interesting to compare WT versus IL-10KO enteroid phenotypes following IFN-γ withdrawal. Lastly, despite receiving the most attention from researchers, DEFA5 is not the most highly expressed α-defensin in murine small intestines. DEFA20 and DEFA24 are more abundant (Castillo et al., 2019); therefore, there are good reasons to investigate other members of α-defensin family.

4.4. Inconsistent reports of the source of epithelial IL-10

When exploring publicly available RNA-sequencing data from *ex vivo* and *in vivo* experiments, we found inconsistent reports of IL-10-positive epithelial

cells. The inconsistency between data sets, beside the chance of false positive and false negative results, might be due to the sequencing design. Specifically, it is noteworthy that the common aim of the mentioned studies is to present a global view of gene expression; therefore, the corresponding choice of read-depth and background cutoff threshold might not be optimal for in-depth characterization of low-expression genes. Second, the inconsistency might be attributed to how each study categorizes cell types through clustering following optional pre-sorting with cell markers. Notably, such “black-or-white” categorization based on cell markers disregards an important aspect of the epithelium; that is, such multi-lineage population is hierarchical, and it experience gradients of differentiation. Additionally, all studies seem to overlook the “inter-cluster” links, or the “branching point” where different differentiation trajectories take place. For example, one study has shown that mature Paneth cells can arise from two different trajectories: 1) through Dll1-positive common progenitor of Paneth and goblet cells, and 2) directly through transit-amplifying cell track (Grün et al., 2016). Nevertheless, despite inconsistencies between datasets in terms of IL-10–positive cell types, it is confirmed that the endogenous production of IL-10 can be found in Paneth cells, but not necessarily exclusive to this cell type.

4.5. Basal IL-10 receptors are expressed on IEC types other than Paneth cells

Multiple studies report consequences of IL-10 upon intestinal carcinoma cell lines, so it is not surprising that cells within the epithelium express IL-10RA.

We detected IL-10RA on the apical membrane of Paneth cells and on the basal side of goblet cells and other cells in the crypt base. These findings are compatible with others' studies showing IL-10 influences stem cells, Paneth cells and goblet cells. In terms of stem cells, different studies showed contrasting outcomes when adding IL-10 to enteroids. Murine WT enteroids derived from whole small intestine and treated with 5 ng/ml IL-10 for 5 days showed inhibition of stem cell expansion, yet the opposite outcome was reported in murine WT enteroids derived from ileum and treated with 10 ng/ml for 3 days (Biton et al., 2018; Deng et al., 2020). These conflicting outcomes might be due to the discrepancies in dose, exposure length, intestinal section where the crypts were isolated, as well as the timing relative to stem cell marker measurements. Our finding that IL-10KO enteroids grew and "budded" similar to WT enteroids, would lead us to conclude that IL-10 does not significantly influence stem cells.

Apart from Paneth cells, using immunofluorescent staining, goblet cells were observed to possess basal IL-10RA. Multiple studies have indicated IL-10 influences goblet cell phenotype. Although the epithelium of IL-10KO mice are more proliferative, they have fewer goblet cells and impaired secretion of mucin-2 (Schwerbrock et al., 2004; Xue et al., 2016). Additionally, it was reported in rhesus macaque explants that neutralization of IL-10 resulted in cytoplasmic vacuolar degeneration in goblet cells (Pan et al., 2013). It is worth pointing out that these outcomes can be due to either the direct effect of IL-10 or the indirect effect from the emergence of other mediators caused by the lack of IL-10. That there is a direct effect of IL-10 upon goblet cells is supported by evidence that

mucin-2 protein misfolding and endoplasmic reticulum stress was resolved by adding IL-10, although that study was conducted using a cell line (Hasnain et al., 2013). While basal IL-10RA was linked to goblet cells, no particular deficiency was identified, and the number of goblet cells was not reduced in IL-10KO enteroids.

Considering the impact of IL-10 in homeostasis, our observations of cells bearing IL-10RA seems relatively conservative. It is likely the case that enteroids fail to express IL-10RA in a pattern resembling *in vivo* expression due to the lack of exogenous stimuli. One example is that epithelial IL-10 receptors can be induced by a variety of microbial metabolites (Alexeev et al., 2018; Kominsky et al., 2014; Lanis et al., 2017; Zheng et al., 2017).

4.6. IL-10R signaling in IEC

The principal signaling pathway of IL-10 through the IL-10R is mainly through STAT3 phosphorylation, but infrequently also STAT1 and STAT5 phosphorylation (Shouval et al., 2014; Weber-Nordtt et al., 1996). STAT3 signaling plays an important regulatory role in the intestinal epithelium, as IEC-specific knockout of STAT3 has been shown to disrupt IEC in enteroids, and aggravate DSS-induced colitis in mice (Jung et al., 2019; Willson et al., 2013). IL-10 can trigger phosphorylation of STAT3 at both serine (SER727) and tyrosine (TYR705) positions. While phospho-TYR705 stabilizes the STAT3 dimer and facilitates translocation of the dimer to the nucleus to activate transcription of target genes, phospho-SER727 was reported to regulate the longevity of STAT3 activation through tyrosine-dephosphorylation (Wakahara et al., 2012; Yang et

al., 2019). Presumably, both phosphorylation events are important in a robust STAT3 response.

Interestingly, cells within both WT and IL-10KO enteroids possess constitutive levels of pSTAT3, yet IL-10KO enteroids seem to have a higher level of constitutive phospho-SER727. In terms of IL-10 stimulation, a faint increase in the signal for STAT3 phosphorylation was detected upon IL-10 basal administration to WT enteroids; however, in IL-10-stimulated IL-10KO enteroids, phospho-STAT3 levels (SER727 and TYR705) were lower than the constitutive levels in untreated IL-10KO enteroids. These observations may be explained by the constitutive expression of IL-10 being coupled with the expression of functional IL-10 receptors in WT, providing a basal level of IL-10R activation. Secondly, in IL-10KO enteroids, exogenous IL-10 possibly activates a different STAT molecule or even inhibits signal transduction through STAT3. The idea of a switch in STAT usage from STAT3 to STAT1 was reported in IL-10-treated macrophages after pre-exposure with IFN-γ (Herrero et al., 2003). Thirdly, given that IEC can produce cytokines other than IL-10 that can activate STAT3, such as IL-6 and IL-15 (Mizoguchi, 2012; Stadnyk, 2002), IL-10KO enteroids might have increased levels of these mediators driving the STAT switch. One of the important model improvements enteroids offer is that the cells are polarized, and we found IL-10R on both side of Paneth cells and basal receptors on other cell types. This introduces the interesting prospect that activation of receptors on one side may trigger a transcriptional program different than activation on the opposite side of the cell. One challenge to testing this idea is getting any agonist

into the lumen of enteroids. Thus, to further explore the signaling pathway of IL-10 in the polarized IECs, a 2D enteroid monolayer system was established from enteroids.

Strikingly, WT enteroid monolayers responded with a more robust phospho-TYR705 signal when stimulated with IL-10 administered apically compared to basally. Unless this is simply due to the number of receptors in each membrane, this result confirms our speculation that apical and basal IL-10R exerts different responses upon stimulation with IL-10. This observation is reinforced by a study reporting that upregulation of epithelial apical IL-10 receptors corresponds with increased phosphorylation of STAT3 following IL-10 stimulation (Kominsky et al., 2014). We also observed that STAT3 in IL-10KO monolayers was less robustly activated with apical IL-10, compared to apically-IL-10-stimulated WT monolayer. This observation implies that epithelial IL-10 influences STAT3-dependent signaling pathway through the apical IL-10 receptor. Importantly, given that IL-10 secreted by cells in the lamina propria, even by IELs, is unlikely to be available to apical receptors on IEC, our evidence suggests that the stimulation of apical IL-10 receptor by epithelial IL-10 is non-redundant to exogenous IL-10.

CHAPTER 5: CONCLUSION

Being the master regulator of gut homeostasis, IL-10 has been regularly shown to play critical roles in mucosal immunity and the epithelial barrier. In this study, we build on the evidence having demonstrated that constitutive epithelial IL-10 secretion likely acts in an autocrine fashion on Paneth cells and supports Paneth cell development. Importantly, we have shown that the role of apically-secreted epithelial-derived IL-10 is likely to be distinct from basally-available exogenous IL-10. This concept is supported by the fact that IL-10KO Paneth cells are deficient in some mediators and that the deficiency is not reversed by the addition of IL-10 to the basal side of the cells. Considering this unique role of epithelial IL-10 in the development and maintenance of the intestinal epithelium, it is paramount to confirm this finding *in vivo* and understand the significance of this IL-10 source in the context of homeostasis in health or disease.

REFERENCES

Abrams, J., Figdor, C. G., De Waal Malefyt, R., Bennett, B., & De Vries, J. E. (1991). Interleukin 10(IL-10) inhibits cytokine synthesis by human monocytes: An autoregulatory role of IL-10 produced by monocytes. *Journal of Experimental Medicine*, *174*(5), 1209–1220.

Alameddine, J., Godefroy, E., Papargyris, L., Sarrabayrouse, G., Tabiasco, J., Bridonneau, C., Yazdanbakhsh, K., Sokol, H., Altare, F., & Jotereau, F. (2019). *Faecalibacterium prausnitzii* skews human DC to prime IL10-producing T cells through TLR2/6/JNK signaling and IL-10, IL-27, CD39, and IDO-1 induction. *Frontiers in Immunology*, *10*, 143.

Alexeev, E. E., Lanis, J. M., Kao, D. J., Campbell, E. L., Kelly, C. J., Battista, K. D., Gerich, M. E., Jenkins, B. R., Walk, S. T., Kominsky, D. J., & Colgan, S. P. (2018). Microbiota-derived indole metabolites promote human and murine intestinal homeostasis through regulation of interleukin-10 receptor. *American Journal of Pathology*, *188*(5), 1183–1194.

Allaire, J. M., Crowley, S. M., Law, H. T., Chang, S. Y., Ko, H. J., & Vallance, B. A. (2018). The intestinal epithelium: Central coordinator of mucosal immunity. *Trends in Immunology*, *39*(9), 677–696.

Almeqdadi, M., Mana, M. D., Roper, J., & Yilmaz, Ö. H. (2019). Gut organoids: Mini-tissues in culture to study intestinal physiology and disease. *American Journal of Physiology - Cell Physiology*, *317*(3), C405–C419.

Altay, G., Larrañaga, E., Tosi, S., Barriga, F. M., Batlle, E., Fernández-Majada, V., & Martínez, E. (2019). Self-organized intestinal epithelial monolayers in crypt and villus-like domains show effective barrier function. *Scientific Reports*, *9*, 10140.

Atarashi, K., Tanoue, T., Shima, T., Imaoka, A., Kuwahara, T., Momose, Y., Cheng, G., Yamasaki, S., Saito, T., Ohba, Y., Taniguchi, T., Takeda, K., Hori, S., Ivanov, I. I., Umesaki, Y., Itoh, K., & Honda, K. (2011). Induction of colonic regulatory T cells by indigenous *Clostridium* species. *Science*, *331*(6015), 337–341.

Autschbach, F., Braunstein, J., Helmke, B., Zuna, I., Schürmann, G., Niemir, Z. I., Wallich, R., Otto, H. F., & Meuer, S. C. (1998). *In situ* expression of interleukin-10 in noninflamed human gut and in inflammatory bowel disease. *American Journal of Pathology*, *153*(1), 121–130.

Avalle, L., Pensa, S., Regis, G., Novelli, F., & Poli, V. (2012). STAT1 and STAT3 in tumorigenesis: A matter of balance. *JAKSTAT*, *1*(2), 65–72.

Ayabe, T., Satchell, D. P., Wilson, C. L., Parks, W. C., Selsted, M. E., & Ouellette, A. J. (2000). Secretion of microbicidal α-defensins by intestinal Paneth cells in response to bacteria. *Nature Immunology*, *1*(2), 113–118.

Bando, J. K., Gilfillan, S., Di Luccia, B., Fachi, J. L., Sécca, C., Cella, M., & Colonna, M. (2020). ILC2s are the predominant source of intestinal ILC-derived IL-10. *Journal of Experimental Medicine*, *217*(2), e20191520.

Beagley, K. W., Fujihashi, K., Lagoo, A. S., Lagoo-Deenadaylan, S., Black, C. A., Murray, A. M., Sharmanov, A. T., Yamamoto, M., McGhee, J. R., & Elson, C. O. (1995). Differences in intraepithelial lymphocyte T cell subsets isolated from murine small versus large intestine. *Journal of Immunology (Baltimore, Md. : 1950)*, *154*(11), 5611–5619.

Beck, P. L., Rosenberg, I. M., Xavier, R. J., Koh, T., Wong, J. F., & Podolsky, D. K. (2003). Transforming growth factor-β mediates intestinal healing and susceptibility to injury in vitro and in vivo through epithelial cells. *American Journal of Pathology*, *162*(2), 597–608.

Berkowitz, L., Pardo-Roa, C., Ramírez, G., Vallejos, O. P., Sebastián, V. P., Riedel, C. A., Álvarez-Lobos, M., & Bueno, S. M. (2019). The absence of interleukin 10 affects the morphology, differentiation, granule content and the production of cryptidin-4 in Paneth cells in mice. *PLoS ONE*, *14*(9), e0221618.

Beumer, J., Puschhof, J., Bauzá-Martinez, J., Martínez-Silgado, A., Elmentaite, R., James, K. R., Ross, A., Hendriks, D., Artegiani, B., Busslinger, G. A., Ponsioen, B., Andersson-Rolf, A., Saftien, A., Boot, C., Kretzschmar, K., Geurts, M. H., Bar-Ephraim, Y. E., Pleguezuelos-Manzano, C., Post, Y., … Clevers, H. (2020). High-resolution mRNA and secretome atlas of human enteroendocrine cells. *Cell*, *181*(6), 1291–1306.

Bevins, C. L., & Salzman, N. H. (2011). Paneth cells, antimicrobial peptides and maintenance of intestinal homeostasis. *Nature Reviews Microbiology*, *9*(5), 356–368.

Bharhani, M. S., Borojevic, R., Basak, S., Ho, E., Zhou, P., & Croitoru, K. (2006). IL-10 protects mouse intestinal epithelial cells from Fas-induced apoptosis via modulating Fas expression and altering caspase-8 and FLIP expression. *American Journal of Physiology - Gastrointestinal and Liver Physiology*, *291*(5), G820–G829.

Birchenough, G. M. H., Nystrom, E. E. L., Johansson, M. E. V., & Hansson, G. C. (2016). A sentinel goblet cell guards the colonic crypt by triggering Nlrp6-dependent Muc2 secretion. *Science*, *352*(6293), 1535–1542.

Biton, M., Haber, A. L., Rogel, N., Burgin, G., Beyaz, S., Schnell, A., Ashenberg, O., Su, C. W., Smillie, C., Shekhar, K., Chen, Z., Wu, C., Ordovas-Montanes, J., Alvarez, D., Herbst, R. H., Zhang, M., Tirosh, I., Dionne, D., Nguyen, L. T., … Xavier, R. J. (2018). T helper cell cytokines modulate intestinal stem cell renewal and differentiation. *Cell*, *175*(5), 1307-1320.e22.

Bourreille, A., Segain, J. P., Raingeard de la Blétière, D., Siavoshian, S., Vallette, G., Galmiche, J. P., & Blottière, H. M. (1999). Lack of interleukin 10 regulation of antigen presentation-associated molecules expressed on colonic epithelial cells. *European Journal of Clinical Investigation*, *29*(1), 48–55.

Bowcutt, R., Forman, R., Glymenaki, M., Carding, S. R., Else, K. J., & Cruickshank, S. M. (2014). Heterogeneity across the murine small and large intestine. *World Journal of Gastroenterology*, *20*(41), 15216–15232.

Brooks, D. G., Walsh, K. B., Elsaesser, H., & Oldstone, M. B. A. (2010). IL-10 directly suppresses CD4 but not CD8 T cell effector and memory responses following acute viral infection. *Proceedings of the National Academy of Sciences of the United States of America*, *107*(7), 3018–3023.

Burger, E., Araujo, A., López-Yglesias, A., Rajala, M. W., Geng, L., Levine, B., Hooper, L. V., Burstein, E., & Yarovinsky, F. (2018). Loss of Paneth cell autophagy causes acute susceptibility to Toxoplasma gondii-mediated inflammation. *Cell Host and Microbe*, *23*(2), 177–190.

Cassatella, M. A., Meda, L., Gasperini, S., Calzetti, F., & Bonora, S. (1994). Interleukin 10 (IL-10) upregulates IL-1 receptor antagonist production from lipopolysaccharide-stimulated human polymorphonuclear leukocytes by delaying mRNA degradation. *Journal of Experimental Medicine*, *179*(5), 1695–1699.

Castillo, P. A., Nonnecke, E. B., Ossorio, D. T., Tran, M. T. N., Goley, S. M., Lönnerdal, B., Underwood, M. A., & Bevins, C. L. (2019). An experimental approach to rigorously assess Paneth cell α-defensin (Defa) mRNA expression in C57BL/6 mice. *Scientific Reports*, *9*, 13115.

Cella, M., Fuchs, A., Vermi, W., Facchetti, F., Otero, K., Lennerz, J. K. M., Doherty, J. M., Mills, J. C., & Colonna, M. (2009). A human natural killer cell subset provides an innate source of IL-22 for mucosal immunity. *Nature*, *457*(7230), 722–725.

Cheifetz, A. S. (2013). Management of active Crohn disease. *JAMA - Journal of the American Medical Association*, *309*(20), 2150–2158.

Clevers, H. C., & Bevins, C. L. (2013). Paneth cells: Maestros of the small intestinal crypts. *Annual Review of Physiology*, *75*, 289–311.

Commins, S., Steinke, J. W., & Borish, L. (2008). The extended IL-10 superfamily: IL-10, IL-19, IL-20, IL-22, IL-24, IL-26, IL-28, and IL-29. *Journal of Allergy and Clinical Immunology*, *121*(5), 1108–1111.

Couper, K. N., Blount, D. G., & Riley, E. M. (2008). IL-10: The master regulator of immunity to infection. *Journal of Immunology (Baltimore, Md. : 1950)*, *180*(9), 5771–5777.

Crespo-Piazuelo, D., Estellé, J., Revilla, M., Criado-Mesas, L., Ramayo-Caldas, Y., Óvilo, C., Fernández, A. I., Ballester, M., & Folch, J. M. (2018). Characterization of bacterial microbiota compositions along the intestinal tract in pigs and their interactions and functions. *Scientific Reports*, *8*, 12727.

de Leeuw, E., Burks, S. R., Li, X., Kao, J. P. Y., & Lu, W. (2007). Structure-dependent functional properties of human defensin 5. *FEBS Letters*, *581*(3), 315–520.

De Smedt, T., Van Mechelen, M., De Becker, G., Urbain, J., Leo, O., & Moser, M. (1997). Effect of interleukin-10 on dendritic cell maturation and function. *European Journal of Immunology*, *27*(5), 1229–1235.

De Winter, H., Elewaut, D., Turovskaya, O., Huflejt, M., Shimeld, C., Hagenbaugh, A., Binder, S., Takahashi, I., Kronenberg, M., & Cheroutre, H. (2002). Regulation of mucosal immune responses by recombinant interleukin 10 produced by intestinal epithelial cells in mice. *Gastroenterology*, *122*(7), 1829–1841.

Deng, F., Hu, J., Yang, X., Wang, Y., Lin, Z., Sun, Q., & Liu, K. (2020). Interleukin-10 expands transit-amplifying cells while depleting Lgr5+ stem cells via inhibition of Wnt and notch signaling. *Biochemical and Biophysical Research Communications*, *533*(4), 1330–1337.

Denning, T. L., Campbell, N. A., Song, F., Garofalo, R. P., Klimpel, G. R., Reyes, V. E., & Ernst, P. B. (2000). Expression of IL-10 receptors on epithelial cells from the murine small and large intestine. *International Immunology*, *12*(2), 133–139.

Dickensheets, H. L., Freeman, S. L., Smith, M. F., & Donnelly, R. P. (1997). Interleukin-10 upregulates tumor necrosis factor receptor type-II (p75) gene expression in endotoxin-stimulated human monocytes. *Blood*, *90*(10), 4162–4171.

Eckmann, L., Jung, H. C., Schürer-Maly, C., Panja, A., Morzycka-Wroblewska, E., & Kagnoff, M. F. (1993). Differential cytokine expression by human intestinal epithelial cell lines: Regulated expression of interleukin 8. *Gastroenterology*, *105*, 1689–1697.

Elphick, D. A., & Mahida, Y. R. (2005). Paneth cells: Their role in innate immunity and inflammatory disease. *Gut*, *54*(12), 1803–1809.

Eriguchi, Y., Nakamura, K., Yokoi, Y., Sugimoto, R., Takahashi, S., Hashimoto, D., Teshima, T., Ayabe, T., Selsted, M. E., & Ouellette, A. J. (2018). Essential role of IFN-γ in T cell-associated intestinal inflammation. *JCI Insight*, *3*(18), e121886.

Ernst, O., Glucksam-Galnoy, Y., Bhatta, B., Athamna, M., Ben-Dror, I., Glick, Y., Gerber, D., & Zor, T. (2019). Exclusive Temporal Stimulation of IL-10 Expression in LPS-Stimulated Mouse Macrophages by cAMP Inducers and Type I Interferons. *Frontiers in Immunology*, *10*, 1788.

Fahlgren, A., Hammarström, S., & Danielsson, Å. (2003). Increased expression of antimicrobial peptides and lysozyme in colonic epithelial cells of patients with ulcerative colitis. *Clinical and Experimental Immunology*, *131*(1), 90–101.

Farin, H. F., Karthaus, W. R., Kujala, P., Rakhshandehroo, M., Schwank, G., Vries, R. G. J., Kalkhoven, E., Nieuwenhuis, E. E. S., & Clevers, H. (2014). Paneth cell extrusion and release of antimicrobial products is directly controlled by immune cell-derived IFN-γ. *Journal of Experimental Medicine*, *211*(7), 1393–1405.

Forbester, J. L., Lees, E. A., Goulding, D., Forrest, S., Yeung, A., Speak, A., Clare, S., Coomber, E. L., Mukhopadhyay, S., Kraiczy, J., Schreiber, F., Lawley, T. D., Hancock, R. E. W., Uhlig, H. H., Zilbauer, M., Powrie, F., & Dougan, G. (2018). Interleukin-22 promotes phagolysosomal fusion to induce protection against *Salmonella enterica* Typhimurium in human epithelial cells. *Proceedings of the National Academy of Sciences of the United States of America*, *115*(40), 10118–10123.

Frick, A., Khare, V., Paul, G., Lang, M., Ferk, F., Knasmüller, S., Beer, A., Oberhuber, G., & Gasche, C. (2018). Overt increase of oxidative stress and DNA damage in murine and human colitis and colitis-associated neoplasia. *Molecular Cancer Research*, *16*(4), 634–642.

Fuss, I. J., Neurath, M. F., Boirivant, M., Fiocchi, C., & Strober, W. (1996). Disparate CD4+ lamina propria (LP) lymphokine secretion profiles in Iinflammatory bowel disease: Crohn's disease LP cells manifest increased secretion of IFN-γ, whereas ulcerative colitis LP cells manifest increased secretion of IL-5. *Journal of Immunology*, *157*(3), 1261–1270.

Gayer, C. P., & Basson, M. D. (2009). The effects of mechanical forces on intestinal physiology and pathology. *Cellular Signalling*, *21*(8), 1237–1244.

George, M. M., Rahman, M., Connors, J., & Stadnyk, A. W. (2019). Opinion: Are organoids the end of model evolution for studying host intestinal epithelium/microbe interactions? *Microorganisms*, *7*(10), 406.

Gerbe, F., Van Es, J. H., Makrini, L., Brulin, B., Mellitzer, G., Robine, S., Romagnolo, B., Shroyer, N. F., Bourgaux, J. F., Pignodel, C., Clevers, H., & Jay, P. (2011). Distinct ATOH1 and Neurog3 requirements define tuft cells as a new secretory cell type in the intestinal epithelium. *Journal of Cell Biology*, *192*(5), 767–780.

Ghosh, D., Porter, E., Shen, B., Lee, S. K., Wilk, D., Drazba, J., Yadav, S. P., Crabb, J. W., Ganz, T., & Bevins, C. L. (2002). Paneth cell trypsin is the processing enzyme for human defensin-5. *Nature Immunology*, *3*(6), 583–590.

Goto, Y. (2019). Epithelial cells as a transmitter of signals from commensal bacteria and host immune cells. *Frontiers in Immunology*, *10*, 2057.

Goto, Y., Obata, T., Kunisawa, J., Sato, S., Ivanov, I. I., Lamichhane, A., Takeyama, N., Kamioka, M., Sakamoto, M., Matsuki, T., Setoyama, H., Imaoka, A., Uematsu, S., Akira, S., Domino, S. E., Kulig, P., Becher, B., Renauld, J. C., Sasakawa, C., … Kiyono, H. (2014). Innate lymphoid cells regulate intestinal epithelial cell glycosylation. *Science*, *345*(6202), 1254009.

Gribble, F. M., & Reimann, F. (2016). Enteroendocrine cells: Chemosensors in the intestinal epithelium. *Annual Review of Physiology*, *78*, 277–299.

Grün, D., Muraro, M. J., Boisset, J. C., Wiebrands, K., Lyubimova, A., Dharmadhikari, G., van den Born, M., van Es, J., Jansen, E., Clevers, H., de Koning, E. J. P., & van Oudenaarden, A. (2016). De novo prediction of stem cell identity using single-cell transcriptome data. *Cell Stem Cell*, *19*(2), 266–277.

Haber, A. L., Biton, M., Rogel, N., Herbst, R. H., Shekhar, K., Smillie, C., Burgin, G., Delorey, T. M., Howitt, M. R., Katz, Y., Tirosh, I., Beyaz, S., Dionne, D., Zhang, M., Raychowdhury, R., Garrett, W. S., Rozenblatt-Rosen, O., Shi, H. N., Yilmaz, O., … Regev, A. (2017). A single-cell survey of the small intestinal epithelium. *Nature*, *551*(7680), 333–339.

Hasnain, S. Z., Tauro, S., Das, I., Tong, H., Chen, A. H., Jeffery, P. L., McDonald, V., Florin, T. H., & McGuckin, M. A. (2013). IL-10 promotes production of intestinal mucus by suppressing protein misfolding and endoplasmic reticulum stress in goblet cells. *Gastroenterology*, *144*(2), 357–368.

Heida, F. H., Beyduz, G., Bulthuis, M. L. C., Kooi, E. M. W., Bos, A. F., Timmer, A., & Hulscher, J. B. F. (2016). Paneth cells in the developing gut: When do they arise and when are they immune competent? *Pediatric Research*, *80*, 306–310.

Herrero, C., Hu, X., Li, W. P., Samuels, S., Sharif, M. N., Kotenko, S., & Ivashkiv, L. B. (2003). Reprogramming of IL-10 activity and signaling by IFN-γ. *Journal of Immunology*, *171*(10), 5034–5041.

Hyun, J., Romero, L., Riveron, R., Flores, C., Kanagavelu, S., Chung, K. D., Alonso, A., Sotolongo, J., Ruiz, J., Manukyan, A., Chun, S., Singh, G., Salas, P., Targan, S. R., & Fukata, M. (2015). Human intestinal epithelial cells express interleukin-10 through Toll-like receptor 4-mediated epithelial-macrophage crosstalk. *Journal of Innate Immunity*, *7*(1), 87–101.

Iliev, I. D., Matteoli, G., & Rescigno, M. (2007). The yin and yang of intestinal epithelial cells in controlling dendritic cell function. *Journal of Experimental Medicine*, *204*(10), 2253–2257.

Inaba, Y., Ashida, T., Ito, T., Ishikawa, C., Tanabe, H., Maemoto, A., Watari, J., Ayabe, T., Mizukami, Y., Fujiya, M., & Kohgo, Y. (2010). Expression of the antimicrobial peptide α-defensin/cryptdins in intestinal crypts decreases at the initial phase of intestinal inflammation in a model of inflammatory bowel disease, IL-10-deficient mice. *Inflammatory Bowel Diseases*, *16*(9), 1488–1495.

Ito, R., Shin-Ya, M., Kishida, T., Urano, A., Takada, R., Sakagami, J., Imanishi, J., Kita, M., Ueda, Y., Iwakura, Y., Kataoka, K., Okanoue, T., & Mazda, O. (2006). Interferon-gamma is causatively involved in experimental inflammatory bowel disease in mice. *Clinical and Experimental Immunology*, *146*(2), 330–338.

Itoh, K., & Hirohata, S. (1995). The role of IL-10 in human B cell activation, proliferation, and differentiation. *Journal of Immunology (Baltimore, Md. : 1950)*, *154*(9), 4341–4350.

Iyer, S. S., & Cheng, G. (2012). Role of interleukin 10 transcriptional regulation in inflammation and autoimmune disease. *Critical Reviews in Immunology*, *31*(1), 23–63.

Jeffery, V., Goldson, A. J., Dainty, J. R., Chieppa, M., & Sobolewski, A. (2017). IL-6 signaling regulates small intestinal crypt homeostasis. *Journal of Immunology*, *199*(1), 303–311.

Jeon, S. G., Kayama, H., Ueda, Y., Takahashi, T., Asahara, T., Tsuji, H., Tsuji, N. M., Kiyono, H., Ma, J. S., Kusu, T., Okumura, R., Hara, H., Yoshida, H., Yamamoto, M., Nomoto, K., & Takeda, K. (2012). Probiotic *Bifidobacterium breve* induces IL-10-producing Tr1 cells in the colon. *PLoS Pathogens*, *8*(5), e1002714.

Jung, H. C., Eckmann, L., Yang, S. K., Panja, A., Fierer, J., Morzycka-Wroblewska, E., & Kagnoff, M. F. (1995). A distinct array of proinflammatory cytokines is expressed in human colon epithelial cells in response to bacterial invasion. *Journal of Clinical Investigation*, *95*(1), 55–65.

Jung, K. B., Kwon, O., Lee, M.-O., Lee, H., Son, Y. S., Habib, O., Oh, J.-H., Cho, H.-S., Jung, C.-R., Kim, J., & Son, M.-Y. (2019). Blockade of STAT3 causes severe in vitro and in vivo maturation defects in intestinal organoids derived from human embryonic stem cells. *Journal of Clinical Medicine*, *8*(7), 976.

Kamanaka, M., Kim, S. T., Wan, Y. Y., Sutterwala, F. S., Lara-Tejero, M., Galán, J. E., Harhaj, E., & Flavell, R. A. (2006). Expression of interleukin-10 in intestinal lymphocytes detected by an interleukin-10 reporter knockin tiger mouse. *Immunity*, *25*(6), 941–952.

Kasten, K. R., Muenzer, J. T., & Caldwell, C. C. (2010). Neutrophils are significant producers of IL-10 during sepsis. *Biochemical and Biophysical Research Communications*, *393*(1), 28–31.

Kennedy, E. A., King, K. Y., & Baldridge, M. T. (2018). Mouse microbiota models: Comparing germ-free mice and antibiotics treatment as tools for modifying gut bacteria. *Frontiers in Physiology*, *9*, 1534.

Khare, V., Krnjic, A., Frick, A., Gmainer, C., Asboth, M., Jimenez, K., Lang, M., Baumgartner, M., Evstatiev, R., & Gasche, C. (2019). Mesalamine and azathioprine modulate junctional complexes and restore epithelial barrier function in intestinal inflammation. *Scientific Reports*, *9*(1), 2842.

Kominsky, D. J., Campbell, E. L., Ehrentraut, S. F., Wilson, K. E., Kelly, C. J., Glover, L. E., Collins, C. B., Bayless, A. J., Saeedi, B., Dobrinskikh, E., Bowers, B. E., MacManus, C. F., Müller, W., Colgan, S. P., & Bruder, D. (2014). IFN-γ–mediated induction of an apical IL-10 receptor on polarized intestinal epithelia. *The Journal of Immunology*, *192*(3), 1267–1276.

Kotenko, S. V., Krause, C. D., Izotova, L. S., Pollack, B. P., Wu, W., & Pestka, S. (1997). Identification and functional characterization of a second chain of the interleukin-10 receptor complex. *EMBO Journal*, *16*(19), 5894–5903.

Kotlarz, D., Beier, R., Murugan, D., Diestelhorst, J., Jensen, O., Boztug, K., Pfeifer, D., Kreipe, H., Pfister, E. D., Baumann, U., Puchalka, J., Bohne, J., Egritas, O., Dalgic, B., Kolho, K. L., Sauerbrey, A., Buderus, S., Güngör, T., Enninger, A., … Klein, C. (2012). Loss of interleukin-10 signaling and infantile inflammatory bowel disease: Implications for diagnosis and therapy. *Gastroenterology*, *143*(2), 347–355.

Kozuka, K., He, Y., Koo-McCoy, S., Kumaraswamy, P., Nie, B., Shaw, K., Chan, P., Leadbetter, M., He, L., Lewis, J. G., Zhong, Z., Charmot, D., Balaa, M., King, A. J., Caldwell, J. S., & Siegel, M. (2017). Development and characterization of a human and mouse intestinal epithelial cell monolayer platform. *Stem Cell Reports*, *9*(6), 1976–1990.

Krndija, D., Marjou, F. El, Guirao, B., Richon, S., Leroy, O., Bellaiche, Y., Hannezo, E., & Vignjevic, D. M. (2019). Active cell migration is critical for steady-state epithelial turnover in the gut. *Science*, *365*(6454), 705–710.

Kucharzik, T., Lügering, N., Pauels, H. G., Domschke, W., & Stoll, R. (1998). IL-4, IL-10 and IL-13 down-regulate monocyte-chemoattracting protein-1 (MCP-1) production in activated intestinal epithelial cells. *Clinical and Experimental Immunology*, *111*(1), 152–157.

Kühn, R., Löhler, J., Rennick, D., Rajewsky, K., & Müller, W. (1993). Interleukin-10-deficient mice develop chronic enterocolitis. *Cell*, *75*(2), 263–274.

Kumar, K. K., Burgess, A. W., & Gulbis, J. M. (2014). Structure and function of LGR5: An enigmatic G-protein coupled receptor marking stem cells. *Protein Science*, *23*(5), 551–565.

Lanis, J. M., Alexeev, E. E., Curtis, V. F., Kitzenberg, D. A., Kao, D. J., Battista, K. D., Gerich, M. E., Glover, L. E., Kominsky, D. J., & Colgan, S. P. (2017). Tryptophan metabolite activation of the aryl hydrocarbon receptor regulates IL-10 receptor expression on intestinal epithelia. *Mucosal Immunology*, *10*(5), 1133–1144.

Latorre, E., Layunta, E., Grasa, L., Pardo, J., García, S., Alcalde, A. I., & Mesonero, J. E. (2018). Toll-like receptors 2 and 4 modulate intestinal IL-10 differently in ileum and colon. *United European Gastroenterology Journal*, *6*(3), 446–453.

Latorre, R., Sternini, C., De Giorgio, R., & Greenwood-Van Meerveld, B. (2016). Enteroendocrine cells: A review of their role in brain-gut communication. *Neurogastroenterology and Motility*, *28*(5), 620–630.

Lee, G. S., Cody, A. S., Johnson, K. C., Zhao, H., Odelberg, S. J., Li, D. Y., & Zhu, W. (2019). Estrogen enhances female small intestine epithelial organoid regeneration. *Journal of Bio-X Research*, *2*(1), 9–15.

Li, C. K. F., Seth, R., Gray, T., Bayston, R., Mahida, Y. R., & Wakelin, D. (1998). Production of proinflammatory cytokines and inflammatory mediators in human intestinal epithelial cells after invasion by Trichinella spiralis. *Infection and Immunity*, *66*(5), 2200–2206.

Lorén, V., Cabré, E., Ojanguren, I., Domènech, E., Pedrosa, E., García-Jaraquemada, A., Mañosa, M., & Manyé, J. (2015). Interleukin-10 enhances the intestinal epithelial barrier in the presence of corticosteroids through p38 MAPK activity in Caco-2 monolayers: A possible mechanism for steroid responsiveness in ulcerative colitis. *PLoS ONE*, *10*(6), e0130921.

Lu, W., & de Leeuw, E. (2013). Pro-inflammatory and pro-apoptotic properties of Human Defensin 5. *Biochemical and Biophysical Research Communications*, *436*(3), 557–562.

Lueschow, S. R., & McElroy, S. J. (2020). The Paneth cell: The curator and defender of the immature small intestine. *Frontiers in Immunology*, *11*, 587.

Madsen, K. L., Lewis, S. A., Tavernini, M. M., Hibbard, J., & Fedorak, R. N. (1997). Interleukin 10 prevents cytokine-induced disruption of T84 monolayer barrier integrity and limits chloride secretion. *Gastroenterology*, *113*(1), 151–159.

Mantis, N. J., Rol, N., & Corthésy, B. (2011). Secretory IgA's complex roles in immunity and mucosal homeostasis in the gut. *Mucosal Immunology*, *4*, 603–611.

Matthews, J. R., Sansom, O. J., & Clarke, A. R. (2011). Absolute requirement for STAT3 function in small-intestine crypt stem cell survival. *Cell Death and Differentiation*, *18*(12), 1934–1943.

Mazmanian, S. K., Round, J. L., & Kasper, D. L. (2008). A microbial symbiosis factor prevents intestinal inflammatory disease. *Nature*, *453*(7195), 620–625.

McDole, J. R., Wheeler, L. W., McDonald, K. G., Wang, B., Konjufca, V., Knoop, K. A., Newberry, R. D., & Miller, M. J. (2012). Goblet cells deliver luminal antigen to CD103 + dendritic cells in the small intestine. *Nature*, *483*(7389), 345–349.

Meran, L., Baulies, A., & Li, V. S. W. (2017). Intestinal stem cell niche: The extracellular matrix and cellular components. *Stem Cells International*, *2017*, 7970385.

Michalsky, M. P., Deitch, E. A., Ding, J., Lu, Q., & Huang, Q. (1997). Interleukin-6 and tumor necrosis factor production in an enterocyte cell model (CACO-2) during exposure to Escherichia coli. *Shock*, *7*(2), 139–146.

Miller, M. J., Knoop, K. A., & Newberry, R. D. (2014). Mind the GAPs: Insights into intestinal epithelial barrier maintenance and luminal antigen delivery. *Mucosal Immunology*, *7*, 452–454.

Mishima, Y., Oka, A., Liu, B., Herzog, J. W., Eun, C. S., Fan, T. J., Bulik-Sullivan, E., Carroll, I. M., Hansen, J. J., Chen, L., Wilson, J. E., Fisher, N. C., Ting, J. P. Y., Nochi, T., Wahl, A., Victor Garcia, J., Karp, C. L., & Balfour Sartor, R. (2019). Microbiota maintain colonic homeostasis by activating TLR2/MyD88/PI3K signaling in IL-10-producing regulatory B cells. *Journal of Clinical Investigation*, *129*(9), 3702–3716.

Mizoguchi, A. (2012). Healing of intestinal inflammation by IL-22. *Inflammatory Bowel Diseases*, *18*(9), 1777–1784.

Moens, E., & Veldhoen, M. (2012). Epithelial barrier biology: Good fences make good neighbours. *Immunology*, *135*(1), 1–8.

Moorefield, E. C., Andres, S. F., Blue, R. E., Van Landeghem, L., Mah, A. T., Santoro, M. A., & Ding, S. (2017). Aging effects on intestinal homeostasis associated with expansion and dysfunction of intestinal epithelial stem cells. *Aging*, *9*(8), 1898–1915.

Moran, C. J., Walters, T. D., Guo, C. H., Kugathasan, S., Klein, C., Turner, D., Wolters, V. M., Bandsma, R. H., Mouzaki, M., Zachos, M., Langer, J. C., Cutz, E., Benseler, S. M., Roifman, C. M., Silverberg, M. S., Griffiths, A. M., Snapper, S. B., & Muise, A. M. (2013). IL-10R polymorphisms are associated with very-early-onset ulcerative colitis. *Inflammatory Bowel Diseases*, *19*(1), 115–123.

Morhardt, T. L., Hayashi, A., Ochi, T., Quirós, M., Kitamoto, S., Nagao-Kitamoto, H., Kuffa, P., Atarashi, K., Honda, K., Kao, J. Y., Nusrat, A., & Kamada, N. (2019). IL-10 produced by macrophages regulates epithelial integrity in the small intestine. *Scientific Reports*, *9*(1), 1223.

Mosser, D. M., & Zhang, X. (2008). Interleukin-10: New perspectives on an old cytokine. *Immunol Rev*, *226*(1), 205–218.

Musuraca, G., De Matteis, S., Napolitano, R., Papayannidis, C., Guadagnuolo, V., Fabbri, F., Cangini, D., Ceccolini, M., Giannini, M. B., Lucchesi, A., Ronconi, S., Mariotti, P., Savini, P., Tani, M., Fattori, P. P., Guidoboni, M., Martinelli, G., Zoli, W., Amadori, D., & Carloni, S. (2015). IL-17/IL-10 double-producing T cells: New link between infections, immunosuppression and acute myeloid leukemia. *Journal of Translational Medicine*, *13*, 229.

Noben, M., Vanhove, W., Arnauts, K., Santo Ramalho, A., Van Assche, G., Vermeire, S., Verfaillie, C., & Ferrante, M. (2017). Human intestinal epithelium in a dish: Current models for research into gastrointestinal pathophysiology. *United European Gastroenterology Journal*, *5*(8), 1073–1081.

Noble, A., Giorgini, A., & Leggat, J. A. (2006). Cytokine-induced IL-10-secreting CD8 T cells represent a phenotypically distinct suppressor T-cell lineage. *Blood*, *107*(11), 4475–4483.

Nozaki, K., Mochizuki, W., Matsumoto, Y., Matsumoto, T., Fukuda, M., Mizutani, T., Watanabe, M., & Nakamura, T. (2016). Co-culture with intestinal epithelial organoids allows efficient expansion and motility analysis of intraepithelial lymphocytes. *Journal of Gastroenterology*, *51*(3), 206–213.

Nyström, E. E. L., Martinez-Abad, B., Arike, L., Birchenough, G. M. H., Nonnecke, E. B., Castillo, P. A., Svensson, F., Bevins, C. L., Hansson, G. C., & Johansson, M. E. V. (2021). An intercrypt subpopulation of goblet cells is essential for colonic mucus barrier function. *Science*, *372*(6539), eabb1590.

O'Farrell, A. M., Liu, Y., Moore, K. W., & Mui, A. L. F. (1998). IL-10 inhibits macrophage activation and proliferation by distinct signaling mechanisms: Evidence for Stat3-dependent and -independent pathways. *EMBO Journal*, *17*(4), 1006–1018.

Oshima, H., Kok, S. Y., Nakayama, M., Murakami, K., Voon, D. C. C., Kimura, T., & Oshima, M. (2019). Stat3 is indispensable for damage-induced crypt regeneration but not for Wnt-driven intestinal tumorigenesis. *FASEB Journal*, *33*(2), 1873–1886.

Pabst, R., Russell, M. W., & Brandtzaeg, P. (2008). Tissue distribution of lymphocytes and plasma cells and the role of the gut. *Trends in Immunology*, *29*(5), 206–208.

Pan, D., Das, A., Lala, W., Kenway-Lynch, C. S., Liu, D. X., Veazey, R. S., & Pahar, B. (2013). Interleukin-10 prevents epithelial cell apoptosis by regulating IFNγ and TNFα expression in rhesus macaque colon explants. *Cytokine*, *64*(1), 30–34.

Pan, D., Kenway-Lynch, C. S., Lala, W., Veazey, R. S., Lackner, A. A., Das, A., & Pahar, B. (2014). Lack of interleukin-10-mediated anti-inflammatory signals and upregulated interferon gamma production are linked to increased intestinal epithelial cell apoptosis in pathogenic simian immunodeficiency virus infection. *Journal of Virology*, *88*(22), 13015–13028.

Panja A, Zhou Z, Mullin G, M. L. (1995). Secretion and regulation of IL-10 by intestinal epithelial cells. *Gastroenterology*, *108*(4), A890.

Panja, A., Siden, E., & Mayer, L. (1995). Synthesis and regulation of accessory/proinflammatory cytokines by intestinal epithelial cells. *Clinical and Experimental Immunology*, *100*(2), 298–305.

Pelaseyed, T., Bergström, J. H., Gustafsson, J. K., Ermund, A., Birchenough, G. M. H., Schütte, A., van der Post, S., Svensson, F., Rodríguez-Piñeiro, A. M., Nyström, E. E. L., Wising, C., Johansson, M. E. V., & Hansson, G. C. (2014). The mucus and mucins of the goblet cells and enterocytes provide the first defense line of the gastrointestinal tract and interact with the immune system. *Immunological Reviews*, *260*(1), 8–20.

Pickert, G., Neufert, C., Leppkes, M., Zheng, Y., Wittkopf, N., Warntjen, M., Lehr, H. A., Hirth, S., Weigmann, B., Wirtz, S., Ouyang, W., Neurath, M. F., & Becker, C. (2009). STAT3 links IL-22 signaling in intestinal epithelial cells to mucosal wound healing. *Journal of Experimental Medicine*, *206*(7), 1465–1472.

Prandi, S., Bromke, M., Hübner, S., Voigt, A., Boehm, U., Meyerhof, W., & Behrens, M. (2013). A subset of mouse colonic goblet cells expresses the bitter taste receptor Tas2r131. *PLoS ONE*, *8*(12), e82820.

Quiros, M., Nishio, H., Neumann, P. A., Siuda, D., Brazil, J. C., Azcutia, V., Hilgarth, R., O'Leary, M. N., Garcia-Hernandez, V., Leoni, G., Feng, M., Bernal, G., Williams, H., Dedhia, P. H., Gerner-Smidt, C., Spence, J., Parkos, C. A., Denning, T. L., & Nusrat, A. (2017). Macrophage-derived IL-10 mediates mucosal repair by epithelial WISP-1 signaling. *Journal of Clinical Investigation*, *127*(9), 3510–3520.

Reinecker, H. C., MacDermott, R. P., Mirau, S., Dignass, A., & Podolsky, D. K. (1996). Intestinal epithelial cells both express and respond to interleukin 15. *Gastroenterology*, *111*(6), 1706–1713.

Richter, K., Perriard, G., Behrendt, R., Schwendener, R. A., Sexl, V., Dunn, R., Kamanaka, M., Flavell, R. A., Roers, A., & Oxenius, A. (2013). Macrophage and T cell produced IL-10 promotes viral chronicity. *PLoS Pathogens*, *9*(11), e1003735.

Rieger, A., & Bar-Or, A. (2008). B-cell-derived interleukin-10 in autoimmune disease: Regulating the regulators. *Nature Reviews Immunology*, *8*(6), 486–487.

Rosas-Arellano, A., Villalobos-González, J. B., Palma-Tirado, L., Beltrán, F. A., Cárabez-Trejo, A., Missirlis, F., & Castro, M. A. (2016). A simple solution for antibody signal enhancement in immunofluorescence and triple immunogold assays. *Histochemistry and Cell Biology*, *146*(4), 421–430.

Rossi, O., Van Berkel, L. A., Chain, F., Tanweer Khan, M., Taverne, N., Sokol, H., Duncan, S. H., Flint, H. J., Harmsen, H. J. M., Langella, P., Samsom, J. N., & Wells, J. M. (2016). *Faecalibacterium prausnitzii* A2-165 has a high capacity to induce IL-10 in human and murine dendritic cells and modulates T cell responses. *Scientific Reports*, *6*, 18507.

Rothenberg, M. E., Nusse, Y., Kalisky, T., Lee, J. J., Dalerba, P., Scheeren, F., Lobo, N., Kulkarni, S., Sim, S., Qian, D., Beachy, P. A., Pasricha, P. J., Quake, S. R., & Clarke, M. F. (2012). Identification of a cKit+ colonic crypt base secretory cell that supports Lgr5+ stem cells in mice. *Gastroenterology*, *142*(5), 1195–1205.

Sabat, R., Grütz, G., Warszawska, K., Kirsch, S., Witte, E., Wolk, K., & Geginat, J. (2010). Biology of interleukin-10. *Cytokine and Growth Factor Reviews*, *21*(5), 331–344.

Salzman, N. H., Polin, R. A., Harris, M. C., Ruchelli, E., Hebra, A., Zirin-Butler, S., Jawad, A., Porter, E. M., & Bevins, C. L. (1998). Enteric defensin expression in necrotizing enterocolitis. *Pediatric Research*, *44*, 20–26.

Sanin, D. E., Prendergast, C. T., & Mountford, A. P. (2015). IL-10 production in macrophages is regulated by a TLR-driven CREB-mediated mechanism that is linked to genes involved in cell metabolism. *Journal of Immunology*, *195*(3), 1218–1232.

Sasaki, N., Sachs, N., Wiebrands, K., Ellenbroek, S. I. J., Fumagalli, A., Lyubimova, A., Begthel, H., Van Born, M. Den, Van Es, J. H., Karthaus, W. R., Li, V. S. W., López-Iglesias, C., Peters, P. J., Van Rheenen, J., Van Oudenaarden, A., & Clevers, H. (2016). Reg4+ deep crypt secretory cells function as epithelial niche for Lgr5+ stem cells in colon. *Proceedings of the National Academy of Sciences of the United States of America*, *113*(37), E5399–E5407.

Sato, T., Stange, D. E., Ferrante, M., Vries, R. G. J., Van Es, J. H., Van Den Brink, S., Van Houdt, W. J., Pronk, A., Van Gorp, J., Siersema, P. D., & Clevers, H. (2011). Long-term expansion of epithelial organoids from human colon, adenoma, adenocarcinoma, and Barrett's epithelium. *Gastroenterology*, *141*(5), 1762–1772.

Sato, T., Van Es, J. H., Snippert, H. J., Stange, D. E., Vries, R. G., Van Den Born, M., Barker, N., Shroyer, N. F., Van De Wetering, M., & Clevers, H. (2011). Paneth cells constitute the niche for Lgr5 stem cells in intestinal crypts. *Nature*, *469*(7330), 415–418.

Sato, T., Vries, R. G., Snippert, H. J., Van De Wetering, M., Barker, N., Stange, D. E., Van Es, J. H., Abo, A., Kujala, P., Peters, P. J., & Clevers, H. (2009). Single Lgr5 stem cells build crypt-villus structures in vitro without a mesenchymal niche. *Nature*, *459*(7244), 262–265.

Saxena, A., Khosraviani, S., Noel, S., Mohan, D., Donner, T., & Hamad, A. R. A. (2015). Interleukin-10 paradox: A potent immunoregulatory cytokine that has been difficult to harness for immunotherapy. *Cytokine*, *74*(1), 27–34.

Schneider, C., O'Leary, C. E., & Locksley, R. M. (2019). Regulation of immune responses by tuft cells. *Nature Reviews Immunology*, *19*(9), 584–593.

Schoenborn, A. A., von Furstenberg, R. J., Valsaraj, S., Hussain, F. S., Stein, M., Shanahan, M. T., Henning, S. J., & Gulati, A. S. (2019). The enteric microbiota regulates jejunal Paneth cell number and function without impacting intestinal stem cells. *Gut Microbes*, *10*(1), 45–58.

Schülke, S. (2018). Induction of interleukin-10 producing dendritic cells as a tool to suppress allergen-specific T helper 2 responses. *Frontiers in Immunology*, *19*(9), 455.

Schwerbrock, N. M. J., Makkink, M. K., van der Sluis, M., Büller, H. A., Einerhand, A. W. C., Sartor, R. B., & Dekker, J. (2004). Interleukin 10-deficient mice exhibit defective colonic Muc2 synthesis before and after induction of colitis by commensal bacteria. *Inflammatory Bowel Diseases*, *10*(6), 811–823.

Sellon, R. K., Tonkonogy, S., Schultz, M., Dieleman, L. A., Grenther, W., Balish, E., Rennick, D. M., & Sartor, R. B. (1998). Resident enteric bacteria are necessary for development of spontaneous colitis and immune system activation in interleukin-10-deficient mice. *Infection and Immunity*, *66*(11), 5224–5231.

Serrano, C., Galán, S., Rubio, J. F., Candelario-Martínez, A., Montes-Gómez, A. E., Chánez-Paredes, S., Cedillo-Barrón, L., Schnoor, M., Meraz-Ríos, M. A., Villegas-Sepúlveda, N., Ortiz-Navarrete, V., & Nava, P. (2019). Compartmentalized response of IL-6/STAT3 signaling in the colonic mucosa mediates colitis development. *Journal of Immunology*, *202*(4), 1239–1249.

Shaw, M. H., Freeman, G. J., Scott, M. F., Fox, B. A., Bzik, D. J., Belkaid, Y., & Yap, G. S. (2006). Tyk2 negatively regulates adaptive Th1 Immunity by mediating IL-10 signaling and promoting IFN-γ-dependent IL-10 reactivation. *Journal of Immunology*, *176*(12), 7263–7271.

Sheridan, B. S., & Lefrançois, L. (2010). Intraepithelial lymphocytes: To serve and protect. *Current Gastroenterology Reports*, *12*(6), 513–521.

Shi, C. Z., Chen, H. Q., Liang, Y., Xia, Y., Yang, Y. Z., Yang, J., Zhang, J. D., Wang, S. H., Liu, J., & Qin, H. L. (2014). Combined probiotic bacteria promotes intestinal epithelial barrier function in interleukin-10-gene-deficient mice. *World Journal of Gastroenterology*, *20*(16), 4636–4647.

Shin, W., Wu, A., Min, S., Shin, Y. C., Fleming, R. Y. D., Eckhardt, S. G., & Kim, H. J. (2020). Spatiotemporal gradient and instability of Wnt induce heterogeneous growth and differentiation of human intestinal organoids. *IScience*, *23*(8), 101372.

Shkoda, A., Ruiz, P. A., Daniel, H., Kim, S. C., Rogler, G., Sartor, R. B., & Haller, D. (2007). Interleukin-10 blocked endoplasmic reticulum stress in intestinal epithelial cells: Impact on chronic inflammation. *Gastroenterology*, *132*(1), 190–207.

Shouval, D. S., Ouahed, J., Biswas, A., Goettel, J. A., Horwitz, B. H., Klein, C., Muise, A. M., & Snapper, S. B. (2014). Interleukin 10 receptor signaling: Master regulator of intestinal mucosal homeostasis in mice and humans. *Advances in Immunology*, *122*, 177–210.

Simmonds, N., Furman, M., Karanika, E., Phillips, A., & Bates, A. W. H. (2014). Paneth cell metaplasia in newly diagnosed inflammatory bowel disease in children. *BMC Gastroenterology*.

Smith, L. K., Boukhaled, G. M., Condotta, S. A., Mazouz, S., Guthmiller, J. J., Vijay, R., Butler, N. S., Bruneau, J., Shoukry, N. H., Krawczyk, C. M., & Richer, M. J. (2018). Interleukin-10 directly inhibits CD8+ T cell function by enhancing N-Glycan branching to decrease antigen sensitivity. *Immunity*, *48*(2), 299–312.

Smith, R. D. (1995). Evidence for autocrine growth inhibition of rat intestinal epithelial (RIE-1) cells by transforming growth factor type-β. *Biochemistry and Molecular Biology International*, *35*(6), 1315–1321.

Smyth, D., Phan, V., Wang, A., & McKay, D. M. (2011). Interferon-γ-induced increases in intestinal epithelial macromolecular permeability requires the Src kinase Fyn. *Laboratory Investigation*, *91*, 764–777.

Snoeck, V., Goddeeris, B., & Cox, E. (2005). The role of enterocytes in the intestinal barrier function and antigen uptake. *Microbes and Infection*, *7*(7–8), 997–1004.

Soderholm, A. T., & Pedicord, V. A. (2019). Intestinal epithelial cells: at the interface of the microbiota and mucosal immunity. *Immunology*, *158*(4), 267–280.

Stadnyk, A. W. (2002). Intestinal epithelial cells as a source of inflammatory cytokines and chemokines. *Canadian Journal of Gastroenterology*, *16*(4), 241–246.

Steiner, T. S., Nataro, J. P., Poteet-Smith, C. E., Smith, J. A., & Guerrant, R. L. (2000). Enteroaggregative *Escherichia coli* expresses a novel flagellin that causes IL-8 release from intestinal epithelial cells. *Journal of Clinical Investigation*, *105*(12), 1769–1777.

Strauch, U. G., Obermeier, F., Grunwald, N., Gürster, S., Dunger, N., Schultz, M., Griese, D. P., Mähler, M., Schölmerich, J., & Rath, H. C. (2005). Influence of intestinal bacteria on induction of regulatory T cells: Lessons from a transfer model of colitis. *Gut*, *54*(11), 1546–1552.

Strober, Warren; Fuss, I. (2013). Pro-Inflammatory Cytokines in the Pathogenesis of IBD. *Gastroenterology*, *140*(6), 1756–1767.

Strzyz, P. (2019). Cryptic migration. *Nature Reviews Molecular Cell Biology*, *20*(10), 572.

Sun, X., Yang, H., Nose, K., Nose, S., Haxhija, E. Q., Koga, H., Feng, Y., & Teitelbaum, D. H. (2007). Decline in intestinal mucosal IL-10 expression and decreased intestinal barrier function in a mouse model of total parenteral nutrition. *American Journal of Physiology - Gastrointestinal and Liver Physiology*, *294*(1), G139–G147.

Tamagawa, Y., Ishimura, N., Uno, G., Yuki, T., Kazumori, H., Ishihara, S., Amano, Y., & Kinoshita, Y. (2012). Notch signaling pathway and Cdx2 expression in the development of Barrett's esophagus. *Laboratory Investigation*, *92*(6), 896–909.

Tanabe, Y., Nishibori, T., Su, L., Arduini, R. M., Baker, D. P., & David, M. (2005). Cutting edge: Role of STAT1, STAT3, and STAT5 in IFN-αβ responses in T lymphocytes. *Journal of Immunology*, *174*(2), 609–613.

Tanaka, M., Saito, H., Kusumi, T., Fukuda, S., Shimoyama, T., Sasaki, Y., Suto, K., Munakata, A., & Kudo, H. (2001). Spatial distribution and histogenesis of colorectal Paneth cell metaplasia in idiopathic inflammatory bowel disease. *Journal of Gastroenterology and Hepatology*, *16*(12), 1353–1359.

Thorne, C. A., Chen, I. W., Sanman, L. E., Cobb, M. H., Wu, L. F., & Altschuler, S. J. (2018). Enteroid monolayers reveal an autonomous WNT and BMP circuit controlling intestinal epithelial growth and organization. *Developmental Cell*, *44*(5), 624–633.

Trandem, K., Zhao, J., Fleming, E., & Perlman, S. (2011). Highly activated cytotoxic CD8 T cells express protective IL-10 at the peak of coronavirus-induced encephalitis. *Journal of Immunology*, *186*(6), 3642–3652.

Trinchieri, G. (2007). Interleukin-10 production by effector T cells: Th1 cells show self control. *Journal of Experimental Medicine*, *204*(2), 239–243.

Ueda, Y., Kayama, H., Jeon, S. G., Kusu, T., Isaka, Y., Rakugi, H., Yamamoto, M., & Takeda, K. (2010). Commensal microbiota induce LPS hyporesponsiveness in colonic macrophages via the production of IL-10. *International Immunology*, *22*(12), 953–962.

Vandenbroucke, R. E., Vanlaere, I., Van Hauwermeiren, F., Van Wonterghem, E., Wilson, C., & Libert, C. (2014). Pro-inflammatory effects of matrix metalloproteinase 7 in acute inflammation. *Mucosal Immunology*, *7*, 579–588.

Verma, R., Balakrishnan, L., Sharma, K., Khan, A. A., Advani, J., Gowda, H., Tripathy, S. P., Suar, M., Pandey, A., Gandotra, S., Prasad, T. S. K., & Shankar, S. (2016). A network map of Interleukin-10 signaling pathway. *Journal of Cell Communication and Signaling*, *10*(1), 61–67.

Vuik, F. E. R., Dicksved, J., Lam, S. Y., Fuhler, G. M., van der Laan, L. J. W., van de Winkel, A., Konstantinov, S. R., Spaander, M. C. W., Peppelenbosch, M. P., Engstrand, L., & Kuipers, E. J. (2019). Composition of the mucosa-associated microbiota along the entire gastrointestinal tract of human individuals. *United European Gastroenterology Journal*, *7*(7), 897–907.

Wakahara, R., Kunimoto, H., Tanino, K., Kojima, H., Inoue, A., Shintaku, H., & Nakajima, K. (2012). Phospho-Ser727 of STAT3 regulates STAT3 activity by enhancing dephosphorylation of phospho-Tyr705 largely through TC45. *Genes to Cells*, *17*(2), 132–145.

Walker, C. R., Hautefort, I., Dalton, J. E., Overweg, K., Egan, C. E., Bongaerts, R. J., Newton, D. J., Cruickshank, S. M., Andrew, E. M., & Carding, S. R. (2013). Intestinal intraepithelial lymphocyte-enterocyte crosstalk regulates production of bactericidal angiogenin 4 by Paneth cells upon microbial challenge. *PLoS ONE*, *8*(12), e84553.

Walker, S. R., Nelson, E. A., Yeh, J. E., Pinello, L., Yuan, G.-C., & Frank, D. A. (2013). STAT5 outcompetes STAT3 to regulate the expression of the oncogenic transcriptional modulator BCL6. *Molecular and Cellular Biology*, *33*(15), 2879–2890.

Wang, F., Wang, J., Liu, D., & Su, Y. (2010). Normalizing genes for real-time polymerase chain reaction in epithelial and nonepithelial cells of mouse small intestine. *Analytical Biochemistry*, *399*(2), 211–217.

Wang, S., Liu, J., Li, L., & Wice, B. M. (2004). Individual subtypes of rnteroendocrine cells in the mouse small intestine exhibit unique patterns of inositol 1,4,5-trisphosphate receptor expression. *Journal of Histochemistry and Cytochemistry*, *52*(1), 53–63.

Weber-Nordtt, R. M., Riley, J. K., Greenlund, A. C., Moore, K. W., Darnell, J. E., & Schreiber, R. D. (1996). Stat3 recruitment by two distinct ligand-induced, tyrosine-phosphorylated docking sites in the interleukin-10 receptor intracellular domain. *Journal of Biological Chemistry*, *271*(44), 27954–27961.

Wehinger, J., Gouilleux, F., Groner, B., Finke, J., Mertelsmann, R., & Weber-Nordt, R. M. (1996). IL-10 induces DNA binding activity of three STAT proteins (Stat1, Stat3, and Stat5) and their distinct combinatorial assembly in the promoters of selected genes. *FEBS Letters*, *394*(3), 365–370.

Werner, T., Shkoda, A., & Haller, D. (2007). Intestinal epithelial cell proteome in IL-10 deficient mice and IL-10 receptor reconstituted epithelial cells: Impact on chronic inflammation. *Journal of Proteome Research*, *6*(9), 3691–3704.

Wilbers, R. H. P., Van Raaij, D. R., Westerhof, L. B., Bakker, J., Smant, G., & Schots, A. (2017). Re-evaluation of IL-10 signaling reveals novel insights on the contribution of the intracellular domain of the IL-10R2 chain. *PLoS ONE*, *12*(10), e0186317.

Willson, T. A., Jurickova, I., Collins, M., & Denson, L. A. (2013). Deletion of intestinal epithelial cell STAT3 promotes T-lymphocyte STAT3 activation and chronic colitis following acute dextran sodium sulfate injury in mice. *Inflammatory Bowel Diseases*, *19*(3), 512–525.

Wilson, C. L., Ouellette, A. J., Satchell, D. P., Ayabe, T., López-Boado, Y. S., Stratman, J. L., Hultgren, S. J., Matrisian, L. M., & Parks, W. C. (1999). Regulation of intestinal α-defensin activation by the metalloproteinase matrilysin in innate host defense. *Science*, *286*(5437), 113–117.

Wittkopf, N., Pickert, G., Billmeier, U., Mahapatro, M., Wirtz, S., Martini, E., Leppkes, M., Neurath, M. F., & Becker, C. (2015). Activation of intestinal epithelial stat3 orchestrates tissue defense during gastrointestinal infection. *PLoS ONE*, *10*(3), e0118401.

Xue, Y., Zhang, H., Sun, X., & Zhu, M. J. (2016). Metformin improves ileal epithelial barrier function in interleukin-10 deficient mice. *PLoS ONE*, *11*(12), e0168670.

Yang, J., Kunimoto, H., Katayama, B., Zhao, H., Shiromizu, T., Wang, L., Ozawa, T., Tomonaga, T., Tsuruta, D., & Nakajima, K. (2019). Phospho-Ser727 triggers a multistep inactivation of STAT3 by rapid dissociation of pY705-SH2 through C-terminal tail modulation. *International Immunology*, *32*(2), 73–88.

Ye, Z., Huang, H., Hao, S., Xu, S., Yu, H., Van Den Hurk, S., & Xiang, J. (2007). IL-10 has a distinct immunoregulatory effect on naive and active T cell subsets. *Journal of Interferon and Cytokine Research*, *27*(12), 1031–1038.

Yue, R., Wei, X., Zhao, J., Zhou, Z., & Zhong, W. (2021). Essential role of IFN-γ in regulating gut antimicrobial peptides and microbiota to protect against alcohol-induced bacterial translocation and hepatic inflammation in mice. *Frontiers in Physiology*, *11*, 629141.

Zheng, L., Kelly, C. J., Battista, K. D., Schaefer, R., Lanis, J. M., Alexeev, E. E., Wang, R. X., Onyiah, J. C., Kominsky, D. J., & Colgan, S. P. (2017). Microbial-derived butyrate promotes epithelial barrier function through IL-10 receptor–dependent repression of claudin-2. *Journal of Immunology*, *199*(8), 2976–2984.

Zhou, P., Streutker, C., Borojevic, R., Wang, Y., & Croitoru, K. (2004). IL-10 modulates intestinal damage and epithelial cell apoptosis in T cell-mediated enteropathy. *American Journal of Physiology - Gastrointestinal and Liver Physiology*, *287*(3), G599–G604.

Zhu, L., Shi, T., Zhong, C., Wang, Y., Chang, M., & Liu, X. (2017). IL-10 and IL-10 receptor mutations in very early onset inflammatory bowel disease. *Gastroenterology Research*, *10*(2), 65–69.

APPENDICES

Confirmation of publication and licensing rights

49 Spadina Ave. Suite 200
Toronto ON M5V 2J1 Canada
www.biorender.com

Confirmation of Publication and Licensing Rights

September 19th, 2021
Science Suite Inc.

Subscription: *Student Plan*
Agreement number: *EK22Z5U61G*
Journal name: *Library and Archives of Canada*

To whom this may concern,

This document is to confirm that **Huong Nguyen** has been granted a license to use the BioRender content, including icons, templates and other original artwork, appearing in the attached completed graphic pursuant to BioRender's Academic License Terms. This license permits BioRender content to be sublicensed for use in journal publications.

All rights and ownership of BioRender content are reserved by BioRender. All completed graphics must be accompanied by the following citation: "Created with BioRender.com".

BioRender content included in the completed graphic is not licensed for any commercial uses beyond publication in a journal. For any commercial use of this figure, users may, if allowed, recreate it in BioRender under an Industry BioRender Plan.

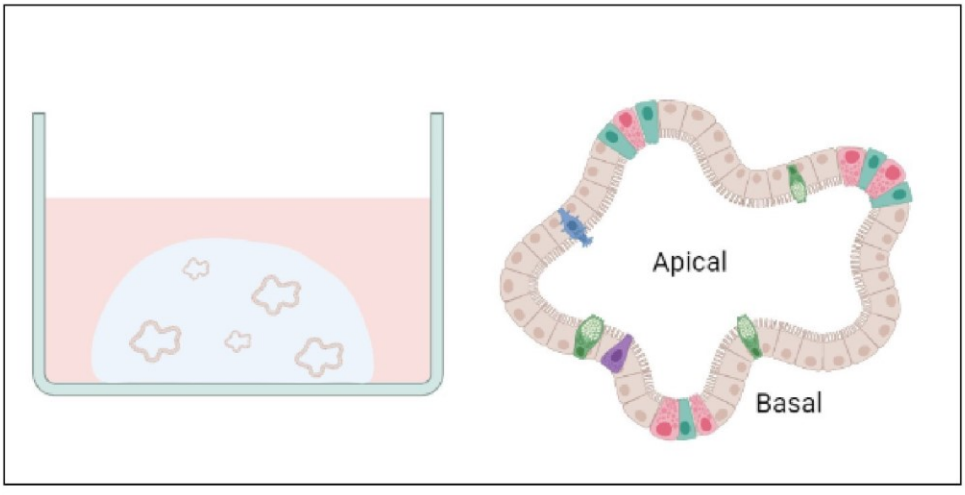

For any questions regarding this document, or other questions about publishing with BioRender refer to our BioRender Publication Guide, or contact BioRender Support at support@biorender.com.

49 Spadina Ave. Suite 200
Toronto ON M5V 2J1 Canada
www.biorender.com

Confirmation of Publication and Licensing Rights

September 19th, 2021
Science Suite Inc.

Subscription:	*Student Plan*
Agreement number:	*MW22Z5U6KB*
Journal name:	*Library and Archives of Canada*

To whom this may concern,

This document is to confirm that **Huong Nguyen** has been granted a license to use the BioRender content, including icons, templates and other original artwork, appearing in the attached completed graphic pursuant to BioRender's Academic License Terms. This license permits BioRender content to be sublicensed for use in journal publications.

All rights and ownership of BioRender content are reserved by BioRender. All completed graphics must be accompanied by the following citation: "Created with BioRender.com".

BioRender content included in the completed graphic is not licensed for any commercial uses beyond publication in a journal. For any commercial use of this figure, users may, if allowed, recreate it in BioRender under an Industry BioRender Plan.

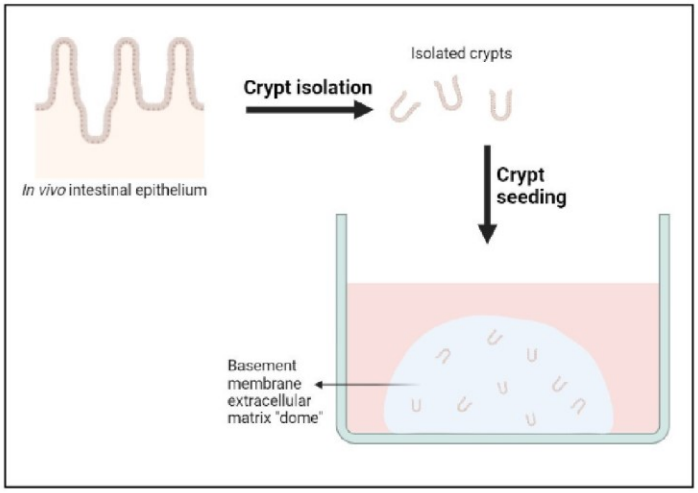

For any questions regarding this document, or other questions about publishing with BioRender refer to our BioRender Publication Guide, or contact BioRender Support at support@biorender.com.

49 Spadina Ave. Suite 200
Toronto ON M5V 2J1 Canada
www.biorender.com

Confirmation of Publication and Licensing Rights

September 20th, 2021
Science Suite Inc.

Subscription:	*Student Plan*
Agreement number:	*ZF22ZABOUQ*
Journal name:	*Library and Archives of Canada*

To whom this may concern,

This document is to confirm that **Huong Nguyen** has been granted a license to use the BioRender content, including icons, templates and other original artwork, appearing in the attached completed graphic pursuant to BioRender's Academic License Terms. This license permits BioRender content to be sublicensed for use in journal publications.

All rights and ownership of BioRender content are reserved by BioRender. All completed graphics must be accompanied by the following citation: "Created with BioRender.com".

BioRender content included in the completed graphic is not licensed for any commercial uses beyond publication in a journal. For any commercial use of this figure, users may, if allowed, recreate it in BioRender under an Industry BioRender Plan.

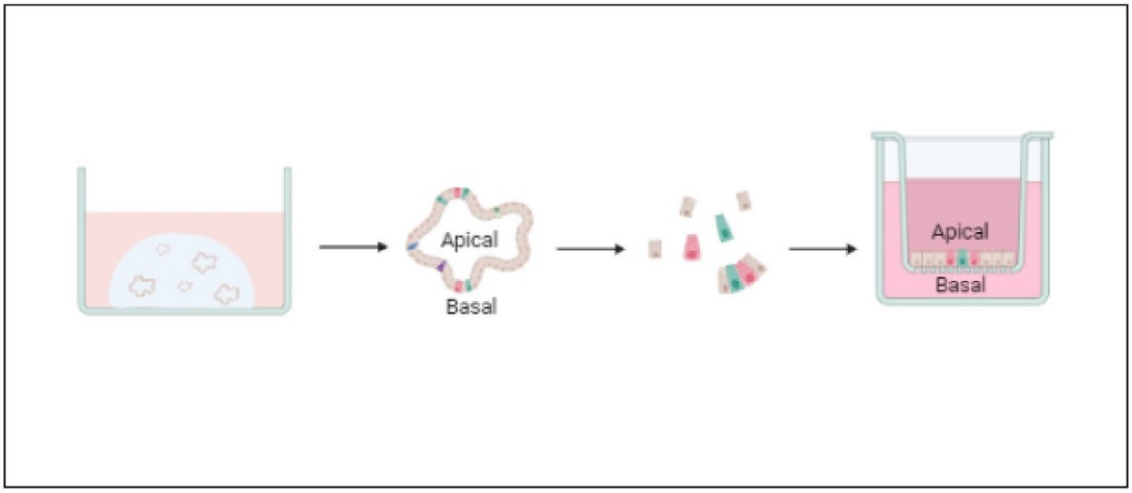

For any questions regarding this document, or other questions about publishing with BioRender refer to our BioRender Publication Guide, or contact BioRender Support at support@biorender.com.

49 Spadina Ave. Suite 200
Toronto ON M5V 2J1 Canada
www.biorender.com

Confirmation of Publication and Licensing Rights

September 19th, 2021
Science Suite Inc.

Subscription:	*Student Plan*
Agreement number:	*JO22Z5U7G2*
Journal name:	*Library and Archives of Canada*

To whom this may concern,

This document is to confirm that **Huong Nguyen** has been granted a license to use the BioRender content, including icons, templates and other original artwork, appearing in the attached completed graphic pursuant to BioRender's Academic License Terms. This license permits BioRender content to be sublicensed for use in journal publications.

All rights and ownership of BioRender content are reserved by BioRender. All completed graphics must be accompanied by the following citation: "Created with BioRender.com".

BioRender content included in the completed graphic is not licensed for any commercial uses beyond publication in a journal. For any commercial use of this figure, users may, if allowed, recreate it in BioRender under an Industry BioRender Plan.

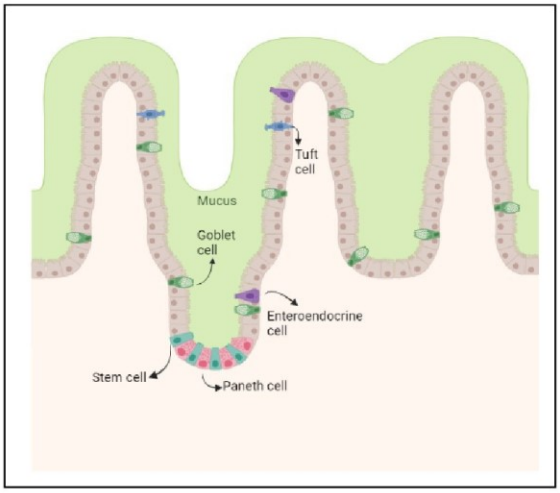

For any questions regarding this document, or other questions about publishing with BioRender refer to our BioRender Publication Guide, or contact BioRender Support at support@biorender.com.

49 Spadina Ave. Suite 200
Toronto ON M5V 2J1 Canada
www.biorender.com

Confirmation of Publication and Licensing Rights

September 19th, 2021
Science Suite Inc.

Subscription:	*Student Plan*
Agreement number:	*YW22Z5U1J9*
Journal name:	*Library and Archives of Canada*

To whom this may concern,

This document is to confirm that **Huong Nguyen** has been granted a license to use the BioRender content, including icons, templates and other original artwork, appearing in the attached completed graphic pursuant to BioRender's Academic License Terms. This license permits BioRender content to be sublicensed for use in journal publications.

All rights and ownership of BioRender content are reserved by BioRender. All completed graphics must be accompanied by the following citation: "Created with BioRender.com".

BioRender content included in the completed graphic is not licensed for any commercial uses beyond publication in a journal. For any commercial use of this figure, users may, if allowed, recreate it in BioRender under an Industry BioRender Plan.

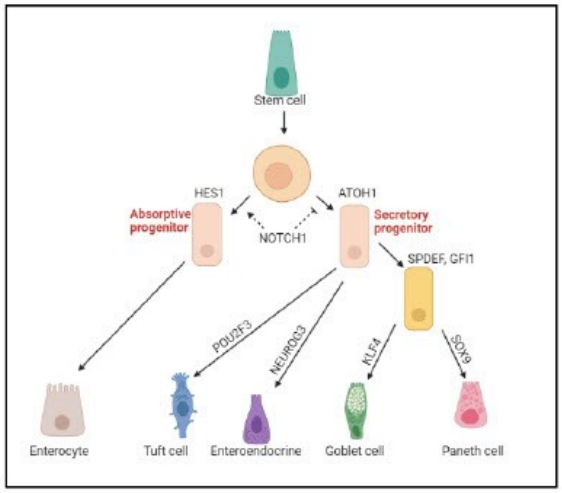

For any questions regarding this document, or other questions about publishing with BioRender refer to our BioRender Publication Guide, or contact BioRender Support at support@biorender.com.

49 Spadina Ave. Suite 200
Toronto ON M5V 2J1 Canada
www.biorender.com

Confirmation of Publication and Licensing Rights

September 19th, 2021
Science Suite Inc.

Subscription:	*Student Plan*
Agreement number:	*QY22Z5UEAH*
Journal name:	*Library and Archives of Canada*

To whom this may concern,

This document is to confirm that **Huong Nguyen** has been granted a license to use the BioRender content, including icons, templates and other original artwork, appearing in the attached completed graphic pursuant to BioRender's Academic License Terms. This license permits BioRender content to be sublicensed for use in journal publications.

All rights and ownership of BioRender content are reserved by BioRender. All completed graphics must be accompanied by the following citation: "Created with BioRender.com".

BioRender content included in the completed graphic is not licensed for any commercial uses beyond publication in a journal. For any commercial use of this figure, users may, if allowed, recreate it in BioRender under an Industry BioRender Plan.

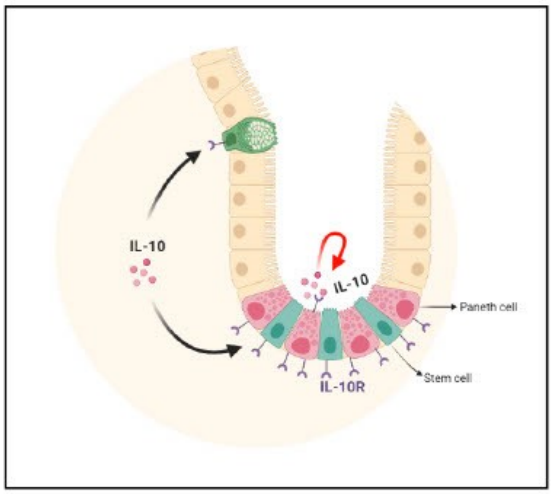

For any questions regarding this document, or other questions about publishing with BioRender refer to our BioRender Publication Guide, or contact BioRender Support at support@biorender.com.